UBIQUITIN AND UBIQUITIN-LIKE PROTEINS IN CELL CYCLE REGULATION

Christine A. Mills

A dissertation submitted to the faculty at the University of North Carolina at Chapel Hill in partial fulfillment of the requirements for the degree of Doctor of Philosophy in the Department of Pharmacology in the School of Medicine.

Chapel Hill
2018

Approved by:

Michael J. Emanuele

Lee Graves

Jean Cook

Gary Johnson

Kerry Bloom

ABSTRACT

Christine A. Mills: Ubiquitin and Ubiquitin-Like Proteins in Cell Cycle Regulation
(Under the direction of Michael J Emanuele)

Cell cycle is a tightly regulated process; however, it is mis-regulated in many cancers, leading to increased proliferation. Our lab is interested in better understanding cell cycle regulation, in particular, regulation by the ubiquitin system, which controls targeted protein degradation. The following work focuses on the modular ubiquitin E3 ligase composed of SKP1/CUL1/F-box protein (SCF) with its substrate adapter Cyclin F. Cyclin F is a unique F-box protein in that it is highly cell cycle regulated, and has been revealed as a key regulator of cell cycle progression despite few of its substrates having been identified. Our lab aims to identify novel Cyclin F substrates, and determine how these substrates regulate cell cycle processes.

The Cyclin F substrate, Nucleolar and Spindle Associated Protein 1 (NUSAP1), is a microtubule binding protein implicated in mitotic spindle stability and chromosome segregation, however, how it functions is unknown. I have identified a novel interaction between NUSAP1 and a small ubiquitin-related modifier (SUMO) E3 ligase composed of Ran Binding Protein 2 (RanBP2), Ran GTPase Activating Protein 1 (RanGAP1) and the SUMO E2 conjugating enzyme, UBC9. This work provides evidence that NUSAP1 may function in the SUMO pathway to promote faithful chromosome segregation.

Cell cycle and metabolic regulation are critical to the growth and proliferation of normal cells, and these systems can be rewired in cancer to promote proliferation. Better understanding how these processes are integrated could provide key insights into how cancers proliferate. The following work identifies Sirtuin 5, a mitochondrial deacylating enzyme, as a novel Cyclin F substrate. Sirtuin 5 is a known regulator of key metabolic processes including gluconeogenesis and urea production, among others. To date, identified Cyclin F substrates are all involved in significant cell cycle processes, however, Sirtuin 5 has never been connected to cell cycle. This data reveals a new role for Sirtuin 5 as a regulator of G1 progression and suggests a possible role in quiescence. Furthermore, this data provides a link between cell cycle progression and metabolism. Additional research is needed to understand what possible metabolites are involved in this regulation, and how it is mis-regulated in cancer.

To my mentors, friends and parents, whose limitless support I have relied upon along the way. Special thanks to Charles Jervis, the teacher who ignited my love of science, Dr. Tara Phelps-Durr, who encouraged me to go farther than I ever imagined, and finally, Dr. Michael J Emanuele, who has helped me grow into an independent scientist and given me confidence in my work. I could not have come this far without you all.

ACKNOWLEDGEMENTS

Special thanks to the Emanuele laboratory and my thesis committee for critical feedback throughout the course of this research. This work was done in part at the University of North Carolina Flow Cytometry and Proteomics Core Facilities.

TABLE OF CONTENTS

LIST OF TABLES

LIST OF FIGURES

LIST OF ABBREVIATIONS

AA	amino acid
AEBSF	4-[2Aminoethyl] benzenesulfonyl fluoride
AKT	RAC-alpha serine/threonine-protein kinase
APC/C	Anaphase Promoting Complex/Cyclosome
apc5	Anaphase-promoting complex subunit 5
ATM	Ataxia telangiectasia mutated
ATP	Adenosine triphosphate
ATR	Ataxia telangiectasia and Rad3-related protein
BSA	Bovine serum albumin
C/EBP-β	CCAAT/Enhancer-Binding Protein beta
Cdc20	Cell division cycle protein 20 homologue
Cdc25A	M-Phase inducer phosphatase 1
Cdc4	Cell division control protein 4
Cdc53	Cell division control protein 53
Cdc6	Cell division control protein 6 homolog
Cdh1	Fizzy-related protein homolog Cdh1
CDK	Cyclin Dependent Kinase
CENP-C	Centromere-associated protein C

CENP-E	Centromere-associated protein E
Chk1	Checkpoint Kinase-1
Chk2	Checkpoint Kinase-2
CP110	Centriolar coiled-coil protein o 110 kDa
CPC	Chromosomal Passenger Complex
CPS1	Carbamoyl phosphate synthase 1
CRAPome	Contaminant Repository for Affinity Purification Mass Spectrometry Data
CRISPR	Clustered regularly interspaced short palindromic repeats
CSK	Cytoskeletal buffer
CUL1	Cullin-1
CUL3	Cullin-3
DMEM	Dulbecco's Modified Eagle Media
DMSO	Dimethyl sulfoxide
DNA	Deoxyribonucleic Acid
DRYGIN	Data Repository of Yeast Genetic Interactions
DTT	Dithiothreitol
DUB	Deubiquitinating enzyme
ECL	Enhanced chemiluminescence

EDTA	Ethylenediaminetetraacetic acid
EdU	5-ethynyl-2'-deoxyuridine
EGTA	Ethylene glycol-bis(β-aminoethyl ether)-N,N,N',N'-tetraacetic acid
Exo1	Exonuclease 1
FASP	Filter-aided sample preparation
FBS	Fetal bovine serum
FF	Firefly luciferase
FoxM1	Forkhead box protein M1
HA	Human influenza hemagglutinin epitope
HEC1	Kinetochore protein NDC80 homolog
HECT	Homologous to E6-AP carboxy terminus
HEPES	4-(2-hydroxyethyl)-1-piperazineethanesulfonic acid
HIS	Hexahistidine tag
HRP	Horseradish peroxidase
hst3	NAD-dependent histone deacetylate hst3
IBR	InBetweenRING domain
IF	Immunofluorescence
IgG	Immunoglobulin G

INCENP	Inner Centromere Protein
IP	Immunoprecipitation
IPTG	isopropyl β-D-1-thiogalactopyranoside
KCl	Potassium chloride
KD	Knock-down
kDa	Kilodalton
KIF4	Chromosome-Associated kinesin KIF4A
KLH	Keyhole Limpet Hemocyanin
KO	Knockout
KOH	Potassium hydroxide
LC	Liquid chromotography
MCC	Mitotic Checkpoint Complex
mcm3	DNA replication licensing factor MCM3
MDM2	E3 ubiquitin-protein ligase Mdm2
MEF	Mouse embryonic fibroblasts
MgCl2	Magnesium chloride
mRNA	messenger ribonucleic acid
MS	Mass spectrometry
NaCl	Sodium chloride

NAD	Nicotinamide adenine dinucleotide
NaF	Sodium fluoride
Nedd8	Neural precursor cell expressed developmentally down-regulated protein 8
NETN	20mM Tris-Cl, pH 8.0, 100mM NaCl, 0.5mM EDTA, 0.5% Nonidet P-40
Ni-NTA	Nickel-nitrilotriacetic acid
NP-40	Nonidet P-40
NSLC	Non small-cell lung cancer
NUSAP1	Nucleolar and Spindle Associated Protein 1
orc3	Origin recognition complex subunit 3
PBS	Phosphate buffered saline
PBST	Phosphate buffered saline, 0.05% tween-20
p-Chk1	phosphorylated Chk1
PFA	Paraformaldehyde
PIAS	Protein Inhibitor of Activated STAT2
PIPES	piperazine-N-N'-bis(2-ethanesulfonic acid)
PLA	Proximity ligation assay
PRC1	Protein Regulator of Cytokinesis 1
PTM	Post-translational modification

RanBP2	Ran Binding Protein 2
RanGAP1	Ran GTPase Activating Protein 1
RB	Retinoblastoma protein
RING	Really Interesting New Gene
RNA	Ribonucleic acid
RNAi	RNA interference
RNase A	Ribonuclease A
RRM2	Ribonucleoside-diphosphate reductase subunit M2
SAC	Spindle Assembly Checkpoint
SAF-A/B	Scaffold Attachment Factor A/B
SAP	SAF-A/B/Acinus/PIAS protein domain
SCF	Skp1/Cul1/F-box
SDS	Sodium dodecyl sulfate
SDS-PAGE	Sodium dodecyl sulfate polyacrylamide gel electrophoresis
siRNA	Small interfering RNA
Sirt5	NAD-dependent protein deacylase sirtuin-5, mitochondrial
Sirt7	NAD-dependent protein deacetylase sirtuin-7
Skp1	Supressor of Kinetochore Protein 1
SLBP	Stem-Loop Binding Protein

sli15	Inner centromere protein-related protein SLI15
SOD1	Cu/Zn superoxide disumutase
SUMO	Small ubiquitin-related modifier
swi5	Transcriptional factor SWI5
TOP2	DNA topoisomerase 2
TOP2A	DNA topoisomerase 2-alpha
TOP2B	DNA topoisomerase 2-beta
TSC	Total spectral counts
UBC9	SUMO-conjugating ezyme
UBD	Ubiquitin Binding Domain
UBL	Ubiquitin-Like proteins
WCE	Whole cell extract
Wee1	Wee1-like protein kinase

CHAPTER 1: INTRODUCTION

1.1 Cell Cycle

Cell growth and division is a highly regulated process during which one cell becomes two daughter cells. This process, known as the cell cycle, is broken up into four phases; G1, S, G2 and Mitosis (M). During G1, cells monitor their surroundings and nutrient availability, assessing whether it is safe to proceed through the cell cycle. If the cell proceeds forward in the cell cycle, G1 acts as a preparatory phase for S, where DNA replication occurs. G1 cells contain only one copy of each chromosome, but to divide, the DNA must be duplicated to ensure that each daughter cell receives the same DNA. To prepare for DNA replication, cells must make nucleotides and proteins, and license DNA replication origins. At the beginning of S, origins fire and DNA replication begins. Once DNA replication is complete and the cells are equipped with two copies of each chromosome, the cells proceed into G2. During G2, the cell ensures that the DNA has been properly replicated and that it is of adequate size to proceed through mitosis. Once it is ready, the cell proceeds to mitosis, where it segregates sister chromatids equally, resulting in two genetically identical daughter cells. Mitosis is composed of six stages; prophase, prometaphase, metaphase, anaphase, telophase and cytokinesis.

Cell cycle progression is tightly controlled to ensure that cells are prepared to proceed before moving to the next phase. At the center of that control are Cyclin Dependent Kinases (CDKs) and their cyclin binding partners, which, when bound,

form active kinase complexes. There are a number of different CDKs and cyclins, which combine in specific pairs. While CDK protein levels remain constant throughout the cell cycle, cyclin protein levels oscillate. When a particular cyclin is expressed, it binds its preferred CDK to promote signaling and cell cycle progression (**Figure 1.1**). It is important to note, that while CDK/Cyclin pairs are considered the core of cell cycle regulation, abundance and activity of hundreds of proteins cycle throughout cell cycle and contribute to proper progression (1).

Cell cycle Checkpoints

There are many checkpoints during the cell cycle to prevent cells from prematurely beginning irreversible processes. These checkpoints are always "active" and monitoring the cellular state. For a cell to proceed past these checkpoints it must satisfy them by fulfilling a number of requirements, with each checkpoint having a unique set of requirements. Cell cycle checkpoints include the restriction point, DNA damage checkpoint, and Spindle Assembly Checkpoint (SAC). Weakened checkpoints can allow the cell to proceed through the next phase of the cell cycle despite being unprepared, which can result in damage to the cell.

The first checkpoint is called the restriction point (2). This checkpoint ensures that cells have enough resources, such as space, growth factors, or nutrients, to proceed safely through the next cell cycle (2). If the cell does not detect enough resources, it may exit the cell cycle during G1 into a state referred to as G0, or quiescence. Quiescence is a suspended state, during which the cell does not cycle and maintains an early G1-like state. If a quiescent cell senses that it has sufficient resources to cycle again, it can re-enter the cell cycle in G1.

The DNA-damage checkpoint, which arrests cell so that damaged DNA can be repaired, is controlled by either of two large kinases. Ataxia telangiectasia mutated (ATM) or Ataxia telangiectasia and Rad3-related protein (ATR) signaling, depending on which stage of the cell cycle the cell it is in at the time of damage. Both ATM and ATR phosphorylate hundreds of target proteins. If DNA damage is sensed in G1, the ATM signaling pathway is activated, preventing cells from entering S-phase before the damage is repaired, ultimately preventing replication of damaged DNA. ATM does this, in part, by phosphorylating and activating Checkpoint Kinase 2 (Chk2), which inhibits M-Phase inducer phosphatase 1 (Cdc25A) (3–7). Normally, Cdc25A dephosphorylates and activates CDK2/Cyclin E to promote S-phase entry, and phosphorylation by ATM in turn prevents activation of CDK2/Cyclin E (8). ATM also phosphorylates p53, releasing it from its inhibitor E3 ubiquitin-protein ligase Mdm2 (MDM2), so it can induce DNA repair proteins as well as the CDK2/Cyclin E and CDK2/Cyclin A inhibitor p21 (9–18).

If DNA damage occurs during S or G2, signaling goes through a similar signaling pathway mediated by ATR, to arrest cells and give the cell time to repair the damage before proceeding through mitosis. At the core of ATR damage response, ATR phosphorylates and activates Checkpoint Kinase 1 (Chk1), which, like Chk2, also inhibits Cdc25A (19–21). During S-phase however, Cdc25A promotes CDK1/Cyclin B activity (22, 23). ATR signaling also activates the CDK1 inhibitor Wee1-like protein kinase (Wee1) (24, 25). If cells slip through the damage checkpoint and into mitosis, cells undergo mitotic catastrophe and die.

Once cells enter mitosis they must satisfy the Spindle Assembly Checkpoint (or SAC). The SAC ensures that cells do not attempt to enter anaphase, where the

cell segregates mitotic chromosomes, until they have made the correct attachments to the mitotic spindles, meaning each sister of a chromosome pair is stably attached to opposite spindle poles (26). This checkpoint is controlled by the Mitotic Checkpoint Complex (MCC) which targets the E3 ubiquitin ligase complex known as the Anaphase Promoting Complex/Cyclosome (APC/C) (27). The MCC sequesters the APC/C substrate adapter protein Cell division cycle protein 20 homologue (Cdc20), preventing the APC/C from being active (28). Once each pair of sister chromatids has been stably attached to opposite poles, the checkpoint is satisfied and APC/C is activated. Once active, APC/C targets Cyclin B for degradation, as well as Securin, the protein that sequesters Separase (29–33). Once Separase is released, it can cleave Cohesin, the proteins holding sister chromatids together, and the cell can enter anaphase where sister chromatids are pulled to opposite poles of the mitotic cell (34, 35).

The Ubiquitin system

Targeted protein degradation is a major component of cell cycle regulation and allows the cell to degrade proteins within a few minutes of degradation onset, offering a quick switch-like mechanism for cells to release from, or even activate checkpoints. For example, once the SAC has been satisfied, cells trigger degradation of Cyclin B via the Anaphase Promoting Complex/Cyclosome (APC/C) and within minutes, Cyclin B is degraded, allowing cells to progress into anaphase.

This process of targeted protein degradation is controlled by the ubiquitin system. Ubiquitin is a small protein (~8.5 kDa), that once conjugated to a substrate, acts as a post-translational modification (PTM) (36, 37). Ubiquitin is highly conserved in eukaryotes, with paralogues identified in prokaryotes. Ubiquitin

is added specifically to substrate lysines through an enzyme cascade composed of E1, E2 and E3 enzymes (37, 38). The first step to this cascade is ATP-dependent ubiquitin activation by the E1, or activating enzyme. This activation results in a thioester linkage between the C-terminus of the ubiquitin and a cysteine in the E1. The ubiquitin molecule is then passed to the catalytic cysteine of an E2, or conjugating enzyme (39). Finally, the E2 interacts with an E3 ubiquitin ligase (discussed in detail below), to ligate the ubiquitin molecule to a substrate lysine via an isopeptide bond with the C-terminal glycine of ubiquitin (39). Alternatively, ubiquitin can be conjugated to the amino-terminal of a target substrate (40).

Ubiquitin can be added to substrates a number of different ways. Mono-ubiquitination refers to a single ubiquitin molecule added to a substrate on a single lysine. Multi-mono-ubiquitination occurs when multiple lysines of the substrate have a single ubiquitin modification. Furthermore, because ubiquitin is itself a protein that contains lysines, it too can be modified by other PTMs or other ubiquitin molecules, resulting in ubiquitin chains. There are many possible chain linkages due ubiquitin containing seven lysines, with different lysine linkages between ubiquitin molecules resulting in different chain topologies, which determine the outcome for the substrate (36, 41, 42).

Polyubiquitination of proteins with K11/K48, (with K denoting the lysine in ubiquitin), linked ubiquitin chains are known to target proteins for degradation through the proteasome (43, 44). The 26S proteasome is a large, multi-subunit machine composed of two primary complexes; the 20S proteasome core and the 19S regulatory cap (45). The ubiquitinated proteins first bind the 19S cap, which regulates their unfolding and entry into the 20S proteasome, which contains a

number of proteolytic enzymes that hydrolyze peptide bonds, ultimately degrading proteins (46, 47). Deubiquitinating enzymes (DUBs) associated with the proteasome cleave ubiquitin from target proteins, allowing it to be recycled (48, 49).

Apart from ubiquitin's role in promoting degradation through the proteasome, ubiquitin also regulates cellular processes such as endocytosis, DNA repair and other signaling pathways (41, 50, 51). Ubiquitination of some proteins may regulate binding partners through mechanisms such as steric hinderance, or even promote complex assembly (52). Ubiquitin can also be conjugated to histones or transcription factors to regulate transcription (52).

Ubiquitin E3 ligases

As described above, ubiquitin is added to substrates via an enzyme cascade, with the last member of the cascade is the E3 ubiquitin ligase. E3 ligases typically fall into one of three families; RING-type, HECT-type or RING-between-RING (RBR) type (53–55). The largest family of E3 ligases, RING-type ubiquitin ligases, are classified by the Really Interesting New Gene (or RING) domain or protein, which recruits an E2 to the enzyme complex (53). In RING-type ligases, the E3 binds a substrate protein and the E2 transfers ubiquitin directly to the substrate, with the E3 acting more as a scaffold and never contacting the ubiquitin directly (53). For HECT-type E3 ubiquitin ligases, which contain a Homologous to E6-AP carboxy terminus (HECT) domain, the E2 binds the E3 and transfers the ubiquitin to a catalytic cysteine on the E3 ligase (54). The E3 then directly transfers ubiquitin to a target substrate. The RING-between-RING enzymes contain two RING domains with an InBetweenRING (IBR) domain between them (55). Similar to HECT-type E3's,

the ubiquitin is first transferred from the E2 to the E3, which then transfers it to a substrate lysine (55).

E3 ligase families can be further broken down into subfamilies, for example, the RING-type ligases include Cullin E3 ligases (56). These are modular E3 ubiquitin ligases based on a Cullin backbone, and were first discovered for their role in the cell cycle (example in Figure 1.2) (56, 57). There are up to nine Cullin proteins, and each uses a specific family of substrate adapter proteins to recruit substrates to the complex. In the following research, the Cullin 1 (CUL1) based E3 ubiquitin ligase, called the SCF (Skp1/CUL1/Fbox protein) is of particular interest. This E3 ligase was the first Cullin based E3 ligase to be identified, and is composed of a CUL1 backbone, which binds a RING protein on its C-terminus and Skp1 (Suppressor of Kinetochore Protein 1) on its N-terminus (58, 59). The Skp1 protein binds an F-box protein, which then recruits specific substrates to the E3 complex for ubiquitination while the RING protein recruits the E2 (58, 59). Humans possess ~70 different F-box proteins, each enabling the SCF unique target specificity.

E3 Ubiquitin ligases are antagonized by DUBs, which remove ubiquitin modifications from targets. There are approximately 100 DUBs, divided up into two different classes; cysteine proteases and metalloproteases (60, 61). While some DUBs have specific activity against certain ubiquitin chain types, some are non-specific and can cleave multiple ubiquitin linkages (60, 61). Some DUBs also have activity against ubiquitin-like proteins, which are discussed further below (61).

Ubiquitin-Like Modifications

Ubiquitin is a member of the ubiquitin family of proteins, which primarily act as PTMs. Ubiquitin-Like proteins (UBLs) are classified into two types; type I have been identified as being conjugated to substrates, while type II have not, with ubiquitin being a type I UBLs. All UBLs undergo the same basic enzyme cascade for activation and conjugation to substrates, but so far, the best characterized of these type I UBLs, besides ubiquitin, include Neural precursor cell expressed developmentally down-regulated protein 8 (Nedd8) and Small Ubiquitin-related Modifier (SUMO).

Nedd8 is the UBL most similar to ubiquitin (62). The role of neddylation in the cell is most closely tied to regulation of Cullin E3 ligases. Neddylation of Cullin backbones aids in recruitment of the ubiquitin loaded E2 and promotes a structural change that brings the E2 and substrate closer together (63–66). Furthermore, it helps stabilize the transition state, during which the E2 and substrate are interacting, allowing chain elongation to occur (63).

While SUMOylation occurs through a similar enzyme cascade as ubiquitin, there are a few key differences (67, 68). The first being that there is only one E2 for the SUMO system compared to the almost 40 E2s for ubiquitin. The SUMO E2, SUMO-conjugating enzyme UBC9, (also referred to as UBE2I), appears more promiscuous than many ubiquitin E2 enzymes (67, 69–71). UBC9 can SUMOylate proteins *in vitro* without an E3 ligase, and it is poorly understood how its activity is regulated by SUMO E3 ligases *in vivo*. Furthermore, little is known about how SUMO E3 ligases identify and interact with substrates. There are also three isoforms of SUMO, SUMO1 and SUMO2/3 (with SUMO2 and SUMO3 being indistinguishable at

the protein level), which can both be conjugated to substrates, however only SUMO2/3 can form SUMO chains (67). Currently, it is unclear what the differences between SUMO1 and SUMO2/3 modification of substrates are, although it has been suggested that SUMO2/3 conjugation plays more of a role in stress response (72, 73). It is also unclear if either paralog is preferred by particular SUMO E3 ligases, although research has suggested that SUMO1 modifications compose the majority of preferential SUMO modifications *in vivo* (74).

SUMOylation may influence many protein characteristics, including localization, dimerization/interactions, activity, and stability. While a few SUMO substrates have been well characterized, there is still debate on the function of the SUMOylation. So far, studies aimed at identifying SUMOylation substrates have relied on stress induced SUMOylation or overexpression of SUMO or the promiscuous E2, UBC9. Using overexpression methods in the identification of SUMO targets is difficult because the SUMO can be used by other UBL pathways, for example the ubiquitin pathway, which results in ubiquitin targets being modified by SUMO instead of ubiquitin. These caveats make it unclear whether the substrates identified in many of these studies are real, or relevant, in normal physiological conditions. Furthermore, many of the methods used to probe the SUMO pathway are methods developed to probe the ubiquitin pathway. While SUMO appears very similar to ubiquitin, these methods may be insufficient to elucidate details of the SUMO pathway. Further research is needed to better understand the role of SUMO in normal, or unstressed, cellular state.

1.2 Cyclin F in Cell Cycle Control

Some members of the ubiquitin pathway are becoming more recognized for key roles in cell cycle progression. One such protein is Cyclin F (Figure 1.2). Cyclin F is the founding member of the F-box containing family of proteins, most of which are substrate adapters for the SCF E3 ubiquitin ligase complex (75–77). Cyclin F is a non-traditional cyclin, as it does not bind to and activate a CDK (78). However, like cyclins, Cyclin F protein levels are highly cell cycle regulated, and it is the most cell cycle regulated F-box protein (75, 78). Cyclin F was first identified as a protein that could rescue the yeast Cdc4 mutant phenotype, which causes a G1 arrest and subsequent death (75). While many of the known Cyclin F substrates alluded to its importance for cell cycle progression, more recent studies have shown that feedback between the APC/C^{Cdh1} and $SCF^{Cyclin\ F}$ is important for promoting the G1-S transition (79, 80). During early G1, when the APC/C substrate adapter Cdh1 is around, the APC/C^{Cdh1} targets Cyclin F for ubiquitination and degradation (79). However, as Cyclin F protein levels slowly accumulate, a switch occurs and the $SCF^{Cyclin\ F}$ targets Cdh1 for ubiquitination and degradation, promoting the transition into S-phase (79). This switch has been shown to be controlled by growth factor signaling through the RAC-alpha serine/threonine-protein kinase (AKT) pathway, which promotes the recruitment of Cyclin F into the SCF complex, resulting in the degradation of Cdh1 (80).

Identified Cyclin F substrates

Identified Cyclin F substrates to date include Centriolar coiled-coil protein of 110 kDa (CP110), Nucleolar and Spindle Associated Protein 1 (NUSAP1), Ribonucleoside-diphosphate reductase subunit M2 (RRM2), Exonuclease 1 (Exo1),

Stem-Loop Binding Protein (SLBP), Cell division control protein 6 homolog (Cdc6), and Fizzy-related protein homolog Cdh1 (79, 81–85). All of these substrates have roles in cell cycle progression and are involved in highly regulated processes.

RRM2, Cdc6 and Exo1 are all important in G1-S transition and DNA replication. RRM2 is a subunit of ribonucleoside-diphosphate reductase complex, which is important for nucleotide synthesis needed for DNA replication. Cdc6 is important for pre-replication complex loading, an event critical to proper DNA replication (86, 87). Degradation of Cdc6 by Cyclin F is important for preventing re-replication (85). Exo1 is required for mismatch repair during DNA replication and strand resection during homologous recombination (88). Exo1 is targeted for degradation by Cyclin F in response to UV-induced DNA damage in G2, likely to prevent excessive strand resection (84).

CP110, NUSAP1 and Cdc6 are all important for G2-M transition and mitotic progression. Along with its role in DNA-replication initiation, Cdc6 prevents premature mitotic entry when un-replicated DNA is present by regulating phosphorylation of Chk1, promoting arrest until DNA replication is completed (86, 87, 89). CP110 controls centrosome duplication, an event critical for the establishment of a bipolar spindle during mitosis, however, centrosome duplication normally only occurs one time in a cell cycle (90). If cells duplicate centrosomes more than once it can lead to multipolar spindles. In cells with reduced levels of Cyclin F, multipolar spindles are more common, leading to mis-segregation phenotypes (81). NUSAP1 is not only implicated in the G2-M transition, but is important for maintenance and stability of the mitotic spindle (91–93). NUSAP1 levels must be tightly controlled however, because overexpression of NUSAP1

results in microtubule bundling which inhibits normal mitotic progression (93). SLBP is also targeted by Cyclin F for degradation during G2, preventing the translation and accumulation of H2A.X and γH2A.X (94). Upon high genotoxic stress, SLBP accumulates and promote the induction of H2A.X and γH2A.X (94).

Finally, Cdh1 plays important roles in a number of cell cycle transitions. As one of the substrate adapter for the APC/C, it is especially important for mitotic exit, where it targets Cyclin B for degradation (30). As mentioned in the previous section, Cyclin F mediated degradation of Cdh1 is also important for the G1-S transition (79, 80).

Despite only a handful of Cyclin F substrates having been identified to date, the evidence is clear that Cyclin F plays key roles in regulating cell cycle progression. Identification of more Cyclin F substrates is needed, and will help further clarify our understanding of cell cycle regulation.

1.3 Cell Cycle mis-regulation in Cancer

Cancer is a disease consisting of over proliferative cells, indicating disruptions in normal cell cycle regulation. Over the years, many cell cycle components have been shown to be mis-regulated in cancers, including CDK4/6/Cyclin D, p53 and mitotic machinery.

Many cancers, including some breast cancers, exhibit amplification of the CDK4/6/Cyclin D pathway. Mitogenic factors, estrogen signaling, or oncogenes can promote the expression of Cyclin D in quiescent cells, promoting their re-entry into the cell cycle (95). This is often associated with amplification of CDK4/6 genes, as well as decreases in the CDK4/6 inhibitor p16 and the downstream CDK4/6/Cyclin D

target; Retinoblastoma protein (RB). All of these changes result in an increase in E2F-mediated transcription of S-phase promoting genes, ultimately promoting proliferation. Several drugs have been developed to target this pathway, including the CDK4/6 inhibitors palbociclib, abemaciclib and ribociclib (96–98).

Cancers commonly have misregulated or weakened cell cycle checkpoints, and will not arrest properly in response to stress such as DNA damage. One clear misregulation of the DNA damage response pathway includes the mutation or loss of p53. p53 is a key player in promoting cell cycle arrest in response to DNA damage, which is the most commonly mutated gene among cancers. For example, p53 is mutated in >90% of triple negative breast cancer (99). Drugs currently in clinical trials include inhibitors of the ubiquitin E3 ligase MDM2, such as idasanutlin, that allow p53 accumulation and activation, which induces cell cycle arrest and/or apoptosis (100, 101) (clinical trials.gov, Dec 2017). The Wee1 inhibitor MK1775 is also currently in clinical trials for treatment of p53 deficient cancers, in which it is shown to improve efficacy of DNA damaging agents (102) (clinicaltrials.gov, Dec 2017). Finally, ATR and Chk1 inhibitors have been developed and are being tested in combination with DNA damaging agents, preventing DNA damage checkpoint-induced cell cycle arrest (103–105) (clinicaltrials.gov, Dec 2017).

Mitosis is a tightly controlled series of events that results in segregation of chromosomes equally into daughter cells. Any failures in this process may result in aneuploidy. Aneuploidy is when a cell contains too many or too few chromosomes, which has serious implications for the resulting daughter cells. Physiologically, cycling aneuploid cells are rare in the body because it typically results in cell death, however many cancer cells are highly aneuploid, and may reach a stable state of

aneuploidy, which in some cases is thought to promote survival (106–108). In recent years, it has been shown that low levels of aneuploidy may promote tumorigenesis (108). In an attempt to cause even higher rates of mis-segregation in cancer cells, with the goal of inducing cell death, mitotic spindle assembly has been targeted by traditional chemotherapeutic agents for years, using spindle poisons. Spindle poisons fall into two categories; 1) microtubule depolymerizing agents or 2) microtubule stabilizing agents (103, 109, 110). While these drugs are commonly used, cells can become resistant to spindle poisons via different mechanisms (111, 112). Cells have a number of checks in place to ensure proper chromosome segregation, including the SAC, and maintenance of spindle stability. Much is known about establishment and maintenance of spindle stability, and it's known that these are processes that are regulated by hundreds of proteins, further research is needed to understand the precise functions of many of those proteins, or how they may promote resistance, or sensitivity to spindle poisons.

The ubiquitin system has also been a target of cancer therapeutics. Bortezomib (PS-341), the reversible proteasome inhibitor, has been approved for treatment of multiple cancers, having been shown to increase the cytotoxic effects of both radiation and chemotherapy (113–118). The NEDD8-activating enzyme inhibitor MLN4924 (or pevonedistat), which inhibits function of CRLs, is currently under clinical trials for use in treatment in a number of cancer types (119) (clinicaltrials.gov, Dec 2017). More specific E3 ligase targeted drugs have also been developed, including CC-220, which specifically targets cerablon (120) (clinicaltrials.gov, Dec 2017). Cerablon is a substrate adapter for the CUL4 based

E3 ubiquitin ligase complex, and treatment with CC-220 promotes E3 ligase activity, leading to increased degradation of certain substrates (120).

While cell cycle and the ubiquitin system have proven to be useful targets for cancer treatment, there is still much to be learned about how these processes are controlled in normal cells, and how they may be mis-regulated in cancer. Better understanding of how cancers re-wire these key programs could provide the insight needed to develop more effective chemotherapeutic agents. The following research has been performed with the intention of better understanding how the ubiquitin system, particularly through the E3 ubiquitin ligase $SCF^{Cyclin\ F}$, function to promote cell cycle progression.

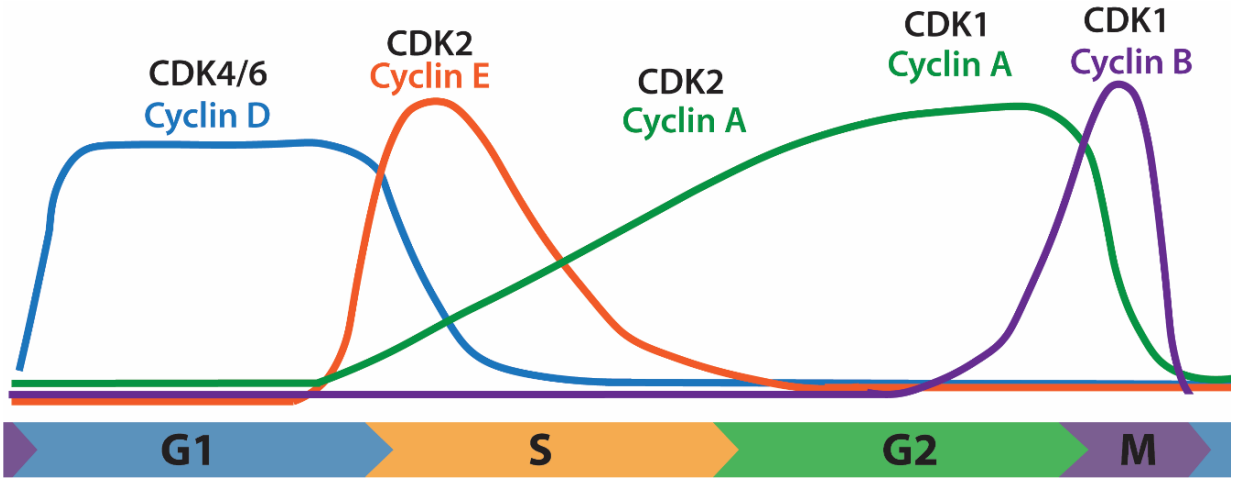

Figure 1.1. Cyclin oscillations through the cell cycle. Each cyclin has precise cell cycle regulated expression, and bind to specific CDKs, forming active kinase complexes that promote cell cycle progression.

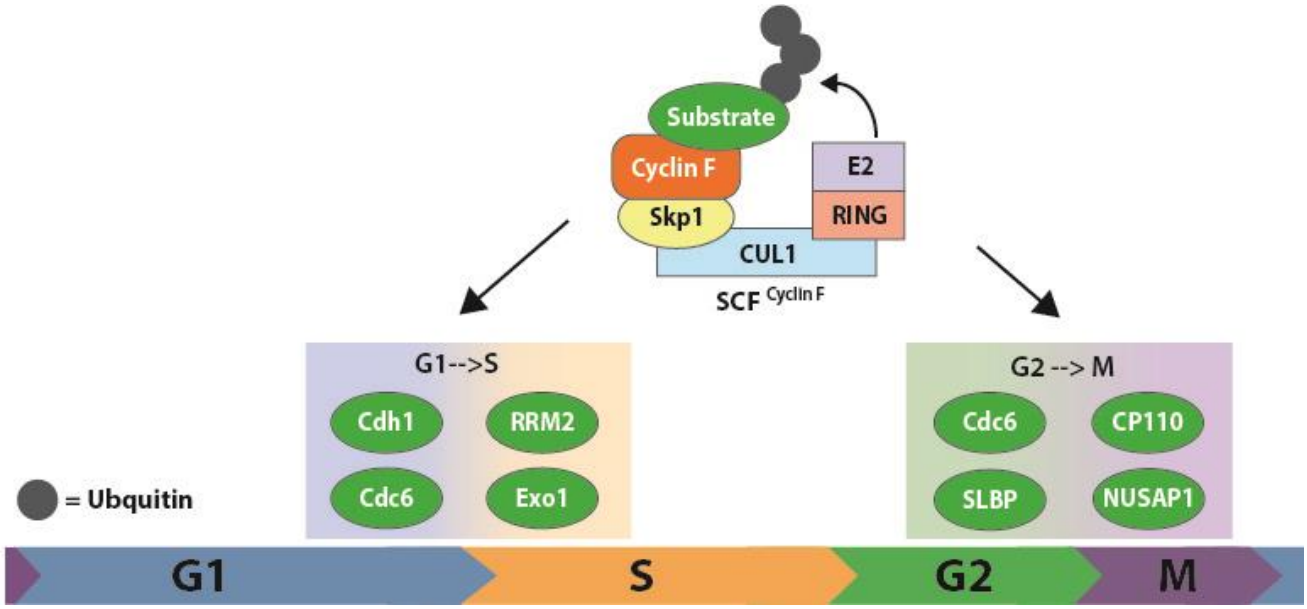

Figure 1.2 Cyclin F and its targets promote cell cycle progression. Cyclin F targets all play key roles in highly regulated cell cycle events. Proper regulation of those events, in part by Cyclin F targeting proteins for degradation, helps ensure proper cell cycle progression.

CHAPTER 2: NUCLEOLAR AND SPINDLE ASSOCIATE PROTEIN 1 (NUSAP1) INTERACTS WITH A SUMO E3 LIGASE COMPLEX DURING CHROMOSOME SEGREGATION[1]

2.1 Introduction

The accurate partitioning of chromosomes during cell division is essential for cell survival and preventing chromosome instability. The movement of chromosomes during mitosis requires the assembly and organization of a bipolar array of microtubules termed the mitotic spindle. Spindle dynamics are controlled by numerous microtubule associated proteins, and the molecular function of many of these remains to be characterized.

Nucleolar and Spindle Associated Protein 1 (NUSAP1) is a mitotic phosphoprotein that binds microtubules and which has been implicated in cell division (91–93, 121–123). NUSAP1 is highly conserved among higher eukaryotes and genetic knockout in mice is embryonic lethal due to chromosome segregation defects (92). NUSAP1 is overexpressed in numerous malignancies, and high levels correlate with poor prognosis in aggressive triple-negative breast cancer (124). A central domain in NUSAP1 directly interacts with microtubules in vitro and in vivo, and its association with the mitotic spindle is controlled by phosphorylation (91,

[1] This chapter previously appeared as an article in the *Journal of Biological Chemistry*. The original citation is as follows: Mills, C. A., Suzuki, A., Arceci, A., Mo, J.Y., Duncan, A., Salmon, E. D., and Emanuele, M.J. (2017) "Nucleolar and Spindle Associated Protein 1 (NUSAP1) interacts with a SUMO E3 ligase complex during chromosome segregation." *JBC* 292(42): 17178-17189.

121, 123). NUSAP1 and has been implicated in mitotic progression, spindle formation and stability (91, 93, 121). In addition, NUSAP1 depletion sensitized a variety of cell types to the chemotherapeutic agent taxol, consistent with its role in spindle formation and stability (82, 125). Furthermore, studies in frog egg extracts have suggested a potential role for NUSAP1 in tethering microtubules to chromatin in a kinetochore independent manner (121).

Mass spectrometry based analysis of spindle associated factors demonstrated that NUSAP1 is among a small group of proteins, that includes PRC1/Ase1 and KIF4, whose binding to microtubules increases after anaphase compared to earlier stages of mitosis (126). Consistent with this observation, NUSAP1 phosphorylation by CDK1/Cyclin B, which is active in early mitosis, displaces it from microtubules (123). Together, these studies point to a crucial role for NUSAP1 is regulating both early and late mitotic events. Importantly, they strongly suggest that there exists a pool of microtubule-free NUSAP1 in early mitosis that could contribute to its function during cell division.

We previously identified NUSAP1 as a substrate for a cell cycle regulated, SCF-type E3 ubiquitin ligase during S/G2 phase (82). NUSAP1 is also targeted for degradation during late mitosis and in early G1 by a second E3 ligase, the Anaphase Promoting Complex/Cyclosome (APC/C) (127). In addition to its regulation by ubiquitin, NUSAP1 was also recovered in large-scale cell cycle phospho-proteomic studies (128, 129). However, the role of NUSAP1 in mitosis remains largely unknown, as does the network of proteins to which it binds during cell division. To gain mechanistic insights into how NUSAP1 regulates cell division, we applied mass spectrometry based proteomics to identify endogenous NUSAP1

interacting proteins. This analysis identified a cell cycle regulated interaction between NUSAP1 and a SUMO (small ubiquitin like modifier) E3 ligase complex.

SUMO is an ubiquitin related protein that is post-translationally appended to substrates, contributing to various aspects of signaling. SUMOylation has been linked transcriptional activation, protein stability, and regulating protein-protein interactions (130, 131). The first described SUMO E3 ligase is composed of three proteins; Ran Binding Protein 2 (RanBP2), Ran GTPase Activating Protein 1 (RanGAP1) and the SUMO E2 conjugating enzyme, UBC9 (69, 132, 133). During interphase, this complex is part of the nuclear pore where it functions in Ran mediated nuclear import and export (134, 135). However, following nuclear envelope breakdown at mitotic entry, the RanBP2 SUMO E3 ligase dissociates from the nuclear pore complex and SUMOylates proteins important for chromosome segregation (132, 136–138). The DNA decatenating enzyme TOP2A is SUMOylated at the metaphase to anaphase transition by the RanBP2 E3; SUMOylation directs TOP2A localization to centromeres, where it functions in sister chromatid disjunction (137). Failure to SUMOylate TOP2A during mitosis has been linked to severe chromosome mis-segregation (137–139). Another RanBP2 SUMO E3 ligase target is Borealin, a member of the Chromosome Passenger Complex (CPC), whose functions are critical to kinetochore-microtubule attachment and chromosome segregation (136, 138). The CPC is composed of Borealin, Survivin, INCENP and Aurora B, and SUMOylation of CPC complex members is highly conserved (140). SUMOylation of the cell cycle transcription factor FoxM1 during G2/M regulates its activity (131, 141). Finally, the kinetochore associated microtubule motor CENP-E is SUMOylated, contributing to its kinetochore localization and function (142).

The most well characterized SUMO ligases described to date are the PIAS family of SUMO E3s. PIAS proteins are a family of conserved SUMO ligases involved in various aspects of cellular physiology, including cell cycle control. PIAS proteins contain an amino-terminal SAP (SAF-A/B, Acinus and PIAS) domain that has been implicated in both enzyme activation and substrate targeting (143). Despite the significant size of the RanBP2-RanGAP1-UBC9 complex (RanBP2 has a predicted molecular weight of 358kDa), it lacks a recognizable SAP domain. Notably, NUSAP1 has an obvious SAP domain in its amino terminus and we propose that NUSAP1 could facilitate RanBP2 ligase function through the amino-terminal SAP domain.

2.2 Results

NUSAP1 localizes to dynamic spindle microtubules near chromatin

NUSAP1 is a cell cycle regulated, microtubule binding protein whose expression has been shown previously, by us and others, to oscillate during the cell cycle (82, 91, 144). However, experiments performed to date were done on relatively short time scales after synchronization and release, making it difficult to know if its dynamics were due to the effects of chemical synchronization. To analyze NUSAP1 protein dynamics throughout an entire cell cycle we performed immunoblots on U2OS cells synchronized using nocodazole, isolated by shake-off, and followed for 28 hours after re-plating (Figure 2.1A). NUSAP1 levels are elevated in mitotic cells compared to asynchronous populations, concomitant with an increase in phosphorylated histone H3 (Ser10), a marker of mitosis. NUSAP1 levels decrease abruptly as cells enter G1-phase, consistent with degradation mediated by the APC/C. NUSAP1 levels remain low through early S-phase, when Cyclin E is expressed and Cdh1 is degraded, and then begin to accumulate after the

expression of Cyclin A, which marks the beginning of S-phase. NUSAP1 is also targeted by another E3 ligase, the $SCF^{Cyclin\ F}$, during S/G2 (82). Interestingly, abundance of the APC/C co-activator Cdc20, Cyclin F, and NUSAP1 are all abruptly diminished at mitotic exit, consistent with their coordinated degradation by APC/C and it other co-activator, Cdh1 (Figure 2.1A and Figure 2.2) (79).

We used high-resolution immunofluorescent (IF) imaging to interrogate the localization of NUSAP1 during mitosis, when its protein levels are at their highest. The specificity of the NUSAP1 antibody was confirmed by comparing anti-NUSAP1 stained cells treated with either control siRNA targeting firefly luciferase (FF) or oligonucleotides targeting NUSAP1. RNAi depletion of NUSAP1 completely eliminated staining, confirming antibody specificity for IF. In prometaphase, NUSAP1 staining was diffuse and localization to specific mitotic structures was not apparent (Figure 2.3). Later in mitosis NUSAP1 did not localize to the whole of the mitotic spindle, like the majority of known microtubule binding proteins in mitosis (Figure 2.1B). Instead, it localizes to the central spindle with the most concentrated area of NUSAP1 being near the chromatin (Figure 2.1B). Highly concentrated NUSAP1 staining in the vicinity of chromatin was visible during metaphase, anaphase and telophase, with the bulk of NUSAP1 appearing to localize to the spindles around chromatin. NUSAP1 localization is coincident with regions of anti-parallel, overlapping microtubules in the central spindle. Notably, this chromatin-centric spindle localization is highly unique among known microtubule binding proteins in mitosis. Interestingly, it is comparable, although not identical, to PRC1 and KIF4, which also show increased microtubule binding after anaphase and control anti-parallel microtubule assemblies in the central spindle (126, 145–147).

This suggests that NUSAP1 represents a unique class of microtubule binding protein that localize in the vicinity of inter-digitated microtubules and that tracks chromatin localization in both early and late mitosis.

The localization of a pool of NUSAP1 on spindle microtubules near chromatin prompted us to determine if NUSAP1 localization is microtubule dependent. Prior to fixation, cells were treated with either DMSO (control) or the microtubule depolymerizing drug nocodazole. NUSAP1 localization is lost when the spindle is depolymerized by nocodazole treatment, confirming that its localization it microtubule dependent (Figure 2.1C). To determine which population of microtubules NUSAP1 localizes to, we depolymerized dynamic spindle microtubules prior to fixation (Figure 2.1C). Cells were cold treated prior to fixation, which leads to the destabilization of microtubules that are not stably attached to kinetochores (k-fibers). NUSAP1 localization to the spindle was lost when non-kinetochore microtubules were depolymerized, suggesting that NUSAP1 localizes to dynamic microtubules during mitosis (Figure 2.1C). This observation, and the diffuse NUSAP1 staining in prometaphase cells, is consistent with the notion that NUSAP1 binds to overlapping spindle microtubules. Finally, we analyzed single focal planes of NUSAP1 and tubulin staining by confocal microscopy. We observed NUSAP1 localization along microtubules, but not at the centromere, centrosome or kinetochore (Figure 2.1D). Together, these data confirm that NUSAP1 is cell cycle regulated, and demonstrate its chromatin-centric localization to dynamic microtubules during mitosis.

Identification of NUSAP1 interacting proteins using mass spectrometry

NUSAP1 has a unique mitotic localization pattern compared to known microtubule binding proteins (Figure 2.1). Since NUSAP1 has been implicated in spindle stability and chromosome segregation we were interested in the mechanism by which NUSAP1 contributes to mitotic progression. To address this question, we analyzed protein interaction partners that bind NUSAP1 using endogenous NUSAP1 immunoprecipitation (IP) followed by protein identification using mass spectrometry (MS/MS). We performed IP experiments using control IgG and endogenous NUSAP1 antibodies in multiple cell lines (HeLa and HEK-293T). In addition, since NUSAP1 levels peak during mitosis (Figure 2.1A) we also performed IPs from both asynchronous and mitotic HEK-293T cells arrested using nocodazole. By performing endogenous IPs in multiple cell lines and physiological conditions we sought to identify the strongest interactors that are most likely to be physiologically relevant in controlling mitotic progression.

We filtered out non-specific interactions identified in control IgG IPs, which were performed in parallel with each experiment, and removed known contaminants based on the CRAPome dataset (148). We then overlapped the remaining interactions between the three IPs to identify the highest-confidence set of NUSAP1 interacting proteins (Figure 2.4A). This resulting list of 14 proteins included the known NUSAP1 interacting protein Importin-β (93).

This analysis identified all three members of the RanBP2 mitotic SUMO E3 ligase complex, which includes RanBP2, RanGAP1 and the SUMO E2 conjugating enzyme UBC9. We identified multiple RanBP2 and RanGAP1 peptides in all three experiments. Despite the fact that NUSAP1 is more abundant in mitotic cells, the

IPs were saturating in that we detected a similar number of NUSAP1 TSCs between asynchronous and mitotic 293T samples. This allowed us to compare the relative number of RanBP2, RanGAP1 and Ubc9 TSCs between asynchronous and mitotic experiments. Our data show an enrichment of all three proteins in the mitotic sample relative to asynchronous cells, indicating that their interaction is cell cycle regulated (Figure 2.4B). Further supporting an interaction between NUSAP1 and RanBP2, their binding was detected in a recent, large scale interactome study using a tagged version of NUSAP1 (93).

To confirm our IP-MS/MS findings we tested whether RanBP2 co-IPed with endogenous NUSAP1 in multiple cell lines. Importantly, isolated endogenous NUSAP1 precipitated from nocodazole arrested U2OS, HeLa, HEK-293T and HCT116 cell lines co-precipitated endogenous RanBP2 (Figure 2.4C). Similarly, when we precipitated endogenous RanBP2 from nocodazole arrested HEK-293T cells we co-precipitated endogenous NUSAP1, as well as its known interactor RanGAP1 (Figure 2.4D). This interaction was also detected in Taxol arrested cells, which prevents microtubule depolymerization, indicating that their interaction is not due to gross changes in microtubule dynamics (Figure 2.5).

To further confirm these findings, we analyzed mitotic HEK-293T cell lysates using size exclusion chromatography to separate proteins and complexes based on their size and shape, followed by endogenous NUSAP1 IP. In this experiment, RanBP2, RanGAP1 and UBC9 co-migrated in a high molecular weight complex (~1 mega-Dalton) (Figure 2.4E, lanes 2-4). There was a small, but detectable amount of NUSAP1 that also co-migrated with those fractions. Importantly, when we precipitated endogenous NUSAP1 from those fractions we co-precipitated both

RanBP2 and RanGAP1 (Figure 2.4F). Together this data strongly supports an interaction between a pool of available NUSAP1 and the RanBP2 SUMO E3 ligase complex.

Interestingly, only a subset of SUMOylated RanGAP1 co-migrated with RanBP2 based on the size exclusion chromatographic analysis. The majority of SUMOylated and unSUMOylated RanGAP1 eluted in fraction of ~500 kDa (Figure 2.4E). This demonstrates that there are RanBP2 bound and unbound pools of RanGAP1 in mitotic 293T cells and contrasts with a recent study suggesting that all of RanBP2 and RanGAP1 are complexed together in HeLa cells (136). The reason for this discrepancy is unknown, but could be cell line dependent. The peak elution of NUSAP1 partially overlapped with the peak elution of RanGAP1 that lacked RanBP2 and IPs from these fractions demonstrate that RanGAP1 and NUSAP1 interact in those fractions (lanes 7-10; Figure 2.4E and F). The full composition of these different NUSAP1 complexes remains unknown.

NUSAP1 does not control RanBP2 localization during mitosis

The RanBP2 complex regulates the SUMOylation of TOP2A and Borealin, both of which have distinct mitotic localization patterns (132, 136–138). In addition, RanBP2 localizes at the kinetochore and on the spindle (149). We hypothesized that NUSAP1 could recruit the RanBP2 SUMO E3 ligase to the spindle. We performed IF; probing for RanBP2 and RanGAP1 localization in control (FF) and NUSAP1 depleted cells. We observed the previously reported RanBP2 and RanGAP1 localization patterns in control depleted cells (150). However, in both U2OS and HeLa cells lines neither RanBP2 nor RanGAP1 localization was affected by NUSAP1 depletion (Figure 2.6A-C, Figure 2.7 and Figure 2.8). Due to previous reports suggesting that

SUMOylation of TOP2 regulates its centromeric localization, we also analyzed the localization of TOP2A and TOP2B on chromatin in control and NUSAP1 depleted cells using biochemical fractionation. Similarly, we observed no change in the localization of TOP2 on chromatin in control and NUSAP1 depleted cells (Figure 2.6D). We conclude that NUSAP1 is not involved in the localization of RanBP2 and RanGAP1, nor that of the RanBP2-RanGAP1-UBC9 SUMO substrate TOP2.

Since our IF staining was unable to distinguish clear co-localization of NUSAP1 with RanBP2 or RanGAP1 and there are soluble pools of NUSAP1, RanBP2 and RanGAP1 during mitosis, we determined where these proteins interact using a proximity ligation assay (PLA; Figure 2.9). PLA relies on the proximity of co-localizing antibodies during immune staining of fixed cells, which allows for the rolling circle amplification of a DNA probe that is detected using fluorescence hybridization. The result is a fluorescent foci at each site of interaction between the target proteins (151). Performing PLA in asynchronous cells with either NUSAP1 or RanGAP1 antibody alone produced a low background (Figure 2.9A), quantified in Figure 4B. Co-staining RanBP2 and RanGAP1 served as a positive control since they interact in both interphase and mitotic cells. Co-staining with NUSAP1 and RanGAP1 antibodies showed a strong increase in the number of foci in the cytosol of mitotic cells (Figure 2.9A and B). Intriguingly, the mitotic cells with the lowest number of foci in the NUSAP1 and RanGAP1 stained samples were in the late stages of mitosis (telophase and after; identified by red triangles). This suggests that the interaction between NUSAP1 and the RanBP2 E3 ligase complex decreases in late mitosis as the cells begin to rebuild their nuclear membranes/pores. Consistent with expression of NUSAP1 late in the cell cycle, and a cell cycle dependent interaction

between NUSAP1 and RanBP2-RanGAP1, the PLA signal was unchanged between single-antibody stained controls (NUSAP1 and RanGAP1 only) and dual-antibody (combined NUSAP1/RanGAP1) stained interphase cells. This supports the observation that NUSAP1 interacts with RanBP2-RanGAP1 in a cell cycle dependent manner, and suggest that NUSAP1 binds RanBP2-RanGAP1 independent of the mitotic spindle, consistent with the binding observed in nocodazole treated cells.

RanBP2 depletion impairs the response to taxol

Previous reports have shown that NUSAP1 depletion sensitizes cells to spindle poisons, such as taxol or nocodazole (82). To determine if RanBP2 depletion would show a consistent phenotype, we depleted cells of RanBP2 using siRNA and treated them with increasing doses of taxol overnight. RanBP2 was effectively depleted by siRNA based on immunoblot analysis (Figure 2.10B). Propidium iodide staining for DNA content in control depleted cells shows a progressive increase in G2/M phase cells in response to taxol, indicating an increased number of cells arresting in response to spindle checkpoint activation (Figure 2.10A). RanBP2 depleted cells had substantially reduced numbers of cells in G2/M phase at all doses of taxol tested, consistent with a defect in maintaining their mitotic arrest in response to checkpoint activation. Consistent with a slippage through mitosis, there was also a reduction in Cyclin B levels in RanBP2 depleted cells compared to controls. At higher doses of taxol the number of surviving cells at time of harvest was also reduced. These data are consistent with our previous studies showing that NUSAP1 depleted cells are sensitive to spindle poisons that activate the spindle checkpoint (82).

2.3 Discussion

NUSAP1 is an important regulator of mitotic progression and chromosome segregation. NUSAP1 is essential for mouse development, and its inactivation by RNAi leads to defects in chromosome segregation (92). The NUSAP1 protein is tightly controlled post-translationally during the cell cycle. Its stability is controlled by at least two E3 ubiquitin ligases: SCFCyclin F during S/G2 phase and by APC/C in G1 (82, 127). Furthermore, NUSAP1 phosphorylation is upregulated during cell cycle progression on upwards of 20 different residues (128, 129). Nevertheless, little is known about where NUSAP1 fits mechanistically in the mitotic spindle apparatus.

We used confocal imaging to determine the precise localization of NUSAP1 on the mitotic spindle, providing a high-resolution snap-shot of NUSAP1 localization at each stage of mitosis. Interestingly, NUSAP1 exhibits a prominent, chromatin-centric localization pattern during metaphase and anaphase that is unique among microtubule binding proteins. We demonstrate here that NUSAP1 is localized on microtubules, and that its localization is dependent on dynamic spindle microtubules, indicating a unique role for NUSAP1 in the process of cell division. The localization of NUSAP1 is most consistent with that of overlapping, inter-digitated spindle microtubules. Consistent with this, we see no significant NUSAP1 staining in prometaphase cells where the spindle poles have not yet separated. We are unaware of another microtubule binding protein with a localization that is fully coincident with chromatin during metaphase and anaphase of mitosis. The PRC1 and KIF4 proteins show the most consistent localization with that of NUSAP1 during metaphase, but localize to the spindle mid-zone at anaphase. However, NUSAP1,

PRC1 and KIF4 all showed increased microtubule binding after anaphase, suggesting a potential relationship between these factors in controlling spindle integrity (126).

To further define the role of NUSAP1 we examined endogenous binding partners using mass spectrometry. Through this analysis we identified and validated a cell cycle regulated interaction between NUSAP1 and the RanBP2-RanGAP1-UBC9 SUMO E3 ligase. Their interaction was identified first using endogenous NUSAP1 pulldown followed by mass spectrometry and was validated by co-IP of both endogenous proteins in multiple cell lines. We were surprised not to identify a larger set of overlapping conditions between datasets, and predict that inter-cell lines differences could be explained by variances in the oncogenic repertoire of the different cell types. An interaction between NUSAP1 and RanBP2 was also detected in a large scale study that globally mapped protein-protein interaction networks, providing further validation for their interaction (152). RanBP2-RanGAP1-UBC9 is a critical SUMO ligase involved in cell division. However, little is known about which substrates it targets, how those substrates are recognized, how its activity is regulated, and how its localization is controlled.

PIAS proteins, the most well characterized family of SUMO E3 ligases, all share a SAP domain (SAFA/B, Acinus, PIAS protein domain) at their N-terminus. While the SAP domain of PIAS proteins has been shown to be involved in nuclear import and DNA binding, PIAS protein SAP domains also mediate substrate interactions. For example, PIAS1 interacts with its substrate C/EBP-β via its SAP domain, with deletion of its SAP domain resulting in failure to SUMOylate C/EBP-β (143). Interestingly, none of the RanBP2-associated SUMO ligase components

contain an identifiable SAP domain. NUSAP1, however, has a well conserved SAP domain at its N-terminus, with nearly all of the key, conserved residues found in the PIAS protein SAP domains (Figure 2.11). Like the PIAS proteins and other SAP domain containing proteins, the NUSAP1 SAP domain has been shown to be important for its interactions with DNA, however, this may not be its only function (153). It is unknown how RanBP2 SUMO ligase is activated and how it specifies substrates for SUMOylation. We speculate that NUSAP1 could be a regulatory subunit for the complex, mediating substrate interactions and/or complex activation, similar to the role of substrate adapters in cullin E3 ligases. Importantly, depletion of NUSAP1 using multiple siRNA reagents does not interfere with RanBP2-RanGAP1 complex assembly (Figure 2.5B). It is noteworthy that despite being the first discovered SUMO E3, little is known about the enzymology of the intact complex, due in large part to the size of RanBP2 (136, 154).

Despite the prominent localization of NUSAP1 during metaphase and anaphase to microtubules in the vicinity of chromatin, its binding to RanBP2-RanGAP1 is cytoplasmic. Thus, NUSAP1 could contribute to mitotic progression through multiple mechanisms: at the site overlapping microtubules on the mitotic spindle and through interactions with RanBP2 in the cytoplasm.

Recent large-scale studies have sought to identify targets of SUMOylation and have even examined cell cycle dependent changes in SUMOylation. However, NUSAP1 has not been identified in any of these large-scale SUMO substrate screens, suggesting it is not a target for SUMOylation, despite these screens often being conducted using mitotic cells (155–158). While this does not rule out NUSAP1

as a SUMO substrate, we currently lack evidence supporting it as target of SUMOylation and were unable to detect NUSAP1 in SUMO pulldowns.

Little is known about how SUMO E3 ligases interact with, and subsequently SUMOylate their targets and how these interactions are regulated. If NUSAP1 did mediate enzymatic activity of the RanBP2 SUMO E3 ligase, this would provide important insight into the functions of not only the RanBP2 complex, but possibly how other SUMO E3 ligases are regulated as well. Further study of the interaction between NUSAP1 and the RanBP2 SUMO E3 ligase, and possibly the SUMO pathway, could elucidate the mechanisms involved in the regulation of other SUMO E3 ligases.

2.4 Materials and Methods

Mammalian cell culture

HEK-293T, U2OS, HCT116 and HeLa cells were grown in Dulbecco's Modified Eagle's Medium (DMEM; Gibco) supplemented with 10% FBS (Atlanta Biologicals) and Pen/Strep (Gibco). For live cell imaging, cells were imaged in Fluorobrite DMEM (Gibco) + 10% FBS. Nocodazole (Sigma 487928) was used at 150 ng/mL for U2OS and 200 ng/mL for 293T. All siRNA transfections were performed using Lipofectamine RNAiMax (Thermo) following manufacturers protocol. Control, non-specific siRNA targeted firefly luciferase (siFF). Three different siRNAs against NUSAP1 were used, each at a concentration of 20nM. The siRNA oligonucleotide sequences used in this study are detailed in Table 2.1.

Immunoblotting and immunoprecipitations

Samples analyzed by immunoblot were lysed in NETN (20mM Tris-Cl, pH 8.0, 100mM NaCl, 0.5mM EDTA, 0.5% Nonidet P-40 (NP-40)) supplemented with 1ug/mL apoprotinin, 1ug/mL pepstatin, 10ug/mL leupeptin, 1mM Na3VO4, 1mM NaF and 1mM AEBSF (4-[2Aminoethyl] benzenesulfonyl fluoride). Protein concentration was estimated using the Bradford assay (Bio-Rad). Laemmli buffer was added to samples, which were then separated by SDS-PAGE gel electrophoresis using home-made or commercially available gels (Bio-Rad). Gels were transferred to nitrocellulose membranes and blotted using standard immunoblotting procedures.

NUSAP1 interacting proteins were identified using endogenous immunoprecipitation followed by tandem mass spectrometry. The mass spectrometry analysis was carried out by the UNC Hooker Proteomics Facility (described below). As a source of starting material, we used asynchronous HEK-293T and HeLa cells, or HEK-293T cells that were arrested in mitosis by overnight incubation in nocodazole. Whole cell extracts (WCE) were prepared on ice in the aforementioned NETN lysis buffer. Protein A/G agarose beads were covalently coupled to control IgG or anti-NUSAP1 antibodies using dimethyl pimelimidate (74). WCE was clarified by centrifugation at 14,000 rpm for 10 minutes at 4°C in a benchtop centrifuge. Clarified lysates were mixed with antibody coated beads on a rotary mixer for 4 hours at 4°C. Samples were quickly washed three times with lysis buffer, eluted using 100mM Glycine, pH 2.5 and neutralized with Tris buffer (pH7.5). Elutions were then digested with trypsin and analyzed by mass spectrometry (see below for details).

For the co-IP experiments in Figure 2, cells were lysed in hypotonic lysis buffer (10mM HEPES, pH 7.9, 10mM KCl, 1.5mM MgCl2, 0.5mM DTT), supplemented with 1ug/mL apoprotinin, 1ug/mL pepstatin, 10ug/mL leupeptin, 1mM Na3VO4, 1mM NaF and 1mM AEBSF (4-[2Aminoethyl] benzenesulfonyl fluoride). Protein A/G DynaBeads (Thermo) were bound to control rabbit IgG, NUSAP1 or RanBP2 antibodies overnight at 4°C. Samples were incubated with beads for 4 hours at 4°C, which were subsequently washed three times in lysis buffer and eluted with 2X Laemmli sample buffer at 95°C for 10 minutes.

Immunological reagents

Commercially available antibodies used in this study, including their use (immunoblotting, immunofluorescence, etc.), catalog numbers and specific dilutions are included in Table 2.2.

An antibody against RanBP2 was generated in-house for these studies. The DNA sequence encoding amino acids 1000-1200 was cloned into the pET28A using traditional PCR amplification to generate an amino-terminally tagged hexahistidine tagged version of the fragment. The cloning was verified by Sanger sequencing and resulting plasmid DNA was introduced into BL21 (DE3) E.coli for recombinant protein production. The expression of the 6HIS-tagged RanBP2 fragment was induced by the addition of IPTG for 22 hours at 18°C. Bacterial pellets that had been frozen and then thawed on wet ice, were diluted in 6HIS purification buffer (20mM Tris pH7.9, 500mM NaCl, 0.5% NP-40, 5mM Imidizole, 0.5mg/ml lysozyme, 0.5mM AEBSF, 1ug/mL apoprotinin, 1ug/mL pepstatin, 10ug/mL leupeptin, 1mM DTT). Cells were sonicated for five minutes and lysates was centrifuged at 15,000 rpm for 30 minutes at 4ºC in a SS-34 fixed angle rotor. Soluble extracts were

incubated in batch with Ni-NTA agarose (Thermo) on a rotary mixer for 90 minutes at 4ºC. Beads washed extensively with 20mM Tris pH7.5, 500mM NaCl, 0.5% NP-40, 30mM Imidizole and then eluted in 20mM Tris pH7.5, 200mM NaCl, 300mM Imidizole. Eluted samples were analyzed by Coomassie blue staining, combined, and tested by Bradford. 6HIS-RanBP21000-1200 was conjugated to KLH and injected into rabbits for antiserum production by Pocono Rabbit Farm & Laboratory (PRF&L, Canadensis, PA). The serum was affinity purified over a column of recombinant protein using described protocols and dialyzed into PBS (159).

For immunoblotting, antibodies were diluted in a solution of 5% nonfat dry milk in phosphate buffered saline, 0.05% tween 20 (PBST). Antibodies were either incubated at room temperature for 2 hours or overnight at 4°C. Detection was performed using HRP conjugated secondary antibodies (Jackson ImmunoResearch Laboratories, Inc; 1:10000), ECL reagent (Pierce), and exposure to film.

Mass Spectrometry analysis

Samples provided in solution were digested using the FASP (Filter assisted sample preparation) protocol. This includes reduction, alkylation, and digested with trypsin. The peptides were extracted, lyophilized, and resuspended in 2% acetonitrile/98% (0.1% formic acid). The peptides were loaded onto a 2 cm long X 360 µm o.d. × 100 µm i.d. microcapillary fused silica precolumn packed with Magic 5 µm C18AQ resin (Michrom Biosciences, Inc.). After sample loading, the precolumn was washed with 95% Solvent A (0.1% formic acid in water) /5% Solvent B (0.1% formic acid in Acetonitrile) for 20 min at a flow rate of 2 uL/min. The pre-column was then connected to a 360 µm o.d. × 75 µm i.d. analytical column packed with 22 cm of 5 µm C18 resin. The peptides were eluted at a flow

rate of 250 nL/min by increasing the percentage of solvent B to 40% with a Nano-Acquity HPLC solvent delivery system (Waters Corp.). The LC system was directly connected through an electrospray ionization source interfaced to an LTQ Orbitrap Velos ion trap mass spectrometer (Thermo Fisher Scientific). The mass spectrometer was controlled by Xcalibur software and operated in the data-dependent mode in which the initial MS scan recorded the mass to charge (m/z) ratios of ions over the range 400–2000. The 10 most abundant ions were automatically selected for subsequent collision-activated dissociation. All files were searched using MASCOT (Matrix Science, Ver. 2.3.02) via Proteome Discoverer (Thermo., Ver. 1.3.0.339) against a recently downloaded human FASTA database. The search parameters included peptide mass tolerance of 10 ppm, fragment ion tolerance of 0.6 mass unit. The search allowed variable modifications for methionine oxidation and carbamidomethylation of Cys.

Gel filtration chromatography

Mitotically arrested 293T cells were analyzed by gel filtration chromatography. Cells were arrested overnight in nocodazole and lysed in hypotonic buffer as described above. The cell extract was clarified via centrifugation followed by filtration through a 0.22 μm syringe filter. Protein complexes in the clarified lysate were then separated using a size exclusion column (Superose 6 10/30, G.E. Healthcare) that had been pre-quilibrated in hypotonic lysis buffer. During separation, 0.4 mL fractions were collected and later analyzed by immunoblot and endogenous NUSAP1 IP.

Chromatin Fractionation

Cells were lysed in CSK buffer (10mM PIPES, pH 7.0, 300mM sucrose, 100mM NaCl, 3mM MgCl2, 0.1% triton X-100) supplemented with 1ug/mL apoprotinin, 1ug/mL pepstatin, 10ug/mL leupeptin, 1mM Na3VO4, 1mM NaF and 1mM AEBSF (4-[2Aminoethyl] benzenesulfonyl fluoride). Protein concentration was determined using Bradford and a portion of the lysate was taken for WCE samples. Samples were then pelleted at 3,000rpm for 5 minutes at 4°C. Supernatant was saved as the soluble fraction (S). Each pellet was washed with CSK buffer on ice and pelleted. The supernatant was removed and the pellet was resuspended in Laemmli buffer diluted in CSK and boiled for 5 minutes before the DNA was sheared using a needle to produce the insoluble fraction (I).

Immunofluorescence Imaging

Cells were plated on poly-L-Lysine coated coverslips approximately one day before fixation. Cells were fixed in PHEM buffer (60mM PIPES, 25mM HEPES, 10mM EGTA, 2mM MgCl2, adjusted to pH 7.0 using KOH) + 3% PFA for 13 minutes at 37°C. Cells were washed with PHEM buffer and permeabilized using PHEM + 0.5% NP-40 for 15 minutes at room temperature. Cells were washed in PBS before blocking in PBS + 5% BSA. All antibodies were subsequently diluted in PBST + 5% BSA. Primary antibodies and their dilutions used: α-NUSAP1 (1:500), α- RanGAP1 (1:100), α-RanBP2 (1:100), α-tubulin (1:200), mouse anti-HEC1 (abcam ab3613; 1:500), guinea pig anti-CENP-C (MBL; 1:1000). Samples were incubated in primary antibody solution for 1h at 37°C. All fluorescent secondary antibodies (anti-mouse Alexa594, anti-rabbit Alexa488, anti-mouse Alexa488, anti-guinea pig Cy5) were diluted 1:200 dilution and incubated for 1h at 37°C. DNA was counter-stained with

1ug/mL Hoechst 33342 for 5 minutes at room temperature. All samples were mounted onto glass slides in ProlongGold media.

The cold stability assay was conducted as detailed in Suzuki et al. Nat Comm 2015 (160). Briefly, cells were treated with ice cold media for 10 minutes before fixation and staining. Proximity Ligation Assay (PLA) was performed using the Sigma Duolink In Situ Red Starter Kit Mouse/Rabbit (DUO92101 Sigma). Cells were plated and fixed as described above. Staining was performed following the DuoLink kit protocol, with primary antibodies against NUSAP1, RanBP2 and RanGAP1 being used at the concentrations described above. Tubulin counterstaining was performed using AlexaFluor488 conjugated α-tubulin at a dilution of 1:100 for 40min at 37°C.

For image acquisition, 3D stacked images were obtained sequentially at 200 nm steps along the z -axis through the cell using MetaMorph 7.8 software (Molecular Devices) and a Nikon Ti inverted microscope equipped with the Orca-ER cooled CCD camera (Nikon) and an 100x/1.4 NA PlanApo objective (Nikon). X, Y, and Z stage movement was controlled by piezo MS2000-500 (ASI). Solid state laser (Andor) illumination at 488, 568, 647 nm were projected through Borealis (Andor) for uniform illumination before a spinning disc confocal head (Yokogawa CSU-10, Perkin Elmer) (161).

Flow Cytometry

Cells were collected and fixed in 70% ethanol. Cells were then washed in 1mL PBS twice, and then resuspended in a solution of PBS containing a final concentration of 25ug/mL propidium iodide (sigma) and 100ug/mL RNase A. Cells were sorted using a Beckman Coulter CyAn ADP. Data was analyzed using FlowJo software.

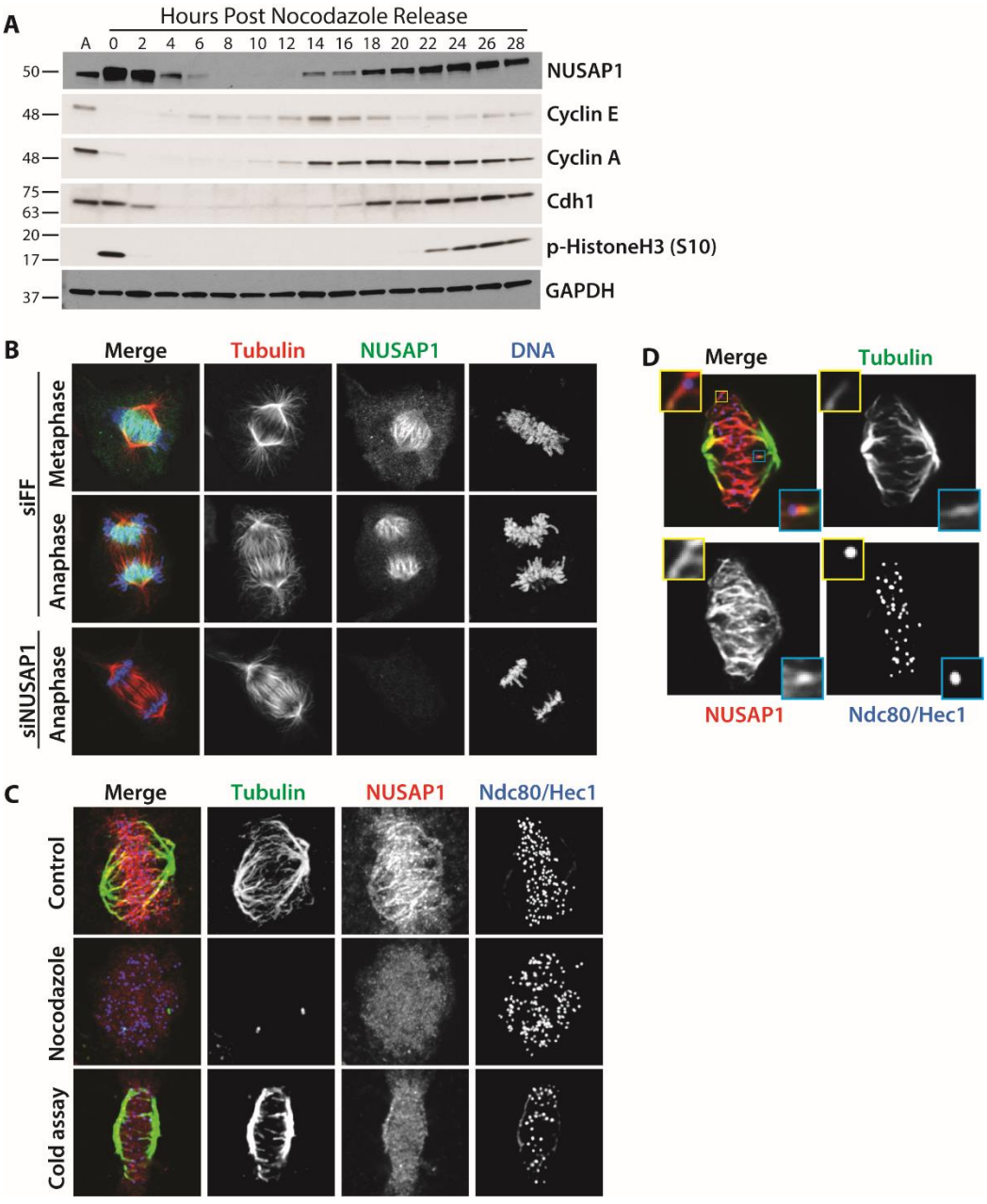

Figure 2.1. NUSAP1 is a cell cycle regulated microtubule binding protein. A) U2OS clls were synchronized by overnight treatment with nocodazole and released by mitotic shake-off. Samples were analyzed by immunoblot as cells progress through the cell cycle. B) NUSAP1 localization to the mitotic spindle analyzing by immunofluorescent imaging of mitosis in U2OS cells. (Scale bars = 10μM.) C) NUSAP1 localization was analyzed in in nocodazole treated cells and following incubation with ice-cold buffer to destabilize non-kinetochore microtubules. (Scale bars indicate 5μM.) D) Single plane confocal imaging of NUSAP1 localization on the spindle during metaphase. Insets highlight two kinetochore-microtubule attachments. (Scale bars indicate 5μM.)

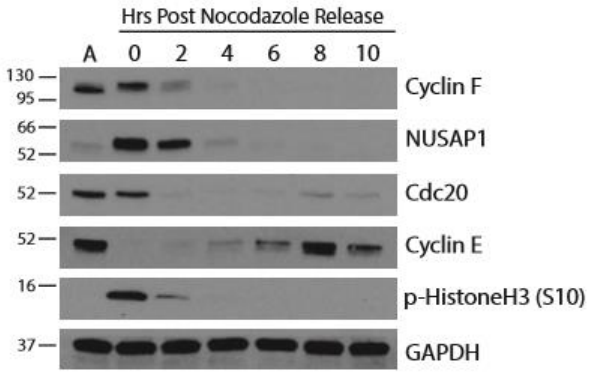

Figure 2.2. NUSAP1 is cell cycle regulated. U2OS Nocodazole release. Cells were arrested in 150ng/mL Nocodazole overnight and released by mitotic shake-off. Time points were taken every 2 hours until 10h.

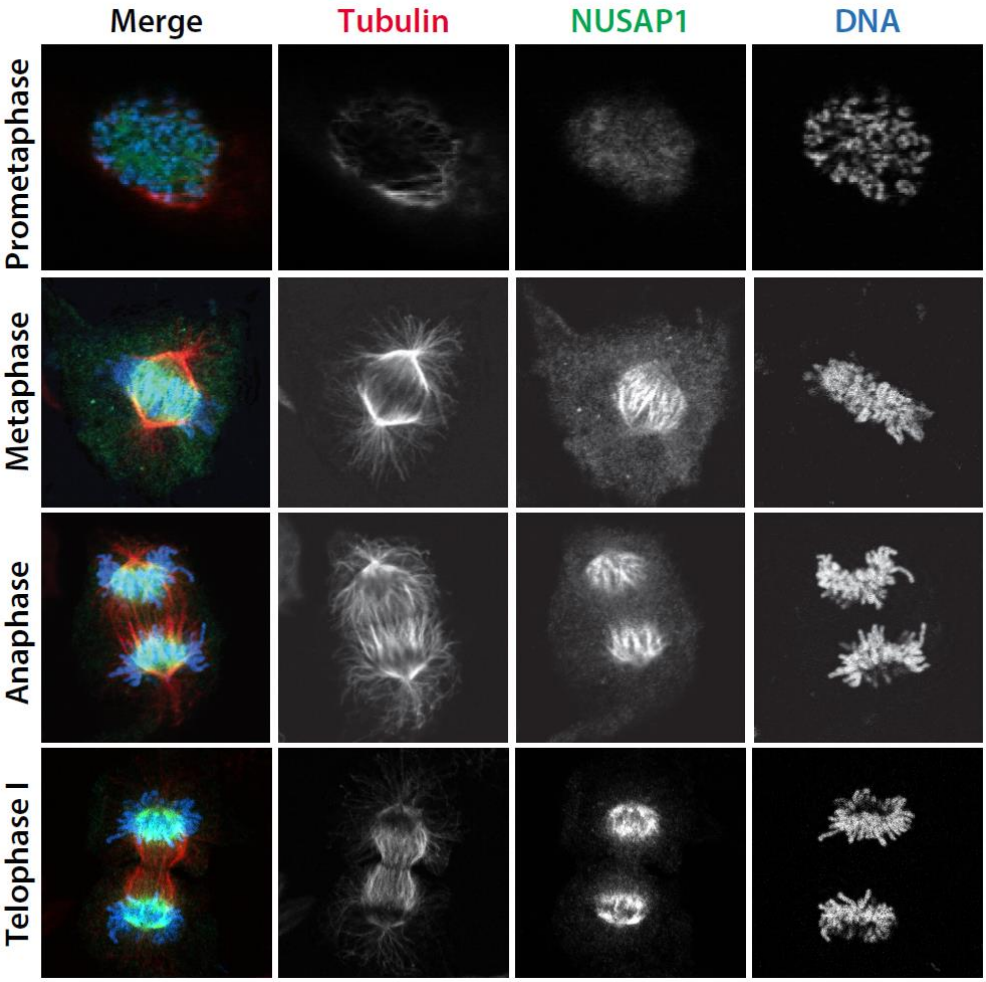

Figure 2.3. NUSAP1 mitotic localization. NUSAP1 localization through mitosis. NUSAP1 localization to the spindle during mitosis in U2OS cells. Metaphase and Anaphase images are replicated from those shown in Figure 1B. Scale bars indicate 10um.

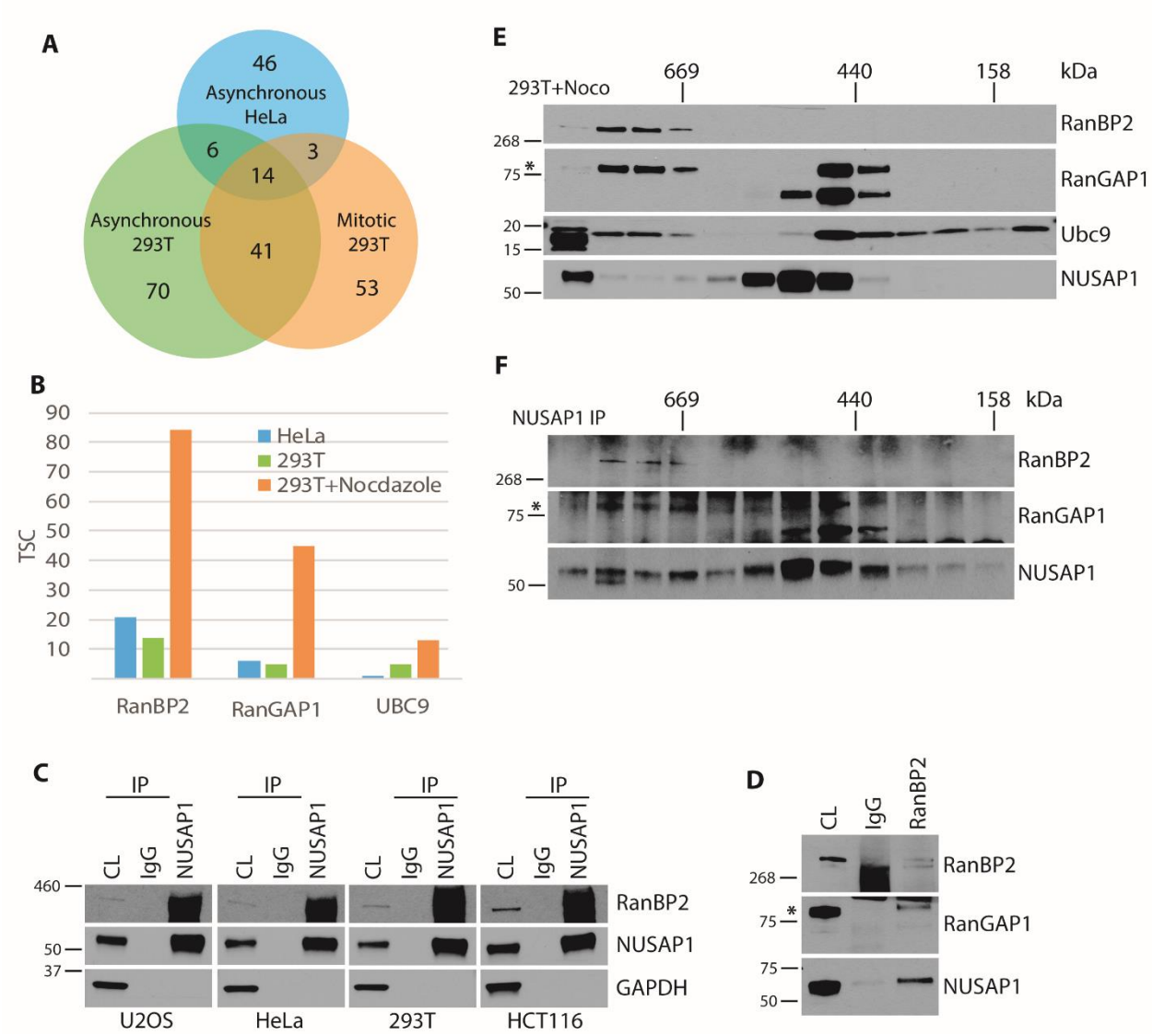

Figure 2.4 NUSAP1 interacts with the RRU in a cell cycle dependent manner. A) Venn diagram showing overlap of IP-MS/MS experiment results. B) Total Spectral Counts (TSC) for each of the RRU complex members determined by mass spectrometry. C) Endogenous NUSAP1 IPs were performed in four different nocodazole arrested cells and analyzed for RanBP2. D) Endogenous RanBP2 IP performed in nocodazole arrested 293T cells. E) Size exclusion chromatography was performed on extracts from nocodazole arrested 293T cells. Extracts were analyzed on a Superose 6 column. Previously tested size markers migrated in the indicated fractions. F) Endogenous NUSAP1 IPs were performed using each of the gel filtration fractions from (E). (*) indicates SUMOylated RanGAP1.

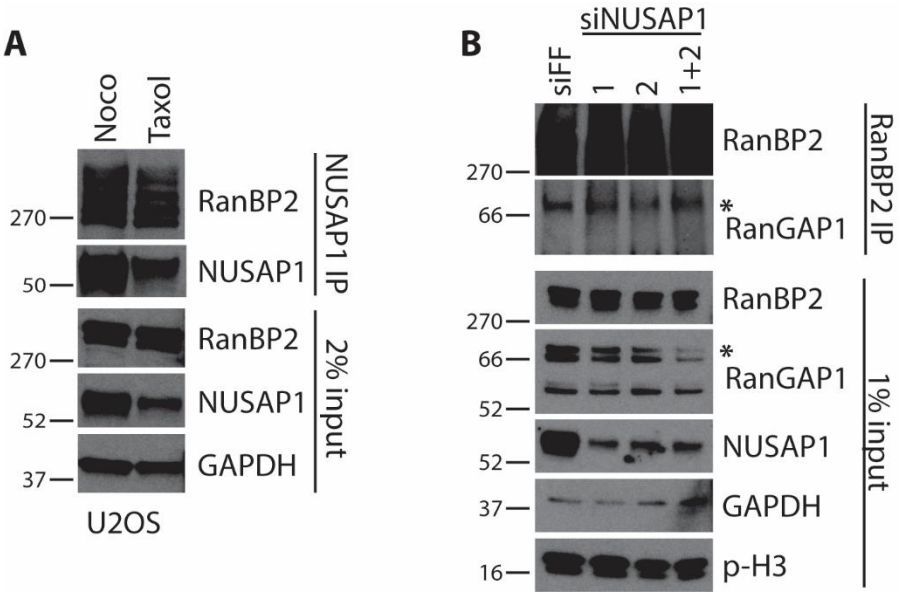

Figure 2.5 RanBP2 co-precipitates with NUSAP1 in both Nocodazole and Taxol arrested cells, and does not influence complex assembly. A) U2OS cells were either arrested using 200ng/mL Nocodazole or 500nM Taxol overnight before collection. Cells were then used for endogenous NUSAP1 IP. B) HEK-293T cells were depleted of NUSAP1 using one of two different siRNAs or a pool of siRNAs. Endogenous RanBP2 IPs were then performed, indicating RanBP2 is still able to associate with SUMOylated RanGAP1 when NUSAP1 is depleted.

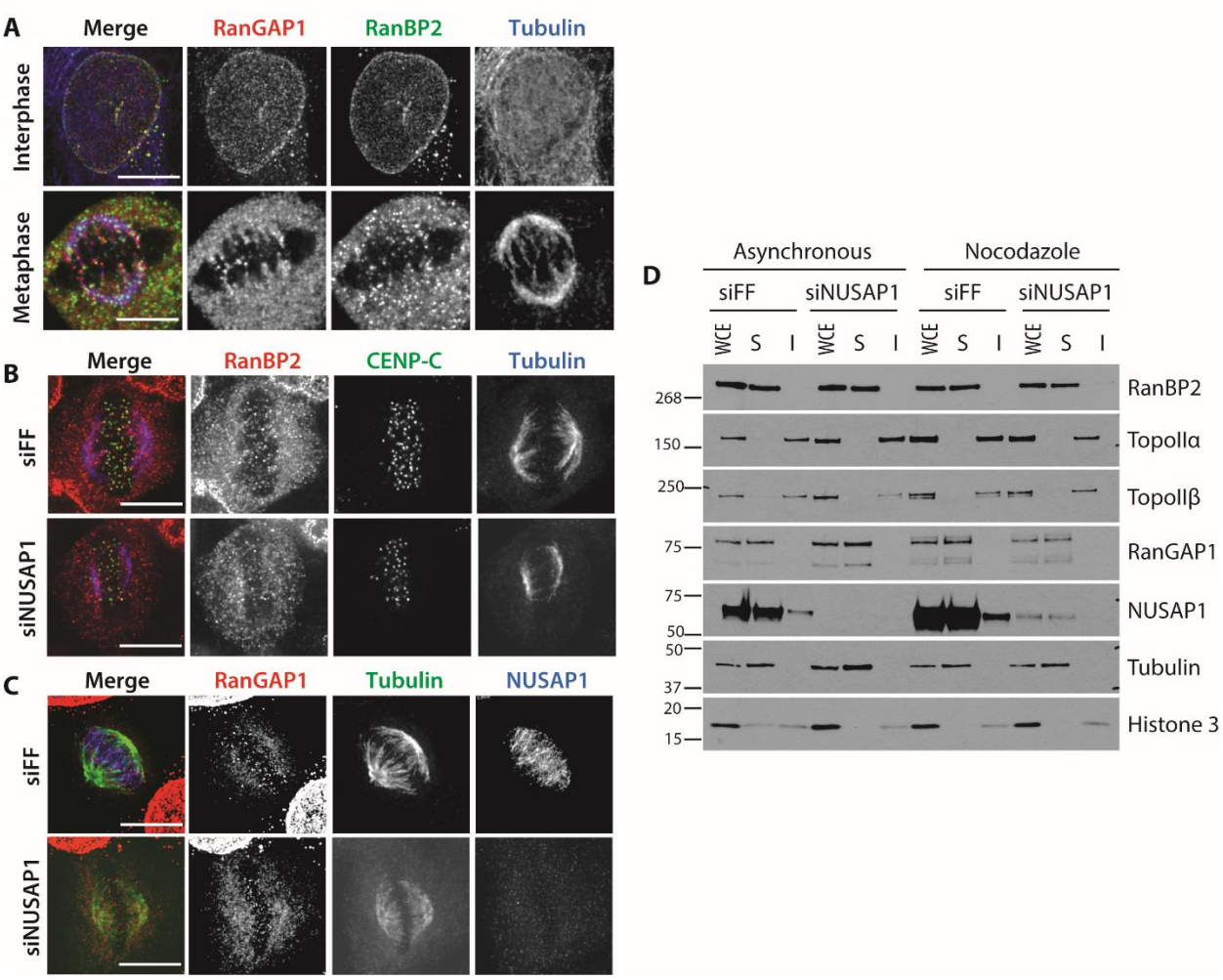

Figure 2.6 NUSAP1 depletion does not affect mitotic localization of the RRU complex. A) Endogenous RanBP2 and RanGAP1 localization in both interphase and metaphase HeLa cells. B) Endogenous RanBP2 localization in either control or NUSAP1 depleted HeLa cells. C) Endogenous RanGAP1 localization in either control or NUSAP1 depleted HeLa cells. D) Chromatin fractionation in U2OS cells. Cells were transfected with either control or NUSAP1 targeting siRNA and split for overnight treatment with either DMSO or nocodazole. (WCE= whole cell lysate; S=soluble (cytoplasmic); I= insoluble (nuclear/chromatin). All scale bars indicate 10μM.)

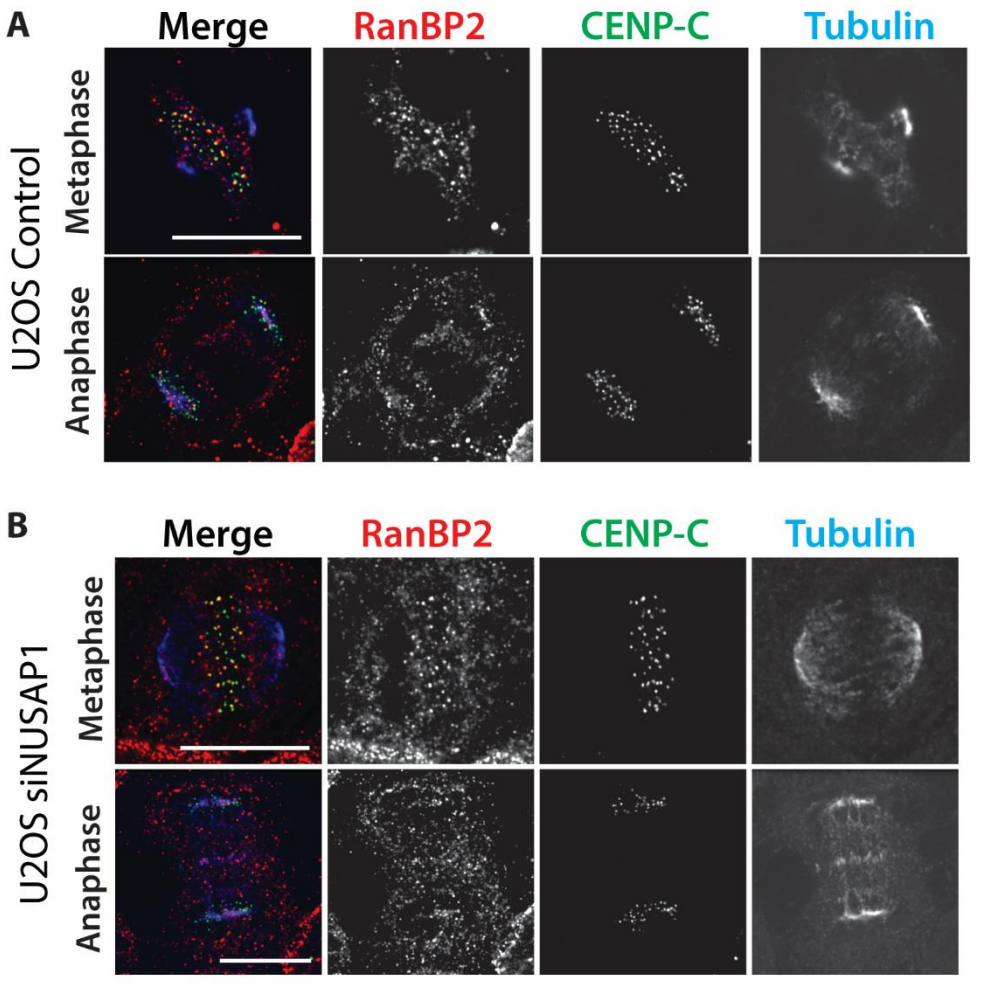

Figure 2.7. NUSAP1 depletion in U2OS cells does not alter RanBP2 localization. Control and NUSAP1 depleted cells were fixed and stained with RanBP2, Tubulin, and CENP-C. (Scale bars indicate 10μM.)

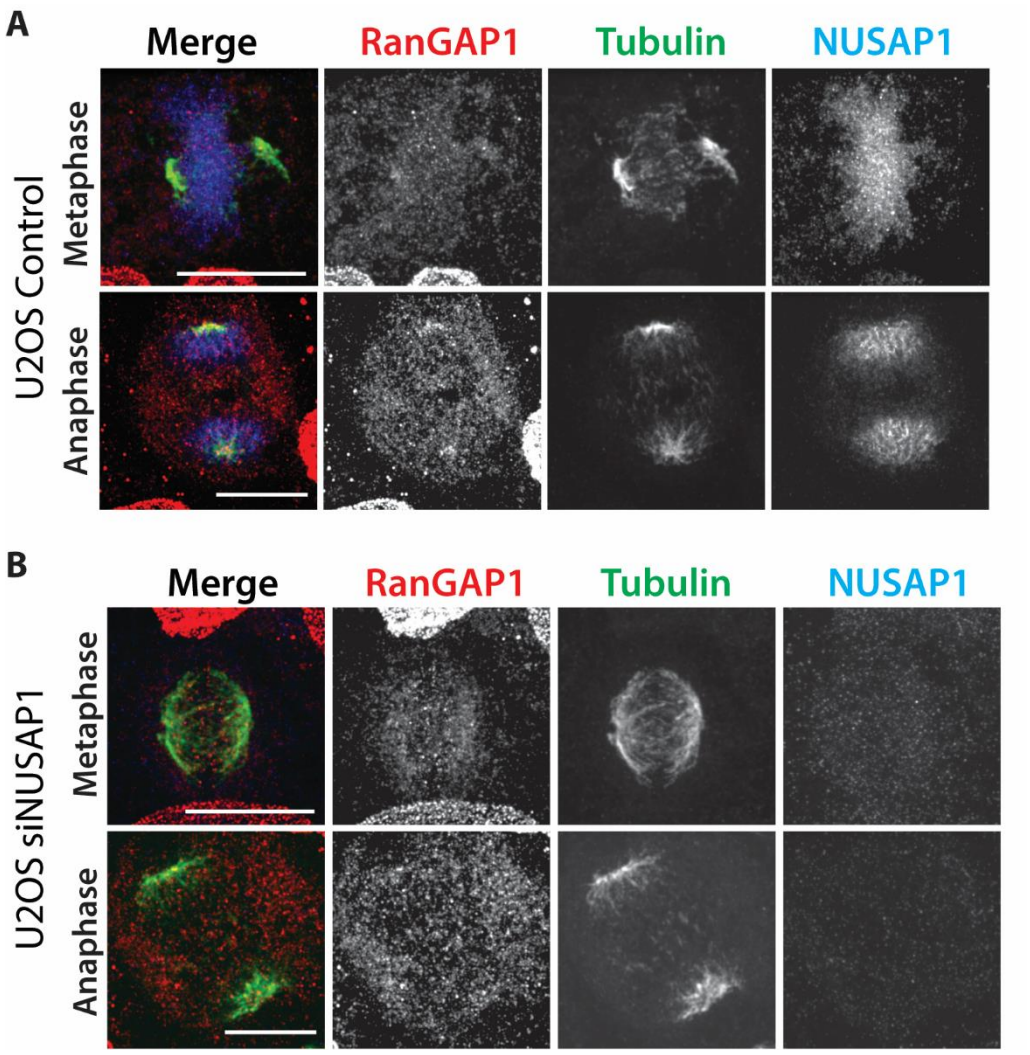

Figure 2.8. NUSAP1 depletion in U2OS cells does not alter RanGAP1 localization. Control and NUSAP1 depleted cells were fixed and stained with RanGAP1, Tubulin and NUSAP1. (Scale bars indicate 10μM.)

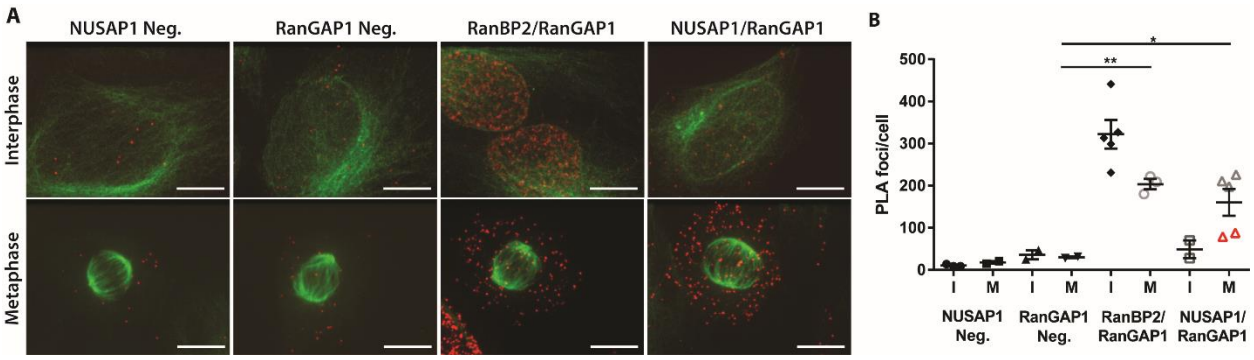

Figure 2.9 NUSAP1 and RanBP2 interact in the cytosol of mitotic cells. A) PLA in U2OS cells using endogenous against NUSAP1, RanGAP1, RanBP2, or control IgG. Tubulin is shown in green with PLA signal in red. (Scale bars indicate 10μM) B) Average number of foci/cell for each PLA condition shown in A. Foci were counted using ImageJ.

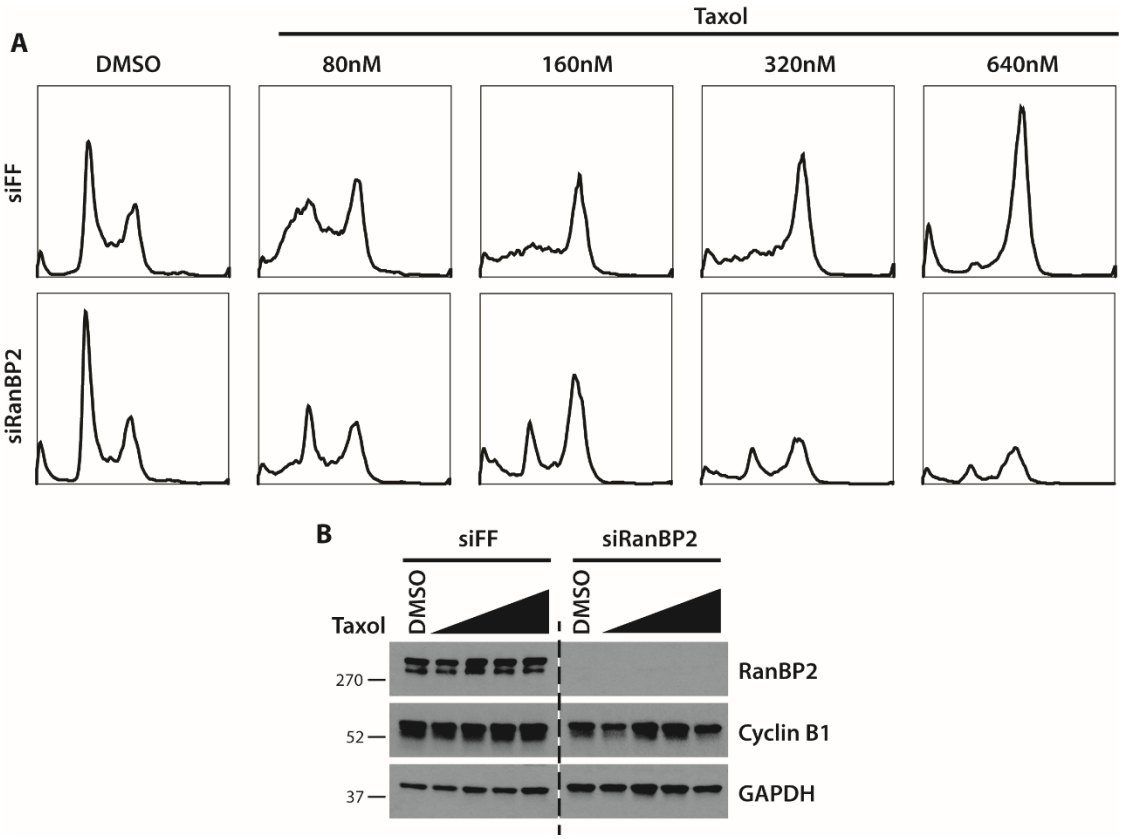

Figure 2.10 RanBP2 knockdown sensitizes cells to taxol treatment. A) U2OS cells were transfected with control of RanBP2 targeting siRNA and then treated overnight with increasing doses of taxol. Cell cycle was analyzed by propidium iodide staining and flow cytometry. B) Immunoblot analysis of cells from (A)

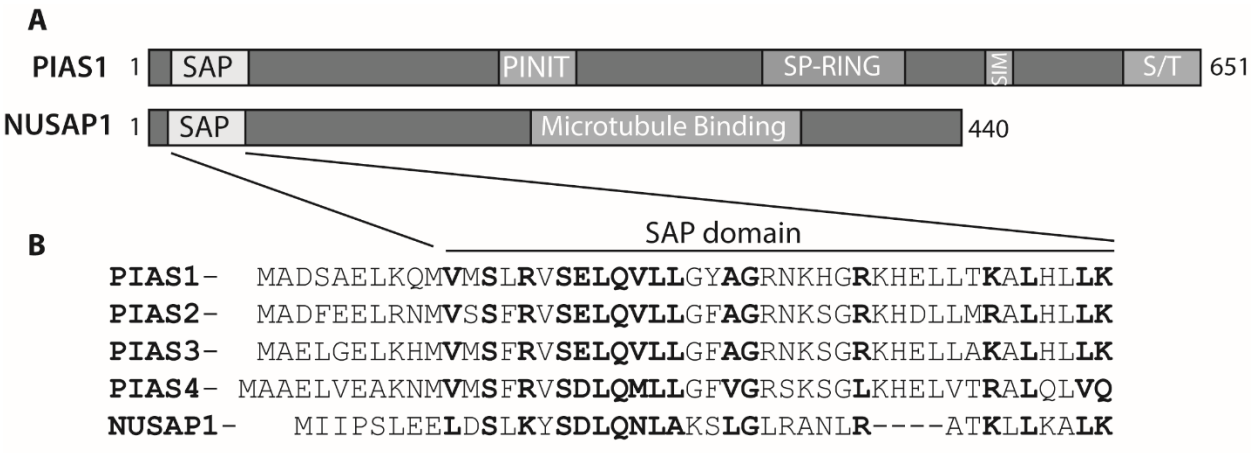

Figure 2.11. NUSAP1 contains a SAP domain in its N-terminus. A) Schematics of NUSAP1 and PIAS1 as a representation of the PIAS family members, which all contain SAP domains approximately 10 AA away from their N-termini. B) Alignment of SAP domains of NUSAP1 and four PIAS protein family members.

Target	siRNA sequence, 5'-3'
Firefly luciferase	CGUACGCGGAAUACUUCGA
NUSAP1 #1	GAUAAUGAGCAUAAGCGUU
NUSAP1 #2	CCACUUUAGUCACGAGAUC
NUSAP1 #3	CAGCCAACGACGCUCGCAA
RanBP2 #1	CGAAACAGCUGUCAAGAAA
RanBP2 #2	GAAAGAAGGUCACUGGGAU
RanBP2 #3	GAAAGGACAUGUAUCACUG
RanBP2 #4	GAAUAACUAUCACAGAAUG

Table 2.1. siRNA oligonucleotides used in Chapter 2.

Target	Company	Catalog number	Dilution
NUSAP1	Proteintech	12024	IB 1:10000; IF 1:500
RanGAP1	abcam	ab119092	IB 1:500; IF 1:100
Ubc9	Santa Cruz	10759	1:1000
Tubulin	Santa Cruz	sc32293	IB 1:1000; IF 1:200
CENP-C	MBL		IF 1:1000
Ndc80/Hec1	abcam	ab3613	IF 1:500
GAPDH	Santa Cruz	sc25778	1:10000
Cyclin E	CST	4129	1:1000
Cyclin A	Santa Cruz	sc751	1:5000
Cdh1 (Fzr1)	abcam	ab3242	1:1000
TopoisomeraseIIα	BDBiosciences	611327	1:2000
TopoisomeraseIIβ	BDBiosciences	611492	1:2000
Cyclin B1	abcam	ab32053	1:10000
Cdc20	Bethyl	A301-107A	1:1000
Cyclin F	Santa Cruz	sc-952	1:2000

Table 2.2. Antibodies used in Chapter 2.

CHAPTER 3: IDENTIFICATION OF A NOVEL SCF$^{CYCLIN\ F}$ TARGET, SIRTUIN 5, LINKING PROLIFERATION AND METABOLIC REGULATION

3.1 Introduction

Precise cell cycle progression is important for maintaining genomic integrity in dividing cells. Cell cycle is highly regulated, in part, by the ubiquitin-proteasome system, which targets proteins for degradation. One Cullin E3 ubiquitin ligase, a modular complex composed of Skp1, CUL1 and F-box protein (SCF) with the substrate adapter Cyclin F, has been identified as an important cell cycle regulator. Most recently, it has been recognized as having an important role in G1-S transition via feedback with the Anaphase Promoting Complex/Cyclosome with its substrate adapter Cdh1 (APC/C^{Cdh1}) during late G1 (79, 80).

Cyclin F is the founding member of the F-box containing family of proteins, most of which act as substrate adapters for the SCF E3 ubiquitin ligase (75–77). As a substrate adapter, Cyclin F recruits substrates to the SCF E3 ubiquitin ligase so that they may be ubiquitinated, which typically results in degradation via the proteasome (76, 77). Cyclin F contains a cyclin homology domain, and is the most highly cell cycle regulated F-box protein with expression during S, G2 and M, and is the only identified F-box protein in all cell cycle trancriptomic profiles performed to date (1, 75, 76). Despite its name, and the presence of a cyclin homology domain, Cyclin F is not a traditional cyclin and does not bind and activate a cyclin dependent kinase (CDK) protein (75, 78).

Identified Cyclin F targets to date include Centriolar coiled-coil protein of 110 kDa (CP110), which is involved in centrosome duplication, an event important for bipolar spindle establishment during mitosis (81, 90). Another substrate of Cyclin F is Nucleolar and Spindle Associated Protein 1 (NUSAP1), a protein implicated in G2-M transition, spindle stability and chromosome segregation (82, 91, 121, 125). Cyclin F also targets ribonucleoside-diphosphate reductase subunit M2 (RRM2), exonuclease 1 (Exo1) and cell-division control protein 6 homolog (cdc6) during S, all of which are important for DNA replication (83–85). RRM2 is important for biosynthesis of deoxyribolnucleotides while Cdc6 is key for DNA replication initiation, and ensuring that the DNA is completely replicated before entering mitosis (86, 87). Exo1, as well as being important for DNA double strand break repair, is important for mismatch repair during DNA replication (88). Targeting of Stem-Loop Binding Protein (SLBP) for degradation by Cyclin F is also important in genotoxic stress response. SLBP promotes translation and accumulation of DNA damage response histones H2A.X and γH2A.X (94). In cycling cells with low genotoxic stress Cyclin F degradation of SLBP helps promote mitotic entry (94). Finally, Cyclin F has been shown to regulate G1-S transition via regulation of another E3 ubiquitin ligase, the APC/C, specifically through regulation of its substrate adapter, Fizzy-related protein homolog Cdh1 (79). During early G1, APC/C^{Cdh1} targets Cyclin F for degradation, however, as Cyclin F protein levels rise, AKT-mediated phosphorylation of Cyclin F promotes its assembly into the SCF, which then targets Cdh1 for degradation (79, 80). This switch is important for promoting the G1-S transition (79, 80).

While a number of Cyclin F substrates have been characterized, using traditional protein-protein interaction, mass spectrometry (MS) based approaches to identify novel Cyclin F substrates has proven challenging. This is, in part, due to the transient nature of F-box-substrate interactions, a feature common to E3 ubiquitin ligase and substrate interactions. Furthermore, the substrate is typically being targeted for degradation, making it difficult to capture. Finally, these experiments are often performed in asynchronous cells, which is problematic because Cyclin F, and many of its substrates, are cell cycle regulated, making it difficult to detect in asynchronous cell extracts. In this report, based on genetic yeast interactions and conservation in the ubiquitin system, we examined whether a human sirtuin could be regulated by Cyclin F.

Here we identify Sirtuin 5 (Sirt5) as a novel $SCF^{Cyclin\ F}$ target important for the G1-S transition. Sirtuins are a class of deacylating enzymes involved in regulating a variety of processes including epigenetic regulation, DNA damage response and metabolism (162, 163). This is the first described role for Sirt5, a mitochondrial sirtuin, in cell cycle control. Sirt5 has specific deacylating activity towards succinyl, malonyl, glutaryl and acetyl post-translational modificiations (PTMs) (164–167). Sirt5 is one of three mitochondrial sirtuins, (Sirtuins 3-5), which are classified by their ability to be imported into the mitochondria, but are not restricted to the mitochondria. Sirt5 also localizes to the cytoplasm and nucleus, however its roles outside of the mitochondria are less clear. Sirt5 is best known for its role in regulating metabolic enzymes, such as carbamoyl phosphate synthase 1 (CPS1), which catalyzes the production of carbamoyl phosphate from ammonia and bicarbonate, which is the first step of the urea cycle (168–170). Sirt5 is also known

to desuccinylate and activate Cu/Zn superoxide disumutase (SOD1), which functions in reactive oxygen species response (171, 172). Sirt5 has been implicated in a number of other metabolic processes as well, including glycolysis, purine metabolism, fatty acid oxidation, as well as the citrate cycle (173). While it is known that Sirt5 is localized to the mitochondria as well as the nucleus and cytoplasm, it has yet to be determined whether it has different activities based on localization.

Here we describe the interaction between Cyclin F and Sirt5, and its impact on the G1-S transition. These data provide a link between cell cycle ubiquitin machinery, and metabolic regulation, a connection of which little has been described.

3.2 Results

Cyclin F was originally identified in a gain-of-function cDNA screen searching for human genes that could rescue the yeast Cdc4 temperature sensitive mutant, which caused G1 arrest and subsequent death (75). Cyclin F was identified as a gene that rescued the G1 arrest phenotype, and based on the fact that it cycled and contained a cyclin homology domain, Cyclin F was classified as a traditional Cyclin (75). However, subsequent studies identified Cyclin F as a substrate adapter for the SCF E3 ubiquitin ligase, and Cdc4 is a yeast F-box substrate adapter (174). Furthermore, Cyclin F can target yeast proteins for degradation, including yeast Cdh1. Knowing this information, we hypothesized that Cyclin F rescued the G1 arrest phenotype in the original Cdc4 mutant screens by targeting a protein for degradation, particularly a protein which prevents S-phase entry. Based on this hypothesis, we interrogated the Data Repository of Yeast Genetic Interactions

(DRYGIN), a database containing data from global synthetic genetic interactions in yeast, for mutants or deletions that also rescue the Cdc4 mutant phenotype as a tool to identify new potential Cyclin F targets (175). To narrow our list down we also compared this to a list of deletions that rescue the Cdc53 mutant G1 arrest phenotype as well (Figure 3.1). Cdc53 is a yeast cullin, which complexes with the F-box protein, Cdc4, to form an E3 ubiquitin ligase. A list of ~40 genes that rescued the G1 arrest and lethality of both the Cdc4 and Cdc53 mutations was identified, which we narrowed down by first eliminating all the genes that had no connection to cell cycle, either directly or through genetic interactions. We then eliminated apc5, orc3 and mcm3 due to their incorporation into large protein complexes with low turnover rates. The yeast specific transcription factor, swi5, was eliminated because no human homologue has been identified. Finally, we chose not to interrogate sli15 because it is a component of the Aurora B complex, which is only active in mitosis. This eliminated all but one gene; hst3, a yeast sirtuin family deacetylase. When we looked at genes with similar genetic interactions to hst3, what we identified was a list of genes important for DNA replication and DNA damage response, indicating a potential role in S-phase entry and progression. Interestingly, hst3 is ubiquitinated by the yeast SCF^{Cdc4} ligase.

Sirtuin 5 stability is increased in the absence of Cyclin F

Since our screen identified a yeast sirtuin as a potential Cyclin F target, we analyzed human sirtuin levels in Cyclin F CRISPR KO HeLa cells, with the expectation that if a sirtuin were a Cyclin F substrate, there would be more sirtuin protein in the Cyclin F KO cells compared to control. Immuno-blotting for human sirtuins in Cyclin F CRISPR KO HeLa cells showed an increase in the mitochondrial

sirtuin, Sirt5 as well as a slight increase in Sirt7 (Figure 3.2A). Elevated Sirt5 protein levels, as well as the known Cyclin F targets Cdh1 and CP110, was observed in both U2OS and 293T cells treated with multiple Cyclin F targeted siRNAs compared to control (firefly luciferase targeted) (Figure 3.2B and C).

To establish whether this elevation in protein level was due to an increase in protein stability, we performed cycloheximide chase in both the control and Cyclin F CRISPR KO HeLa cells (Figure 3.2D). Cycloheximide prevents translation of new protein from mRNA, allowing us to measure half-life of the proteins present at time of treatment. Cells were treated with cycloheximide and samples were collected every two hours, for eight hours, and samples were analyzed via immunoblot. Cycloheximide treatment of control cells showed that both Sirt5 and Sirt7 have a half-life between 3-6 hours, consistent with previously published data for both Sirt5 and Sirt7 (Figure 3.2D) (176, 177). No difference in Sirt7 half-life was observed in Cyclin F CRISPR KO HeLa cells, however a marked increase in the half-life of Sirt5 protein was observed, with the protein becoming so stable the half-life was greater than eight hours (Figure 3.2D). Together, these data show that Sirt5 protein is more stable in the absence of Cyclin F.

Sirtuin 5 interacts with Cyclin F

To determine if Cyclin F and Sirt5 can interact, we performed Myc and Flag immuno-precipitations (IPs) from cells co-expressing a Flag-Sirt5 together with Myc-Cyclin F in 293T cells, in the presence or absence of the proteasome inhibitor Bortezomib. In the Myc-Cyclin F IPs, Flag-Sirt5 signal was detected in the Bortezomib treated sample, indicating an interaction (Figure 3.3A). This was confirmed by the reverse Flag-Sirt5 IP, using the same samples, showing Myc-

Cyclin F co-precipitating in both the co-expressed samples (Figure 3.3A). Furthermore, there was an increase in the amount Myc-Cyclin F protein pulled down in the Bortezomib treated sample compared to co-expression alone (Figure 3.3A). To further confirm this interaction, we transiently expressed a Flag-Cyclin F and HA-Sirt5 in U2OS cells for 48h. The cells were fixed and analyzed by Proximity Ligation Assay (PLA), using primary antibodies against Flag and HA epitopes. PLA allows for fluorescent detection of each site of interaction. In negative controls, which were transfected with empty Flag or HA vectors, or empty vector with either Flag-Cyclin F or HA-Sirt5, no PLA signal (red) was detected (Figure 3.4). In cells co-expressing Flag-Cyclin F and HA-Sirt5, PLA signal was detectable throughout the cell. These data confirm an interaction between Cyclin F and Sirt5, and suggests that it occurs in the cytoplasm of cells (Figure 3.5). This conclusion is supported by mitochondrial fractionation data, which shows Cyclin F is excluded from the mitochondria while Sirt5 is found in both the mitochondria and cytoplasm (data not shown).

$SCF^{Cyclin\ F}$ can ubiquitinate Sirtuin 5

To establish whether Cyclin F could ubiquitinate Sirt5 we performed and *in vivo* ubiquitination assay. For this assay, we express a hexa-HIS-ubiquitin construct in cells, together with our potential substrate and substrate adapter. Ubiquitin is covalently linked to substrates, so the use of HIS-Ubiquitin allows for lysis and subsequent pulldowns under denaturing conditions, to distinguish between ubiquitinated and ubiquitin-interacting proteins. If a protein is ubiquitinated, a higher molecular weight species will appear in the HIS pulldown sample when immuno-blotted. Expression of HA-Sirt5 with HIS-ubiquitin alone did not produce any signal in the HIS pulldown, however, the addition of Myc-Cyclin F resulted in a

multiple banding pattern of HA signal in the HIS pulldown, indicating that Sirt5 is ubiquitinated in the presence of Cyclin F (Figure 3.5). Further experiments, such as *in vitro* ubiquitination assays, are needed to confirm this result.

Sirt5 protein levels influence G1 timing

To date, identified Cyclin F targets have been shown to play key roles in cell cycle progression. However, while Sirt5 has been implicated in a number of metabolic processes, it has no obvious role in cell cycle. To determine whether Sirt5 could play a role in cell cycle progression, particularly G1-S transition, we performed flow cytometry analysis of propidium iodide (PI) stained Sirt5 CRISPR KO 293 cells. Sirt5 CRISPR KO 293 cells exhibit a notable decrease in the G1 population (~20%) compared to control, which is compensated for by an overall increase in S/G2/M (Figure 3.7). When compared to controls, the Sirt5 CRISPR KO cells also had elevated Cyclin A protein levels, a cyclin that is expressed during S/G2/M (Figure 3.7). To confirm that this cell cycle alteration was due to Sirt5 loss, we re-expressed wild type Flag-Sirt5, and the catalytically dead mutant, Flag-Sirt5^{HY}, and performed PI staining and flow analysis. Re-expression of the Flag-Sirt5^{WT} for either 48h or 72h, rescued the cell cycle phenotype, while re-expression of Flag-Sirt5^{HY} rescued to a lesser degree (Figure 3.7). Together, this data indicates that Sirt5 protein levels influence G1-S transition timing.

While a clear redistribution of cell cycle phases occurs in the absence of Sirt5, Sirt5 KO cells appeared to have the same doubling time as control cells. This suggests that Sirt5 CRISPR KO cells spend less time in G1, but more time in S/G2/M. To determine why cells were spending more time in subsequent phases we examined DNA damage pathway activation. If cells exit G1 prematurely, we would

expect these cells would undergo replication stress, and possibly accumulate DNA damage, which would slow S-phase progression. To test this hypothesis, control and Sirt5 CRISPR KO cells were immuno-blotted for phospho-Chk1 (p-Chk1 (S345)), a protein that is phosphorylated by ATR in response to DNA damage. Analysis showed that p-Chk1 was elevated in Sirt5 CRISPR KO cells compared to controls, indicating an activated DNA damage response (Figure 3.8). Further experiments are needed to examine activation of other DNA damage response proteins, and to determine whether this damage is linked to replication stress.

Sirt5 protein levels increase with G0 arrest

Since Sirt5 expression increases the number of cells prior to the start of DNA replication, we analyzed Sirt5 protein levels in proliferating and quiescent cells. We arrested normal human fibroblast (NHF) cells in G0, using either serum depletion or contact inhibition. Interestingly, G0 arrest resulted in an increase in Sirt5 protein, as well as a decrease in Cyclin F protein levels, compared to cycling cells (Figure 3.9A). Furthermore, RPE1 cells grown in varying amounts of serum show a clear correlation between Sirt5 protein level and serum concentration, with more Sirt5 accumulation in cells grown in lower concentrations of serum (Figure 3.9B). This further supports that as cells enter G0 Sirt5 protein levels increase, however, more data is needed to determine whether Sirt5 plays a role in establishing and maintaining G0 arrest.

3.3 Discussion

Cyclin F has proven to be a key regulator of cell cycle progression, even though only a handful of substrates have been identified. Cyclin F regulation of

Cdh1 is important for G1-S transition, while its regulation of CP110 and NUSAP1 is important for G2/M progression.

During G1, both Cyclin F levels and activity, are tightly regulated by both APC/C^{Cdh1} and AKT signaling. This regulation is important for G1-S transition timing, however, only a couple of Cyclin F substrates have been linked to G1 exit/S-phase entry. In an attempt to identify Cyclin F targets that are important in G1-S transition, we utilized the DRYGIN database to identify potential substrates based on conservation of the ubiquitin system in yeast. Ultimately, we identified human Sirt5, a mitochondrial deacylating enzyme, as a potential Cyclin F substrate.

Sirt5 has been linked in numerous ways to metabolic regulation, however, it has not been previously linked to cell cycle regulation. Our data indicate that Sirt5 protein levels influence G1-S transition timing, with Sirt5 depletion resulting in premature G1 exit and extended S/G2/M. This phenotype is common to other key G1-S transition regulators, including Cdh1 depletion or Cyclin E overexpression (178, 179). Importantly, using EdU incorporation assays, it has previously been shown that when Cyclin F protein is depleted, cells spend longer in G1 compared to control cells (79). In addition, Cyclin F null MEFs are slow to enter S after release from serum withdrawal (77). We hypothesize, that along with targeting other substrates, Sirt5 is an important $SCF^{Cyclin\ F}$ target for G1 exit, and Sirt5 levels must dip below a certain threshold for cells to enter S phase (Figure 3.10). Furthermore, maintaining higher Sirt5 levels may be important for maintaining a G0 arrest. This could be linked to metabolic reprogramming that occurs in G0 cells. For instance, the urea cycle, which Sirt5 has been shown to promote, is increased in quiescent cells (180). Future research will focus on whether particular Sirt5 targets, and

possible affected metabolites, are most important for G1-S transition, as well as which pool of Sirt5 is being regulated by Cyclin F (i.e. cytoplasmic vs mitochondrial). As it is possible that Sirt5 regulated metabolites involved in G1-S transition are different from those involved in G0 regulation, experiments will also focus on G0 establishment and maintenance.

Surprisingly, Sirt5 protein levels are increased in some cancer types, including breast cancer and non-small cell lung cancers (NSLCs) (181, 182). It has been shown that increased Sirt5 protein levels in NSLCs may promote resistance to nucleoside analogs such as 5-fluorouracil. 5-fluorouracil is metabolized into an analog of uracil and can be incorporated into mRNA during transcription, which prevents that RNA from being read correctly by ribosomes. Furthermore, it inhibits production of thymidine triphosphate, which is needed for DNA synthesis. Cells with increased Sirt5 protein levels may be more resistant because they are spending more time in G1 or possibly even G0. However, Sirt5 has been implicated in *de novo* DNA synthesis, and it is possible that with increased Sirt5, there is increased nucleotide synthesis, preventing the 5-fluorouracil from being incorporated as much as it would be in Sirt5 low cells. Future experiments are needed to better understand the role of Sirt5 in cancer survival and cell cycle.

Together, our data describe a new Cyclin F target, Sirt5, and support a novel role for Sirt5 in cell cycle progression. This provides a novel link between metabolism and cell cycle progression. Future research is required to better understand which metabolites are being influenced by Sirt5 degradation, and how they promote or inhibit cell cycle.

3.4 Materials and Methods

Mammalian cell culture

HEK-293T, U2OS, RPE-1, NHF and HeLa cells were grown in Dulbecco's Modified Eagle's Medium (DMEM; Gibco) supplemented with 10% FBS (Seradigm, VWR) and Pen/Strep (Gibco). Sirtuin 5 CRISPR KO and control 293 cells, a generous gift from Matthew Hirschey, were grown in DMEM. Nocodazole (Sigma 487928) was used at 150 ng/mL for U2OS and 200 ng/mL for 293T. All siRNA transfections were performed using Lipofectamine RNAiMax (Thermo) following manufacturers protocol. Control, non-specific siRNA targeted firefly luciferase (siFF). Two different siRNAs against Cyclin F were used, each at a concentration of 30nM. The siRNA oligonucleotide sequences used in this study are detailed in Table 3.1. All plasmid transfections were performed using lipofectamine 2000 (Thermo) or lipofectamine 3000 (Thermo) according to manufacturer protocols.

Immunoblotting and immunoprecipitations

Samples analyzed by immunoblot were lysed in NETN (20mM Tris-Cl, pH 8.0, 100mM NaCl, 0.5mM EDTA, 0.5% Nonidet P-40 (NP-40)) supplemented with 1ug/mL apoprotinin, 1ug/mL pepstatin, 10ug/mL leupeptin, 1mM Na_3VO_4, 1mM NaF and 1mM AEBSF (4-[2Aminoethyl] benzenesulfonyl fluoride). Protein concentration was estimated using the Bradford assay (Bio-Rad). Laemmli buffer was added to samples, which were then separated by SDS-PAGE gel electrophoresis using home-made or commercially available gels (Bio-Rad). Gels were transferred to nitrocellulose membranes and blotted using standard immunoblotting procedures.

For the co-IP experiments in Figure 2, cells were lysed in NETN, supplemented with 1ug/mL apoprotinin, 1ug/mL pepstatin, 10ug/mL leupeptin,

1mM Na3VO4, 1mM NaF and 1mM AEBSF (4-[2Aminoethyl] benzenesulfonyl fluoride). Protein A/G DynaBeads (Thermo) were bound to control rabbit IgG, Flag or Myc antibodies overnight at 4°C. Samples were incubated with beads for 4 hours at 4°C, which were subsequently washed three times in lysis buffer and eluted with 2X Laemmli sample buffer at 95°C for 10 minutes.

For the *in vivo* ubiquitination assay, cells were transfected with a combination of empty pcDNA3.1, 6XHIS-Ubiquitin, pcDNA-Sirt5-HA and Myc-Cyclin F (see figure for combinations) for a total of 5ug DNA/transfection using lipofectamine 2000 (Thermo). Cells were treated with 10 uM MG132 4h before harvesting. HIS pulldowns were performed as previously described in Choudhury et al. 2016, 80% cell suspension was lysed in denaturing conditions in buffer 1 (6M Guanidine-HCl, 0.1 M Na_2HPO4/NaH_2PO_4, 0.01 M Tris/HCL [pH 8.0], 15mM Imidizole, and 10mM β-mercaptoethanol [βME]). Lysates were sonicated and loaded onto pre-washed Ni^{2+}-NTA resin and incubated for 4h, rotating, at room temperature. Samples were then washed three times, first using buffer 1, followed by buffer 2 (8M urea, 0.1 M $Na_2HPO4/NaH2PO4$, 0.01 M Tris/HCL [pH 8.0]), then buffer 3 (8M urea, 0.1 M $Na_2HPO4/NaH2PO4$, 0.01 M Tris/HCL [pH 6.3]) plus 0.2% Triton X-100, and finally with buffer 3 plus 0.1% Triton X-100. Samples were then eluted by incubating 20min in buffer 4 (200 mM imidazole, 0.15 M Tris/HCl [pH 6.7], 30% glycerol and 0.72M βME, 5% SDS). The remaining 20% of cell suspension was lysed in NETN supplemented with 1ug/mL apoprotinin, 1ug/mL pepstatin, 10ug/mL leupeptin, 1mM Na3VO4, 1mM NaF and 1mM AEBSF and protein content was measured using Bradford assay. Samples were analyzed by immune-blot.

Immunological reagents

Commercially available antibodies used in this study, including their use (immunoblotting, immunofluorescence, etc.), catalog numbers and specific dilutions are included in Table 3.2.

For immunoblotting, antibodies were diluted in a solution of 5% nonfat dry milk in phosphate buffered saline, 0.05% tween 20 (PBST). Antibodies were either incubated at room temperature for 2 hours or overnight at 4°C. Detection was performed using HRP conjugated secondary antibodies (Jackson ImmunoResearch Laboratories, Inc; 1:10000), ECL reagent (Pierce), and exposure to film.

Flow Cytometry

Cells were collected and fixed in 70% ethanol. Cells were then washed in 1mL PBS twice, and then resuspended in a solution of PBS containing a final concentration of 25ug/mL propidium iodide (sigma) and 100ug/mL RNase A. Cells were sorted using a ThermoFisher Attune Nxt. Data was analyzed using FlowJo software.

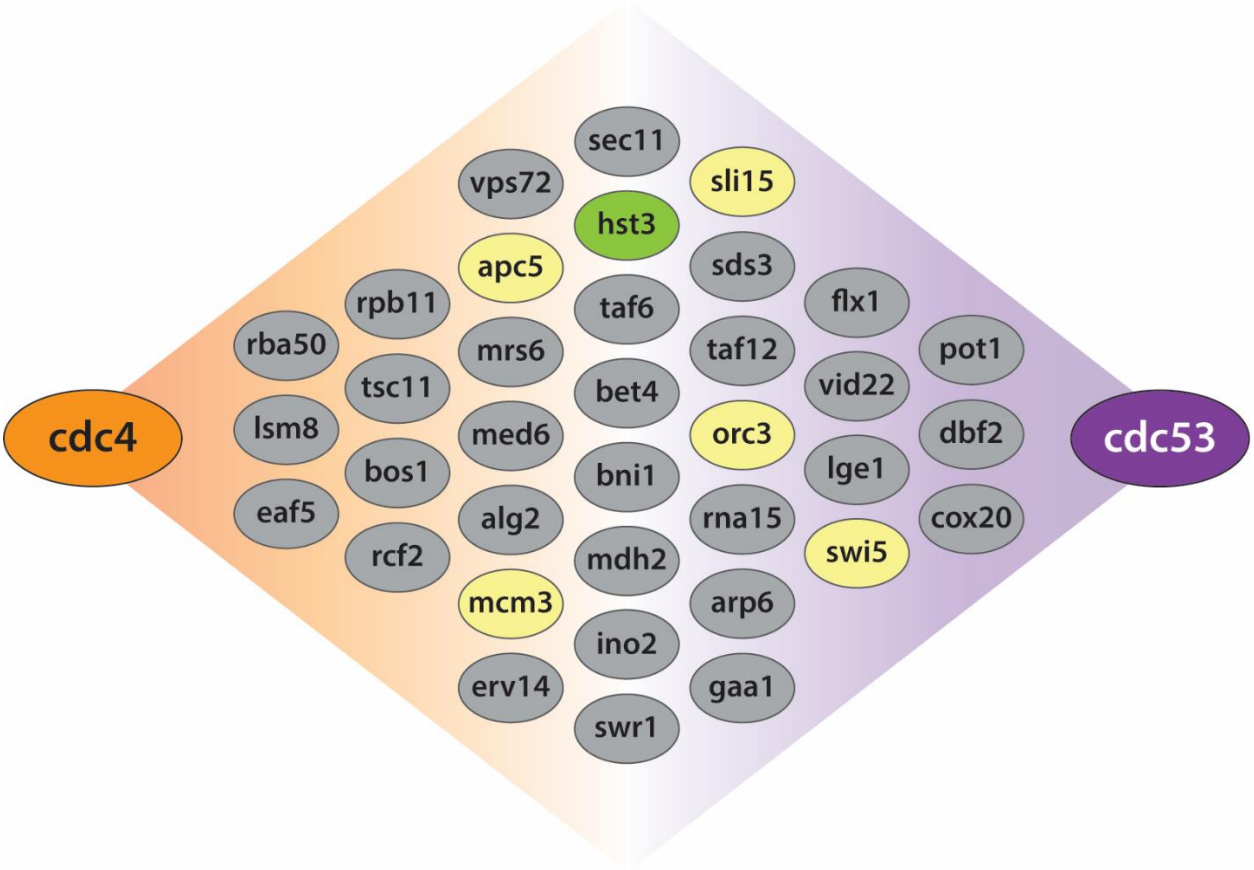

Figure 3.1. Schematic representing results of DRYGIN screen for potential Cyclin F substrates. To search for potential Cyclin F substrates, the DRYGIN database was interrogated for gene deletions or mutations that would rescue both the yeast Cdc4 and Cdc53 mutant cell cycle arrest phenotypes. Gray circles indicate genes with no connection to cell cycle regulation either directly, or through genetic interactions. Yellow circles indicate genes that are cell cycle relevant, but have been eliminated due to low turnover rate, no role in G1 or S, or having no human homolog. Green circle indicates potential Cyclin F target.

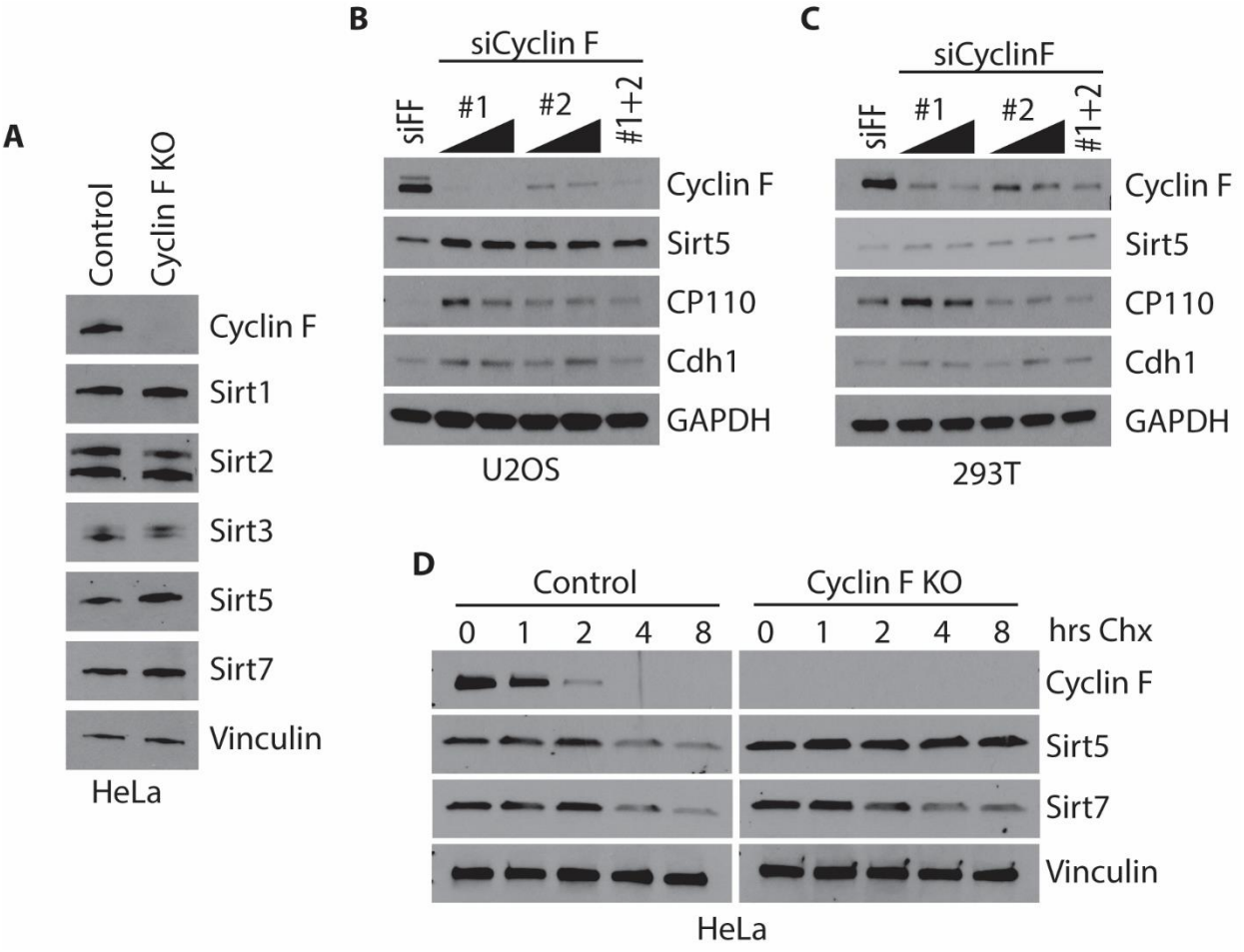

Figure 3.2 Sirt5 stability is increased in the absence of Cyclin F. A) Sirt5 protein levels are increased in Cyclin F CRISPR KO HeLa cells compared to controls. B) and C) Sirt5 protein levels, as well as known Cyclin F targets CP110 and Cdh1, are increased in both U2OS (B) and 293T (C) cells depleted of Cyclin F for 48h using 30-50nM siRNA. D) Cycloheximide treatment in both control and Cyclin F CRISPR KO HeLa cells. Sirt5 protein half-life is extended in Cyclin F CRISPR KO cells compared to controls while Sirt7 remains the same between cells lines.

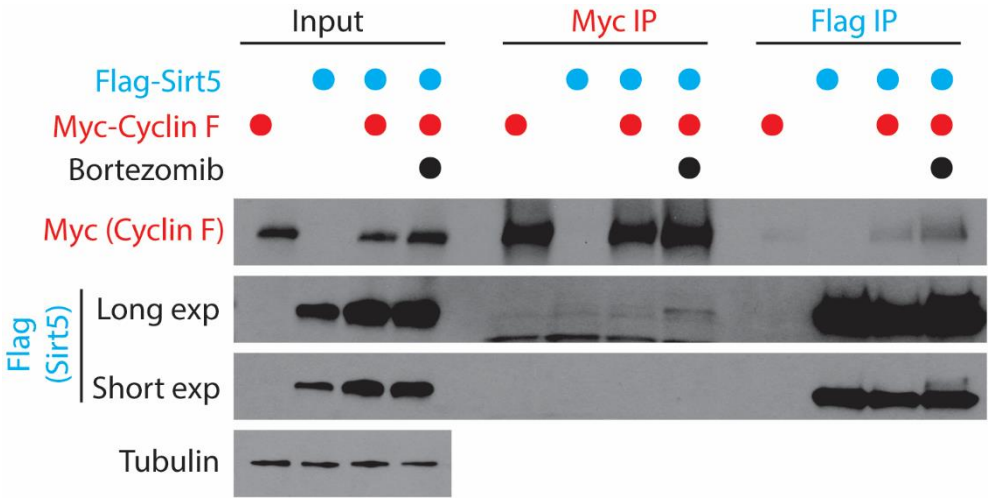

Figure 3.3 Sirt5 and Cyclin F co-immunoprecipitate. Flag-Sirt5 and Myc-Cyclin F were co-expressed in 293T cells, with or without 150nM Bortezomib treatment. Cells were then lysed and split between Flag and Myc IPs. Exp=Exposure.

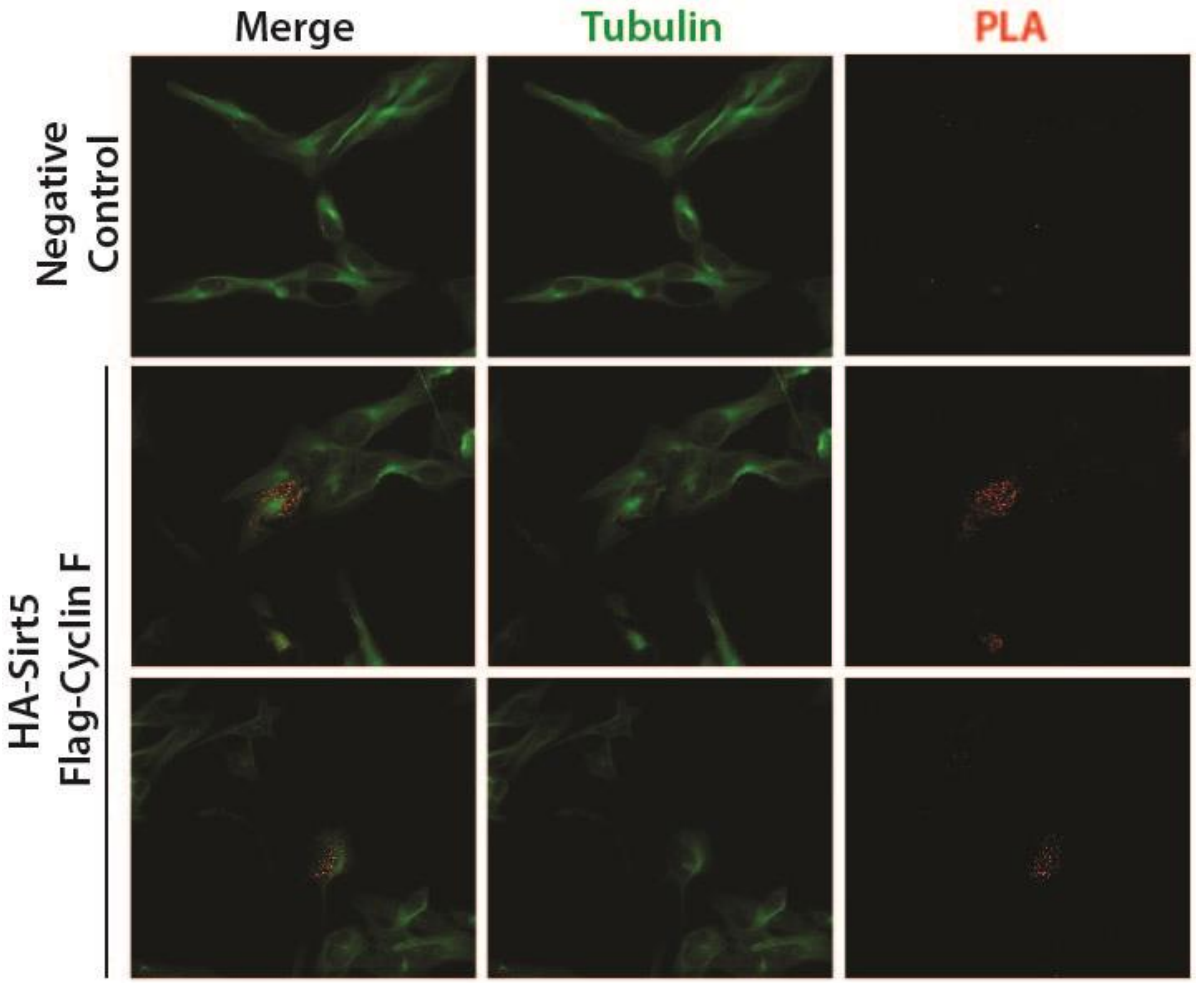

Figure 3.4 Sirt5 and Cyclin F interact in cells. U2OS cells were co-transfected with HA-Sirt5 and Flag-Cyclin F, fixed and used for PLA to detect site of interaction. PLA signal (red foci) is visible in cells throughout the cytoplasm.

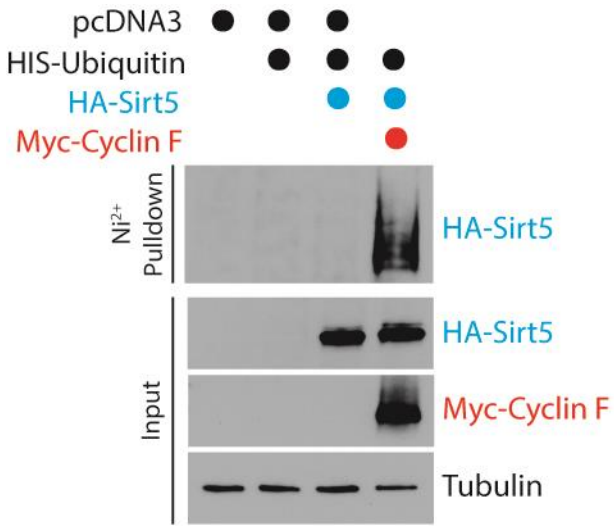

Figure 3.5. Sirt5 is ubiquitinated in the presence of Cyclin F. 293T cells were transfected with a combination empty vector (pcDNA), 6HIS-Ubiquitin, HA-Sirt5 or Myc-Cyclin F. Cells were treated with MG132 and lysed under denaturing conditions, and used for HIS pulldowns.

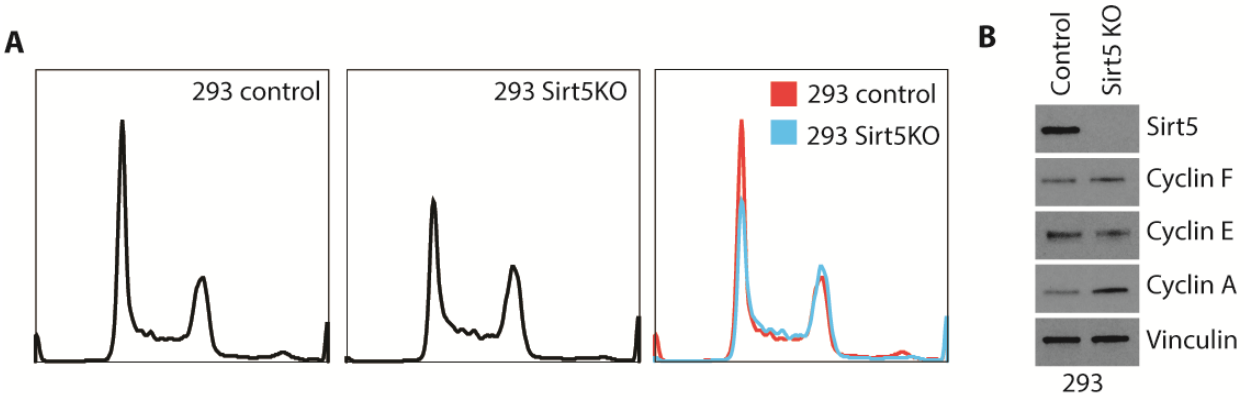

Figure 3.6. Sirt5 CRISPR KO cells exhibit redistribution of cell cycle phases. A) Control and Sirt5 CRISPR KO cells were stained using propidium iodide and analyzed using flow cytometry. Sirt5 KO cells show clear decrease in G1 population in comparison to controls. B) Immunoblot analysis of control and Sirt5 CRISPR KO cells show that Sirt5 KO cells have elevated levels of the S/G2/M cyclin, Cyclin A.

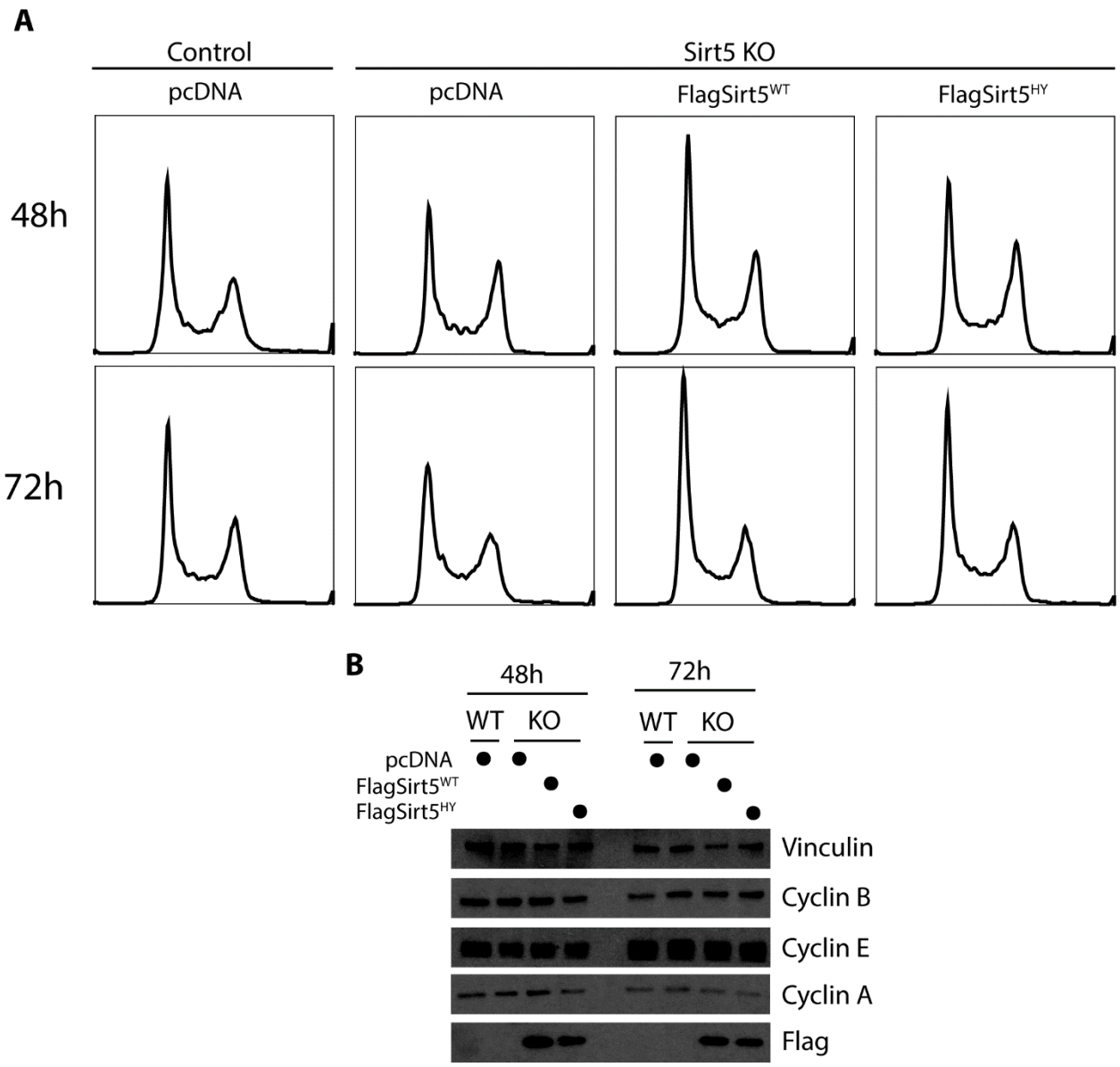

Figure 3.7. Sirt5 protein expression influences G1 timing. A) Cell cycle distribution of control or Sirt5 CRISPR KO 293 cells using propidium iodide staining. Cells were transfected with either empty, Flag-Sirt5^{WT} or Flag-Sirt5^{HY} plasmids and cell cycle was analyzed both 48h and 72h post-transfection. B) Western blot of samples from A.

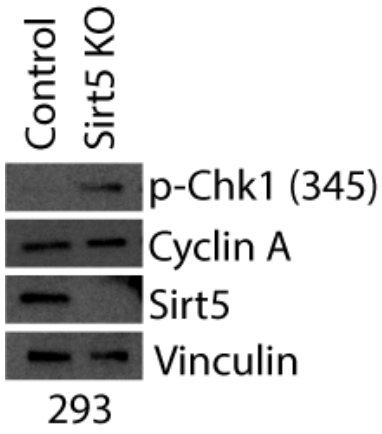

Figure 3.8. Sirt5 KO cells exhibit activated DNA damage response. Sirt5 CRISPR KO 293 cells have increased p-Chk1 (S345), which is phosphorylated by ATR in response to DNA damage, compared to control cells.

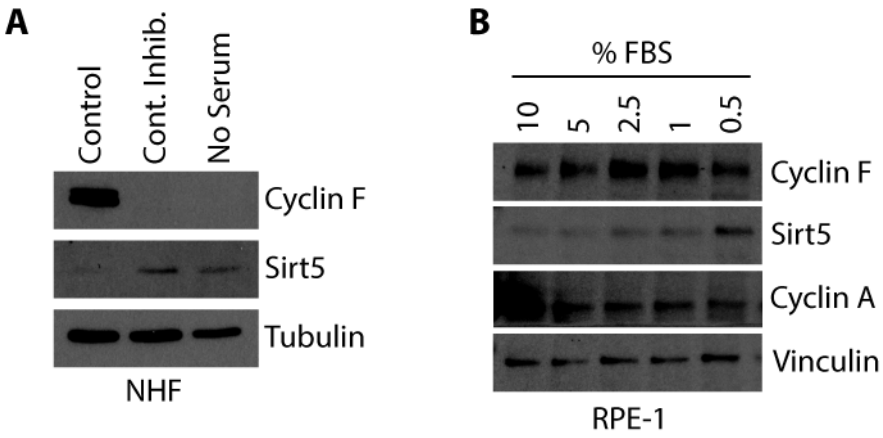

Figure 3.9. Sirt5 protein levels are increased in G0 arrested cells. A) NHF cells were grown under normal conditions, contact inhibited, or no serum (FBS) for 48h. B) RPE1 cells grown in normal media were transferred to media containing lower concentrations of FBS for 24h and then collected and analyzed via immune-blot.

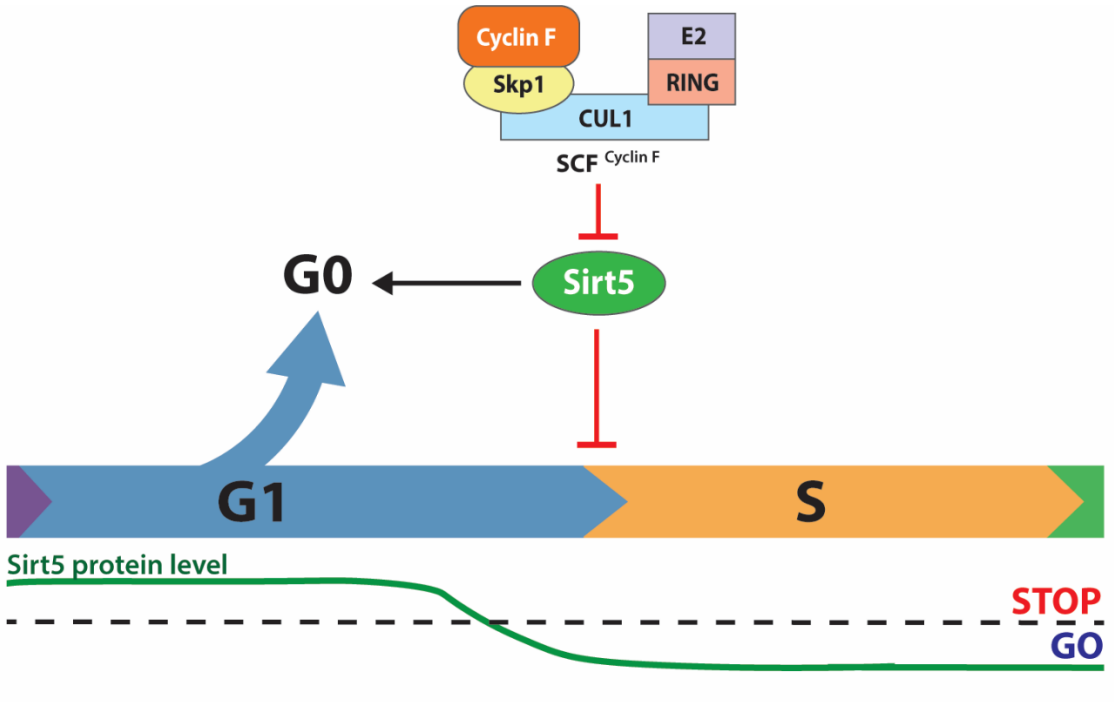

Figure 3.10. Proposed model for Sirt5 role in cell cycle progression. Our data indicate that Sirt5 protein must decrease to a specific threshold for cells to exit G1, and this protein decrease is regulated by protein degradation mediated by $SCF^{CyclinF}$. Cells with increase Sirt5 may not effectively exit G1, or it may promote G0 entry.

Target	siRNA sequence, 5'-3'
Firefly luciferase	CGUACGCGGAAUACUUCGA
Cyclin F #1	UAGCCUACCUCUACAAUGA
Cyclin F #2	GCACCCGGUUUAUCAGUAA
Sirtuin 5 #1	GGAGAUCCAUGGUAGCUUA
Sirtuin 5 #2	GAGUCCAAUUUGUCCAGCU
Sirtuin 5 #3	CCAGCGUCCACACGAAACCAGAUUU
Sirtuin 5 #4	CCAAGUCGAUUGAUUUCCCAGCUAU

Table 3.1 siRNA oligonucleotides used in Chapter 3.

Target	Company	Catalog number	Dilution
Cyclin F	Santa Cruz	sc-952	1:2000
Sirtuin 5	CST	8782	1:2000
Cdh1 (Fzr1)	abcam	ab3242	1:1000
Tubulin	Santa Cruz	sc32293	IB 1:1000; IF 1:200
GAPDH	Santa Cruz	sc25778	1:10000
Cyclin E	CST	4129	1:5000
Cyclin A	Santa Cruz	sc751	1:5000
Cyclin B1	abcam	ab32053	1:10000
Vinculin	Santa Cruz	sc-25336	1:5000
Sirtuin 1	CST	9487	1:1000
Sirtuin 2	CST	12650	1:2000
Sirtuin 3	CST	5490	1:2000
Sirtuin 7	CST	5360	1:1000
CP110	Bethyl	A301-343A	1:1000
Myc tag	Santa Cruz	sc-40	1:2000
FLAG-HRP	Sigma	A8592	1:5000
FLAG	Sigma	F3165	IP:
HA	Covance	MMS-101P	1:1000
phospho-Chk1 (S345)	CST	2341S	1:1000

Table 3.2 Antibodies used in Chapter 3.

CHAPTER 4: CONCLUSIONS AND FUTURE DIRECTIONS

The $SCF^{Cyclin\ F}$ is a key regulator of cell cycle progression. Substrate ubiquitination and degradation by Cyclin F is important in regulating key processes, including DNA replication and mitotic progression. The research reported here identifies further roles for both Cyclin F and its substrates in both G1/S progression and mitotic processes. We show that the Cyclin F substrate; Nucleolar and Spindle Associated 1 (NUSAP1) interacts with a SUMO E3 ligase during mitosis. Furthermore, we identify the metabolic enzyme, Sirtuin 5, as a new Cyclin F substrate and demonstrate that Sirt5 protein levels impact G1/S progression. While both of these projects shed new light on the functions of Cyclin F in proliferating cells, more work is needed to understand the impact of these regulations.

NUSAP1 promotes spindle stability and chromosome segregation in mitotic cells, however, it is unknown how it functions. The above works (Chapter 2) identify a cell cycle regulated interaction between NUSAP1 and a SUMO E3 ligase composed of Ran Binding Protein 2 (RanBP2), Ran GTPase Activating Protein 1 (RanGAP1) and the SUMO E2 conjugating enzyme, UBC9. Furthermore, we show this interaction occurs independent of microtubules, in the cytoplasm of mitotic cells. While we were able to characterize this interaction, the functional meaning of this interaction remains unclear. Further research is needed to understand how NUSAP1 interacts with the complex and completely rule out whether NUSAP1 is a SUMO substrate of

this complex. If it is not, the role of NUSAP1 in the RanBP2 SUMO E3 ligase needs to be determined.

Little is known about how SUMO E3 ligases identify and interact with substrates. Based on a SAF-A/B, Acinus, PIAS protein domain (SAP domain) within NUSAP1, we speculate that NUSAP1 could be important for identification, and subsequent SUMOylation of some RanBP2 SUMO E3 ligase substrates. SAP domains are present at the N-terminus in all PIAS proteins, the most highly characterized class of SUMO E3 ligases, and are important for the identification and SUMOylation of a subset of PIAS SUMO targets. The RanBP2 complex does not contain a SAP domain, however, NUSAP1, like PIAS proteins, contains a SAP domain at its N-terminus. If NUSAP1 is important for RanBP2 substrate identification in mitotic cells, it would greatly further our understanding of how the RanBP2 SUMO E3 ligase functions.

In Chapter 3 we identify Sirt5 as a novel $SCF^{Cyclin\ F}$ substrate. Sirt5 is a mitochondrial deacylating enzyme that regulates a number of metabolic processes. Interestingly, our data show that Sirt5 may also have a role in G1/S progression, and possibly quiescence establishment and maintenance. While this data is promising, more research is needed to better characterize Sirt5 regulation, as well as the cell cycle phenotypes associated with Sirt5 overexpression or depletion. Cell cycle synchronization experiments are needed to determine when Sirt5 is targeted for degradation. Furthermore, more ubiquitination assays are needed to confirm Cyclin F mediated ubiquitination of Sirt5.

Our data show the Sirt5 protein levels influence cell cycle distribution. We hypothesize that Sirt5 is likely regulating a metabolic process that feeds back into cell cycle regulation. A number of metabolic processes, that have been previously identified as cell cycle regulated, are good candidates for this regulation, including nucleoside and amino acid metabolism as well as glycolysis. These are processes Sirt5 has already been implicated in regulating. Metabolic assays performed in both Sirt5 and Cyclin F knockout or over expression are needed to determine whether this is true.

REFERENCES

1. Fischer, M., Grossmann, P., Padi, M., and DeCaprio, J. A. (2016) Integration of TP53, DREAM, MMB-FOXM1 and RB-E2F target gene analyses identifies cell cycle gene regulatory networks. *Nucleic Acids Res.* **44**, 6070–6086

2. Pardee, A. B. (1974) A Restriction Point for Control of Normal Animal Cell Proliferation. *Proc. Natl. Acad. Sci. U. S. A.* **71**, 1286–1290

3. Matsuoka, S., Huang, M., and Elledge, S. J. (1998) Linkage of ATM to Cell Cycle Regulation by the Chk2 Protein Kinase. *Science.* **282**, 1893–1897

4. Matsuoka, S., Rotman, G., Ogawa, A., Shiloh, Y., Tamai, K., and Elledge, S. J. (2000) Ataxia telangiectasia-mutated phosphorylates Chk2 in vivo and in vitro. *PNAS*. **97**, 10389–10394

5. Falck, J., Mailand, N., Syljuåsen, R. G., Bartek, J., and Lukas, J. (2001) The ATM-Chk2-Cdc25A checkpoint pathway guards against radioresistant DNA synthesis. *Nature*. **410**, 842–847

6. Jinno, S., Suto, K., Nagata, A., Igarashi, M., Kanaoka, Y., Nojima, H., and Okayama, H. (1994) Cdc25A is a novel phosphatase functioning early in the cell cycle. *EMBO J.* **13**, 1549–56

7. Hoffmann, I., Draetta, G., and Karsenti, E. (1994) Activation of the phosphatase activity of human cdc25A by a cdk2-cyclin E dependent phosphorylation at the G1/S transition. *EMBO J.* **13**, 4302–10

8. Costanzo, V., Robertson, K., Ying, C. Y., Kim, E., Avvedimento, E., Gottesman, M., Grieco, D., and Gautier, J. (2000) Reconstitution of an ATM-dependent checkpoint that inhibits chromosomal DNA replication following DNA damage. *Mol. Cell*. **6**, 649–659

9. Khanna, K. K., Keating, K. E., Kozlov, S., Scott, S., Gatei, M., Hobson, K., Taya, Y., Gabrielli, B., Chan, D., Lees-Miller, S. P., and Lavin, M. F. (1998) ATM associates with and phosphorylates p53: mapping the region of interaction. *Nat. Genet.* **20**, 398–400

10. Banin, S., Moyal, L., Shieh, S.-Y., Taya, Y., Anderson, C. W., Chessa, L., Smorodinsky, N. I., Prives, C., Reiss, Y., Shiloh, Y., and Ziv, Y. (1998) Enhanced Phosphorylation of p53 by ATM in Response to DNA Damage. *Science.* **281**, 1674–1677

11. Canman, C. E., Lim, D.-S., Cimprich, K. A., Taya, Y., Tamai, K., Sakaguchi, K., Appella, E., Kastan, M. B., and Siliciano, J. D. (1998) Activation of the ATM Kinase by Ionizing Radiation and Phosphorylation of p53. *Science.* **281**, 1677–1679

12. Kubbutat, M. H. G., Jones, S. N., and Vousden, K. H. (1997) Regulation of p53 stability by Mdm2. *Nature*. **387**, 299–303

13. Haupt, Y., Maya, R., Kazaz, A., and Oren, M. (2001) Mdm2 promotes the rapid degradation of p53. *Nature*. **387**, 296–299

14. Shieh, S. Y., Ikeda, M., Taya, Y., and Prives, C. (1997) DNA damage-induced phosphorylation of p53 alleviates inhibition by MDM2. *Cell*. **91**, 325–334

15. Bunz, F. (1998) Requirement for p53 and p21 to Sustain G2 Arrest After DNA Damage. *Science.* **282**, 1497–1501

16. Waldman, T., Kinzler, K. W., and Vogelstein2, B. (1995) p21 Is Necessary for the p53-mediated G1 Arrest in Human Cancer Cells. *Cancer Res.* **55**, 5187–5190

17. Macleod, K. F., Sherry, N., Hannon, G., Beach, D., Tokino, T., Kinzler, K., Vogelstein, B., and Jacks, T. (1995) p53-Dependent and independent expression of p21 during cell growth, differentiation, and DNA damage. *Genes Dev.* **9**, 935–944

18. Hirao, A., Kong, Y.-Y., Matsuoka, S., Wakeham, A., Ruland, J., Yoshida, H., Liu, D., Elledge, S. J., and Mak, T. W. (2000) DNA Damage-Induced Activation of p53 by the Checkpoint Kinase Chk2. *Science.* **287**, 1824–1827

19. Zhao, H., and Piwnica-Worms, H. (2001) ATR-Mediated Checkpoint Pathways Regulate Phosphorylation and Activation of Human Chk1. *Mol. Cell. Biol.* **21**, 4129–4139

20. Sanchez, Y., Wong, C., Thoma, R. S., Richman, R., Wu, Z., Piwnica-Worms, H., and Elledge, S. J. (1997) Conservation of the Chk1 Checkpoint Pathway in Mammals: Linkage of DNA Damage to Cdk Regulation Through Cdc25. *Science.* **277**, 1497–1501

21. Liu, Q., Guntuku, S., Cui, X.-S., Matsuoka, S., Cortez, D., Tamai, K., Luo, G., Carattini-Rivera, S., Demayo, F., Bradley, A., Donehower, L. A., and Elledge, S. J. (2000) Chk1 is an essential kinase that is regulated by Atr and required for the G2/M DNA damage checkpoint. *Genes Dev.* **14**, 1448–1459

22. Timofeev, O., Cizmecioglu, O., Settele, F., Kempf, T., and Hoffmann, I. (2010) Cdc25 Phosphatases Are Required for Timely Assembly of CDK1-Cyclin B at the G2/M Transition. *J. Biol. Chem.* **285**, 16978–16990

23. Tumurbaatar, I., Cizmecioglu, O., Hoffmann, I., Grummt, I., and Voit, R. (2011) Human Cdc14B promotes progression through mitosis by dephosphorylating Cdc25 and regulating Cdk1/cyclin B activity. *PLoS One*. **6**, e14711

24. Parker, L. L., and Piwnica-worms, H. (1992) Inactivation of the p34cdc2-Cyclin B Complex by the Human WEE1 Tyrosine Kinase. *Science.* **257**, 1955–1957

25. Watanabe, N., Broome, M., and Hunter, T. (1995) Regulation of the human WEE1Hu CDK tyrosine 15-kinase during the cell cycle. *EMBO J.* **14**, 1878–91

26. Musacchio, A., and Salmon, E. D. (2007) The Spindle-Assembly Checkpoint in Space and Time. *Nat. Rev.* **8**, 379–393

27. Sudakin, V., Chan, G. K. T., and Yen, T. J. (2001) Checkpoint inhibition of the

APC/C in HeLa cells is mediated by a complex of BUBR1, BUB3, CDC20, and MAD2. *J. Cell Biol.* **154**, 925–936

28. Izawa, D., and Pines, J. (2015) The mitotic checkpoint complex binds a second CDC20 to inhibit active APC/C. *Nature*. **517**, 631–634

29. Wäsch, R., and Cross, F. R. (2002) APC-dependent proteolysis of the mitotic cyclin Clb2 is essential for mitotic exit. *Nature*. **418**, 556–562

30. Raff, J. W., Jeffers, K., and Huang, J.-Y. (2002) The roles of Fzy/Cdc20 and Fzr/Cdh1 in regulating the destruction of cyclin B in space and time. *J. Cell Biol.* **157**, 1139–1149

31. Hagting, A., Den Elzen, N., Vodermaier, H. C., Waizenegger, I. C., Peters, J.-M., and Pines, J. (2002) Human securin proteolysis is controlled by the spindle checkpoint and reveals when the APC/C switches from activation by Cdc20 to Cdh1. *J. Cell Biol.* **157**, 1125–1137

32. Zou, H., Mcgarry, T. J., Bernal, T., and Kirschner, M. W. (1999) Identification of a Vertebrate Sister-Chromatid Separation Inhibitor Involved in Transformation and Tumorigenesis. *Science.* **285**, 418–422

33. Waizenegger, I. C., Giménez-Abián, J. F., Wernic, D., and Peters, J. M. (2002) Regulation of human separase by securin binding and autocleavage. *Curr. Biol.* **12**, 1368–1378

34. Michaelis, C., Ciosk, R., and Nasmyth, K. (1997) Cohesins: Chromosomal proteins that prevent premature separation of sister chromatids. *Cell*. **91**, 35–45

35. Hauf, S., Waizenegger, I. C., and Peters, J.-M. (2001) Cohesin Cleavage by Separase Required for Anaphase and Cytokinesis in Human Cells. *Science.* **293**, 1320–1323

36. Schlesinger, D. H., Goldstein, G., and Koppel, N. (1975) The Complete Amino Acid Sequence of Ubiquitin, an Adenylate Cyclase Stimulating Polypeptide Probably Universal in Living Cells. *Biochemistry*. **14**, 2214–2218

37. Hershko, A., and Ciechanover, A. (1998) The ubiquitin system. *Annu. Rev. Biochem.* **67**, 425–479

38. Cheffner, M., Nuber, U., and Hubregtse, J. M. (1995) Protein ubiquitination involving an E1-E2-E3 enzyme ubiquitin thioester cascade. *Nature*. **373**, 1995

39. Hershko, A., Heller, H., Elias, S., and Ciechanover, A. (1983) Components of Ubiquitin-Protein Ligase System: Resolution, Affinity Purification, and Role in Protein Breakdown. *J. Biol. Chem.* **258**, 8206–8214

40. Breitschopf, K., Bengal, E., Ziv, T., Admon, A., and Ciechanover, A. (1998) A novel site for ubiquitination: The N-terminal residue, and not internal lysines of MyoD, is essential for conjugation and degradation of the protein. *EMBO J.* **17**, 5964–5973

41. Mukhopadhyay, D., and Riezman, H. (2007) Proteasome-Independent

Functions of Ubiquitin in Endocytosis and Signaling. *Science.* **315**, 201–205

42. Nakasone, M. A., Livnat-levanon, N., Glickman, M. H., Cohen, R. E., and Fushman, D. (2013) Mixed-Linkage Ubiquitin Chains Send Mixed Messages. *Structure*. **21**, 727–740

43. Chau, V., Tobias, J. W., Bachmair, A., Marriott, D., Ecker, D. J., Gonda, D. K., and Varshavsky, A. (1989) A Multiubiquitin Chain is Confined to Specific Lysine in a Targeted Short-Lived Protein. *Science.* **243**, 1576–1583

44. Min, M., Mevissen, T. E. T., De Luca, M., Komander, D., and Lindon, C. (2015) Efficient APC/C substrate degradation in cells undergoing mitotic exit depends on K11 ubiquitin linkages. *Mol. Biol. Cell*. **26**, 4325–4332

45. Lander, G. C., Estrin, E., Matyskiela, M. E., Bashore, C., Nogales, E., and Martin, A. (2012) Complete subunit architecture of the proteasome regulatory particle. *Nature*. **482**, 186–193

46. Groll, M., Ditzel, L., Lowe, J., Stock, D., Bochtler, M., Bartunik, H. D., and Huber, R. (1997) Structure of 20S proteasome from yeast at 2.4A resolution. *Nature*. **386**, 463–471

47. Liu, C.-W., Millen, L., Roman, T. B., Xiong, H., Gilbert, H. F., Noiva, R., Demartino, G. N., and Thomas, P. J. (2002) Conformational Remodeling of Proteasomal Substrates by PA700, the 19 S Regulatory Complex of the 26 S Proteasome. *J. Biol. Chem.* **277**, 26815–26820

48. Yao, T., and Cohen, R. E. (2002) A cryptic protease couples deubiquitination and degradation by the proteasome. *Nature*. **419**, 403–407

49. Cope, G. A., Suh, G. S. B., Aravind, L., Schwarz, S. E., Zipursky, S. L., Koonin, E. V., and Deshaies, R. J. (2002) Role of Rpn11 Metalloprotease in Deubiquitination and Degradation by the 26S Proteasome. *Science.* **298**, 611–615

50. Schnell, J. D., and Hicke, L. (2003) Non-traditional Functions of Ubiquitin and Ubiquitin-binding Proteins. *J. Biol. Chem.* **278**, 35857–35860

51. McDowell, G. S., and Philpott, A. (2013) Non-canonical ubiquitylation: Mechanisms and consequences. *Int. J. Biochem. Cell Biol.* **45**, 1833–1842

52. Hochstrasser, M. (2009) Origin and function of ubiquitin-like proteins. *Nature*. **458**, 422–429

53. Deshaies, R. J., and Joazeiro, C. A. P. (2009) RING Domain E3 Ubiquitin Ligases. *Annu. Rev. Biochem.* **78**, 399–434

54. Bernassola, F., Karin, M., Ciechanover, A., and Melino, G. (2008) The HECT Family of E3 Ubiquitin Ligases: Multiple Players in Cancer Development. *Cancer Cell*. **14**, 10–21

55. Dove, K. K., and Klevit, R. E. (2017) RING-Between-RING E3 Ligases: Emerging Themes amid the Variations. *J. Mol. Biol.* **429**, 3363–3375

56. Petroski, M. D., and Deshaies, R. J. (2005) Function and regulation of cullin-RING ubiquitin ligases. *Nat. Rev.* **6**, 9–20

57. Deshaies, R. J. (1999) SCF and Cullin/RING H2-Based Ubiquitin Ligases. *Annu Rev Cell Dev Biol*. **15**, 435–467

58. Lyapina, S. A., Correll, C. C., Kipreos, E. T., and Deshaies, R. J. (1998) Human CUL1 forms an evolutionarily conserved ubiquitin ligase complex (SCF) with SKP1 and an F-box protein. *Proc. Natl. Acad. Sci. U. S. A.* **95**, 7451–7456

59. Zheng, N., Schulman, B. A., Song, L., Miller, J. J., Jeffrey, P. D., Wang, P., Chu, C., Koepp, D. M., Elledge, S. J., Paganok, M., Conaway{, R. C., Conaway{, J. W., Harper, J. W., and Pavletich, N. P. (2002) Structure of the Cul1–Rbx1–Skp1–F box Skp2 SCF ubiquitin ligase complex. *Nature*. **416**, 703–709

60. Reyes Turcu, F. E., Ventii, K. H., and Wilkinson, K. D. (2009) Regulation and Cellular Roles of Ubiquitin-specific Deubiquitinating Enzymes. *Annu. Rev. Biochem.* **78**, 363–397

61. Nijman, S. M. B., Luna-Vargas, M. P. A., Velds, A., Brummelkamp, T. R., Dirac, A. M. G., Sixma, T. K., and Bernards, R. (2005) A Genomic and Functional Inventory of Deubiquitinating Enzymes. *Cell*. **123**, 773–786

62. Kamitani, T., Kito, K., Nguyen, H. P., and Yeh, E. T. H. (1997) Characterization of NEDD8, a Developmentally Down-regulated Ubiquitin-like Protein*. *J. Biol. Chem.* **272**, 28557–28562

63. Saha, A., and Deshaies, R. J. (2008) Multimodal Activation of the Ubiquitin Ligase SCF by Nedd8 Conjugation. *Mol. Cell*. **32**, 21–31

64. Kawakami, T., Chiba, T., Suzuki, T., Iwai, K., Yamanaka, K., Minato, N., Suzuki, H., Shimbara, N., Hidaka, Y., Osaka, F., Omata, M., and Tanaka, K. (2001) NEDD8 recruits E2-ubiquitin to SCF E3 ligase. *EMBO J.* **20**, 4003–4012

65. Hori, T., Osaka, F., Chiba, T., Miyamoto, C., Okabayashi, K., Shimbara, N., Kato, S., and Tanaka, K. (1999) Covalent modification of all members of human cullin family proteins by NEDD8. *Oncogene*. **18**, 6829–6834

66. Wu, K., Chen, A., and Pan, Z.-Q. (2000) Conjugation of Nedd8 to CUL1 Enhances the Ability of the ROC1-CUL1 Complex to Promote Ubiquitin Polymerization. *J. Biol. Chem.* **275**, 32317–32324

67. Tatham, M. H., Jaffray, E., Vaughan, O. a., Desterro, J. M. P., Botting, C. H., Naismith, J. H., and Hay, R. T. (2001) Polymeric Chains of SUMO-2 and SUMO-3 are Conjugated to Protein Substrates by SAE1/SAE2 and Ubc9. *J. Biol. Chem.* **276**, 35368–35374

68. Desterro, J. M. P., Rodriguez, M. S., Kemp, G. D., and Hay, R. T. (1999) Identification of the Enzyme Required for Activation of the Small Ubiquitin-like Protein SUMO-1. *J. Biol. Chem.* **274**, 10618–10624

69. Saitoh, H., Sparrow, D. B., Shiomi, T., Pu, R. T., Nishimoto, T., Mohun, T. J., and Dasso, M. (1998) Ubc9p and the conjugation of SUMO-1 to RanGAP1 and RanBP2. *Curr. Biol.* **8**, 121–4

70. Desterro, J. M. P., Thomson, J., and Hay, R. T. (1997) Ubch9 conjugates SUMO but not ubiquitin. *FEBS Lett.* **417**, 297–300

71. Lee, G. W., Melchior, F., Matunis, M. J., Mahajan, R., Tian, Q., and Anderson, P. (1998) Modification of Ran GTPase-activating Protein by the Small Ubiquitin-related Modifier SUMO-1 Requires Ubc9, an E2-type Ubiquitin-conjugating Enzyme Homologue. *J. Biol. Chem.* **273**, 6503–6507

72. Saitoh, H., and Hinchey, J. (2000) Functional Heterogeneity of Small Ubiquitin-related Protein Modifiers SUMO-1 versus SUMO-2/3. *J. Biol. Chem.* **275**, 3252–6258

73. Vertegaal, A. C. O., Andersen, J. S., Ogg, S. C., Hay, R. T., Mann, M., and Lamond, A. I. (2006) Distinct and Overlapping Sets of SUMO-1 and SUMO-2 Target Proteins Revealed by Quantitative Proteomics. *Mol. Cell. Proteomics*. **5**, 2298–2310

74. Becker, J., Barysch, S. V, Karaca, S., Dittner, C., Hsiao, H.-H., Berriel Diaz, M., Herzig, S., Urlaub, H., and Melchior, F. (2013) Detecting endogenous SUMO targets in mammalian cells and tissues. *Nat. Struct. Mol. Biol.* **20**, 525–31

75. Bai, C., Richman, R., and Elledge, S. J. (1994) Human cyclin F. *EMBO J.* **13**, 6087–6098

76. Bai, C., Sen, P., and Hofmann, K. (1996) SKP1 Connects Cell Cycle Regulators to the Ubiquitin Proteolysis Machinery through a Novel Motif, the F-Box. *Cell*. **86**, 263–274

77. Tetzlaff, M. T., Bai, C., Finegold, M., Wilson, J., Wade Harper, J., Mahon, K. A., Elledge, S. J., and McLean, M. (2004) Cyclin F Disruption Compromises Placental Development and Affects Normal Cell Cycle Execution. *Mol. Cell. Biol.* **24**, 2487–2498

78. D'Angiolella, V., Esencay, M., and Pagano, M. (2013) A cyclin without cyclin-dependent kinases: cyclin F controls genome stability through ubiquitin-mediated proteolysis. *Trends Cell Biol.* **23**, 135–140

79. Choudhury, R., Bonacci, T., Arceci, A., Lahiri, D., Mills, C. A., Kernan, J. L., Branigan, T. B., Decaprio, J. A., Burke, D. J., Emanuele, M. J., Correspondence, M. J. E., Lahiri, D., Mills, C. A., Kernan, J. L., Branigan, T. B., and Emanuele, M. J. (2016) APC/C and SCF(cyclin F) Constitute a Reciprocal Feedback Circuit Controlling S-Phase Entry. *Cell Rep.* **16**, 3359–3372

80. Choudhury, R., Bonacci, T., Wang, X., Kernan, J. L., Liu, P., Correspondence, M. J. E., Truong, A., Arceci, A., Zhang, Y., Mills, C. A., and Emanuele, M. J. (2017) The E3 Ubiquitin Ligase SCF(Cyclin F) Transmits AKT Signaling to the

Cell-Cycle Machinery. *Cell Rep.* **20**, 3212–3222

81. D'Angiolella, V., Donato, V., Vijayakumar, S., Saraf, A., Florens, L., Washburn, M. P., Dynlacht, B., Pagano, M., D 'angiolella, V., Donato, V., Vijayakumar, S., Saraf, A., Florens, L., Washburn, M. P., Dynlacht, B., and Pagano, M. (2010) SCF(Cyclin F) controls centrosome homeostasis and mitotic fidelity through CP110 degradation. *Nature*. **466**, 138–142

82. Emanuele, M. J., Elia, A. E. H., Xu, Q., Thoma, C. R., Izhar, L., Leng, Y., Guo, A., Chen, Y.-N., Rush, J., Hsu, P. W.-C., Yen, H.-C. S., and Elledge, S. J. (2011) Global identification of modular cullin-RING ligase substrates. *Cell*. **147**, 459–74

83. D'Angiolella, V., Donato, V., Forrester, F. M., Jeong, Y.-T., Pellacani, C., Kudo, Y., Saraf, A., Florens, L., Washburn, M. P., and Pagano, M. (2012) Cyclin F-Mediated Degradation of Ribonucleotide Reductase M2 Controls Genome Integrity and DNA Repair. *Cell*. **149**, 1023–1034

84. Elia, A. E. H., Boardman, A. P., Wang, D. C., Koren, I., Gygi, S. P., Elledge Correspondence, S. J., Huttlin, E. L., Everley, R. A., Dephoure, N., Zhou, C., and Elledge, S. J. (2015) Quantitative Proteomic Atlas of Ubiquitination and Acetylation in the DNA Damage Response Molecular Cell Resource Quantitative Proteomic Atlas of Ubiquitination and Acetylation in the DNA Damage Response. *Mol. Cell*. **59**, 867–881

85. Walter, D., Hoffmann, S., Komseli, E.-S., Rappsilber, J., Gorgoulis, V., and Storgaard Sørensen, C. (2016) SCF Cyclin F-dependent degradation of CDC6 suppresses DNA re-replication. *Nat. Commun.* **7**, 1–10

86. Yan, Z., DeGregori, J., Shohet, R., Leone, G., Stillman, B., Nevins, J. R., and Williams, R. S. (1998) Cdc6 is regulated by E2F and is essential for DNA replication in mammalian cells. *Proc. Natl. Acad. Sci. U. S. A.* **95**, 3603–8

87. Ndez, J. M., and Stillman, B. (2000) Chromatin Association of Human Origin Recognition Complex, Cdc6, and Minichromosome Maintenance Proteins during the Cell Cycle: Assembly of Prereplication Complexes in Late Mitosis. *Mol. Cell. Biol.* **20**, 8602–8612

88. Tran, P. T., Erdeniz, N., Symington, L. S., and Liskay, R. M. (2004) EXO1-A multi-tasking eukaryotic nuclease. *DNA Repair (Amst).* **3**, 1549–1559

89. Clay-Farrace, L., Pelizon, C., Santamaria, D., Pines, J., and Laskey, R. A. (2003) Human replication protein Cdc6 prevents mitosis through a checkpoint mechanism that implicates Chk1. *EMBO J.* **22**, 704–712

90. Chen, Z., Indjeian, V. B., McManus, M., Wang, L., and Dynlacht, B. D. (2002) CP110, a cell cycle-dependent CDK substrate, regulates centrosome duplication in human cells. *Dev. Cell*. **3**, 339–350

91. Raemaekers, T., Ribbeck, K., Beaudouin, J., Annaert, W., Van Camp, M., Stockmans, I., Smets, N., Bouillon, R., Ellenberg, J., and Carmeliet, G. (2003) NuSAP, a novel microtubule-associated protein involved in mitotic spindle

organization. *J. Cell Biol.* **162**, 1017–29

92. Vanden Bosch, A., Raemaekers, T., Denayer, S., Torrekens, S., Smets, N., Moermans, K., Dewerchin, M., Carmeliet, P., and Carmeliet, G. (2010) NuSAP is essential for chromatin-induced spindle formation during early embryogenesis. *J. Cell Sci.* **123**, 3244–55

93. Ribbeck, K., Groen, A. C., Santarella, R., Bohnsack, M. T., Raemaekers, T., Köcher, T., Gentzel, M., Görlich, D., Wilm, M., Carmeliet, G., Mitchison, T. J., Ellenberg, J., Hoenger, A., and Mattaj, I. W. (2006) NuSAP, a mitotic RanGTP target that stabilizes and cross-links microtubules. *Mol. Biol. Cell*. **17**, 2646–60

94. Dankert, J. F., Rona, G., Clijsters, L., Geter, P., Skaar, J. R., Bermudez-Hernandez, K., Sassani, E., Fenyö, D., Ueberheide, B., Schneider, R., and Pagano, M. (2016) Cyclin F-Mediated Degradation of SLBP Limits H2A.X Accumulation and Apoptosis upon Genotoxic Stress in G2. *Mol. Cell*. **64**, 507–519

95. Bretones, G., Delgado, M. D., and León, J. (2014) Myc and cell cycle control. *Biochim. Biophys. Acta*. **1849**, 506–516

96. Fry, D. W., Harvey, P. J., Keller, P. R., Elliott, W. L., Meade, M., Trachet, E., Albassam, M., Zheng, X., Leopold, W. R., Pryer, N. K., and Toogood, P. L. (2004) Specific inhibition of cyclin-dependent kinase 4/6 by PD 0332991 and associated antitumor activity in human tumor xenografts. *Mol. Cancer Ther.* **3**, 1427–1438

97. Tate, S. C., Cai, S., Ajamie, R. T., Burke, T., Beckmann, R. P., Chan, E. M., De Dios, A., Wishart, G. N., Gelbert, L. M., and Cronier, D. M. (2014) Semi-Mechanistic Pharmacokinetic/Pharmacodynamic Modeling of the Antitumor Activity of LY2835219, a New Cyclin-Dependent Kinase 4/6 Inhibitor, in Mice Bearing Human Tumor Xenografts. *Clin Cancer Res*. **20**, 3763–3774

98. Rader, J., Russell, M. R., Hart, L. S., Nakazawa, M. S., Belcastro, L. T., Martinez, D., Li, Y., Carpenter, E. L., Attiyeh, E. F., Diskin, S. J., Kim, S., Parasuraman, S., Caponigro, G., Schnepp, R. W., Wood, A. C., Pawel, B., Cole, K. A., and Maris, J. M. (2013) Dual CDK4/CDK6 Inhibition Induces Cell-Cycle Arrest and Senescence in Neuroblastoma. *Clin Cancer Res*. **19**, 6173–6182

99. Cancer Genome Atlas Network, T. (2012) Comprehensive molecular portraits of human breast tumours. *Nature*. **490**, 61–70

100. Vassilev, L. T., Vu, B. T., Graves, B., Carvajal, D., Podlaski, F., Filipovic, Z., Kong, N., Kammlott, U., Lukacs, C., Klein, C., Fotouhi, N., and Liu, E. A. (2004) In Vivo activation of the p53 pathway by small-molecule antagonists of mdm2. *Science.* **303**, 844–848

101. Ding, Q., Zhang, Z., Liu, J.-J., Jiang, N., Zhang, J., Ross, T. M., Chu, X.-J., Bartkovitz, D., Podlaski, F., Janson, C., Tovar, C., Filipovic, Z. M., Higgins, B., Glenn, K., Packman, K., Vassilev, L. T., and Graves, B. (2013) Discovery of

RG7388, a Potent and Selective p53−MDM2 Inhibitor in Clinical Development. *J. Med. Chem.* **56**, 5979–5983

102. Hirai, H., Iwasawa, Y., Okada, M., Arai, T., Nishibata, T., Kobayashi, M., Kimura, T., Kaneko, N., Ohtani, J., Yamanaka, K., Itadani, H., Takahashi-Suzuki, I., Fukasawa, K., Oki, H., Nambu, T., Jiang, J., Sakai, T., Arakawa, H., Sakamoto, T., Sagara, T., Yoshizumi, T., Mizuarai, S., and Kotani, H. (2009) Small-molecule inhibition of Wee1 kinase by MK-1775 selectively sensitizes p53-deficient tumor cells to DNA-damaging agents. *Mol. Cancer Ther.* **8**, 2992–3000

103. Visconti, R., Della Monica, R., and Grieco, D. (2016) Cell cycle checkpoint in cancer: A therapeutically targetable double-edged sword. *J. Exp. Clin. Cancer Res.* **35**, 1–8

104. Hall, A. B., Newsome, D., Wang, Y., Boucher, D. M., Eustace, B., Gu, Y., Hare, B., Johnson, M. A., Milton, S., Murphy, C. E., Takemoto, D., Tolman, C., Wood, M., Charlton, P., Charrier, J.-D., Furey, B., Golec, J., Reaper, P. M., and Pollard, J. R. (2014) Potentiation of tumor responses to DNA damaging therapy by the selective ATR inhibitor VX-970. *Oncotarget*. **5**, 5674–5685

105. Walton, M. I., Eve, P. D., Hayes, A., Henley, A. T., Valenti, M. R., De, A. K., Brandon, H., Box, G., Boxall, K. J., Tall, M., Swales, K., Matthews, T. P., Mchardy, T., Lainchbury, M., Osborne, J., Hunter, J. E., Perkins, N. D., Aherne, G. W., Reader, J. C., Raynaud, F. I., Eccles, S. A., Collins, I., and Garrett, M. D. (2015) The clinical development candidate CCT245737 is an orally active CHK1 inhibitor with preclinical activity in RAS mutant NSCLC and Eμ-MYC driven B-cell lymphoma. *Oncotarget*. **7**, 2329–2342

106. Lengauer, C., Kinzler, K. W., and Vogelstein, B. (1998) Genetic instabilities in human cancers. *Nature*. **396**, 643–9

107. Schvartzman, J.-M., Sotillo, R., and Benezra, R. (2010) Mitotic chromosomal instability and cancer: mouse modelling of the human disease. *Nat. Rev.* **10**, 102–15

108. Silk, A. D., Zasadil, L. M., Holland, A. J., Vitre, B., Cleveland, D. W., and Weaver, B. a (2013) Chromosome missegregation rate predicts whether aneuploidy will promote or suppress tumors. *Proc. Natl. Acad. Sci.* **110**, E4134-4141

109. Zhou, J., and Giannakakou, P. (2005) Targeting Microtubules for Cancer Chemotherapy. *Curr. Med. Chem. -Anti-Cancer Agents*. **5**, 65–71

110. Matson, D. R., and Stukenberg, P. T. (2011) Spindle poisons and cell fate: a tale of two pathways. *Mol. Interv.* **11**, 141–50

111. Kavallaris, M., Kuo, D. Y., Burkhart, C. A., Regl, D. L., Norris, M. D., Haber, M., and Horwitz, S. B. (1997) Taxol-resistant epithelial ovarian tumors are associated with altered expression of specific beta-tubulin isotypes. *J. Clin. Invest.* **100**, 1282–1293

112. Zhang, Y., Yang, S. H., and Guo, X. L. (2017) New insights into Vinca alkaloids resistance mechanism and circumvention in lung cancer. *Biomed. Pharmacother.* **96**, 659–666

113. Adams, J., Palombella, V. J., Sausville, E. A., Johnson, J., Destree, A., Lazarus, D. D., Maas, J., Pien, C. S., Prakash, S., and Elliott, P. J. (1999) Proteasome Inhibitors: A Novel Class of Potent and Effective Antitumor Agents. *Cancer Res.* **59**, 2615–2622

114. Teicher, B. A., Ara, G., Herbst, R., Palombella, V. J., and Adams, J. (1999) The Proteasome Inhibitor PS-341 in Cancer Therapy. *Clin. Cancer Res.* **5**, 2638–2645

115. Cacan, E., Spring, A. M., Kumari, A., Greer, S. F., and Garnett-Benson, C. (2015) Combination treatment with sublethal ionizing radiation and the proteasome inhibitor, bortezomib, enhances death-receptor mediated apoptosis and anti-tumor immune attack. *Int. J. Mol. Sci.* **16**, 30405–30421

116. Huang, C. Y., Wei, C. C., Chen, K. C., Chen, H. J., Cheng, A. L., and Chen, K. F. (2012) Bortezomib enhances radiation-induced apoptosis in solid tumors by inhibiting CIP2A. *Cancer Lett.* **317**, 9–15

117. Tamatani, T., Takamaru, N., Hara, K., Kinouchi, M., Kuribayashi, N., Ohe, G., Uchida, D., Fujisawa, K., Nagai, H., and Miyamoto, Y. (2013) Bortezomib-enhanced radiosensitization through the suppression of radiation-induced nuclear factor-κB activity in human oral cancer cells. *Int. J. Oncol.* **42**, 935–944

118. Horton, T. M., Gannavarapu, A., Blaney, S. M., D'Argenio, D. Z., Plon, S. E., and Berg, S. L. (2006) Bortezomib interactions with chemotherapy agents in acute leukemia in vitro. *Cancer Chemother. Pharmacol.* **58**, 13–23

119. Soucy, T. A., Smith, P. G., Milhollen, M. A., Berger, A. J., Gavin, J. M., Adhikari, S., Brownell, J. E., Burke, K. E., Cardin, D. P., and Cullis, C. A. (2009) An inhibitor of NEDD8-activating enzyme as a novel approach to treat cancer. *Nature*. **458**, 732–737

120. Matyskiela, M. E., Zhang, W., Man, H.-W., Muller, G., Khambatta, G., Baculi, F., Hickman, M., Lebrun, L., Pagarigan, B., Carmel, G., Lu, C.-C., Lu, G., Riley, M., Satoh, Y., Schafer, P., Daniel, T. O., Carmichael, J., Cathers, B. E., and Chamberlain, P. P. (2017) A Cereblon Modulator (CC-220) with Improved Degradation of Ikaros and Aiolos. *J. Med. Chem.* 10.1021/acs.jmedchem.6b01921

121. Ribbeck, K., Raemaekers, T., Carmeliet, G., and Mattaj, I. W. (2007) A role for NuSAP in linking microtubules to mitotic chromosomes. *Curr. Biol.* **17**, 230–236

122. Xie, P., Li, L., Xing, G., Tian, C., Yin, Y., He, F., and Zhang, L. (2011) ATM-mediated NuSAP phosphorylation induces mitotic arrest. *Biochem. Biophys. Res. Commun.* **404**, 413–418

123. Chou, H., Wang, T., Lee, S., Hsu, P., Tsai, M., and Chang, C. (2011) Phosphorylation of NuSAP by Cdk1 regulates its interaction with microtubules in mitosis. *Cell Cycle*. **10**, 4083–4089

124. Chen, L., Yang, L., Qiao, F., Hu, X., Li, S., Yao, L., Yang, X.-L., and Shao, Z.-M. (2015) High Levels of Nucleolar Spindle-Associated Protein and Reduced Levels of BRCA1 Expression Predict Poor Prognosis in Triple-Negative Breast Cancer. *PLoS One*. **10**, e0140572

125. Okamoto, A., Higo, M., Shiiba, M., Nakashima, D., Koyama, T., Miyamoto, I., Kasama, H., Kasamatsu, A., Ogawara, K., Yokoe, H., Tanzawa, H., and Uzawa, K. (2015) Down-Regulation of Nucleolar and Spindle-Associated Protein 1 (NUSAP1) Expression Suppresses Tumor and Cell Proliferation and Enhances Anti-Tumor Effect of Paclitaxel in Oral Squamous Cell Carcinoma. *PLoS One*. **10**, e0142252

126. Ozlü, N., Monigatti, F., Renard, B. Y., Field, C. M., Steen, H., Mitchison, T. J., and Steen, J. J. (2010) Binding partner switching on microtubules and aurora-B in the mitosis to cytokinesis transition. *Mol. Cell. Proteomics*. **9**, 336–350

127. Song, L., and Rape, M. (2010) Regulated degradation of spindle assembly factors by the anaphase-promoting complex. *Mol. Cell*. **38**, 369–82

128. Dephoure, N., Zhou, C., Villén, J., Beausoleil, S. a, Bakalarski, C. E., Elledge, S. J., and Gygi, S. P. (2008) A quantitative atlas of mitotic phosphorylation. *Proc. Natl. Acad. Sci. U. S. A.* **105**, 10762–7

129. Olsen, J. V, Vermeulen, M., Santamaria, A., Kumar, C., Miller, M. L., Jensen, L. J., Gnad, F., Cox, J., Jensen, T. S., Nigg, E. A., Brunak, S., Mann, M., Martin, L., Jensen, L. J., Gnad, F., Cox, J., Jensen, T. S., Nigg, E. A., Brunak, S., and Mann, M. (2010) Quantitative phosphoproteomics reveals widespread full phosphorylation site occupancy during mitosis. *Sci. Signal.* **3**, ra3

130. Dasso, M. (2008) Emerging roles of the SUMO pathway in mitosis. *Cell Div.* **3**, 5

131. Myatt, S. S., Kongsema, M., Man, C. W.-Y., Kelly, D. J., Gomes, a R., Khongkow, P., Karunarathna, U., Zona, S., Langer, J. K., Dunsby, C. W., Coombes, R. C., French, P. M., Brosens, J. J., and Lam, E. W.-F. (2013) SUMOylation inhibits FOXM1 activity and delays mitotic transition. *Oncogene*. **33**, 1–14

132. Pichler, A., Gast, A., Seeler, J. S., Dejean, A., and Melchior, F. (2002) The nucleoporin RanBP2 has SUMO1 E3 ligase activity. *Cell*. **108**, 109–20

133. Saitoh, H., Pu, R., Cavenagh, M., and Dasso, M. (1997) RanBP2 associates with Ubc9p and a modified form of RanGAP1. *Proc. Natl. Acad. Sci. U. S. A.* **94**, 3736–41

134. Mahajan, R., Delphin, C., Guan, T., Gerace, L., and Melchior, F. (1997) A Small Ubiquitin-Related Polypeptide Involved in Targeting RanGAP1 to Nuclear Pore Complex Protein RanBP2. *Cell*. **88**, 97–107

135. Mahajan, R., Gerace, L., and Melchior, F. (1998) Molecular characterization of the SUMO-1 modification of RanGAP1 and its role in nuclear envelope association. *J. Cell Biol.* **140**, 259–70

136. Werner, A., Flotho, A., and Melchior, F. (2012) The RanBP2/RanGAP1*SUMO1/Ubc9 complex is a multisubunit SUMO E3 ligase. *Mol. Cell*. **46**, 287–98

137. Dawlaty, M. M., Malureanu, L., Jeganathan, K. B., Kao, E., Sustmann, C., Tahk, S., Shuai, K., Grosschedl, R., and van Deursen, J. M. (2008) Resolution of sister centromeres requires RanBP2-mediated SUMOylation of topoisomerase IIalpha. *Cell*. **133**, 103–15

138. Klein, U. R., Haindl, M., Nigg, E. A., and Muller, S. (2009) RanBP2 and SENP3 Function in a Mitotic SUMO2/3 Conjugation-Deconjugation Cycle on Borealin. *Mol. Biol. Cell*. **20**, 410–418

139. Bachant, J., Alcasabas, A., Blat, Y., Kleckner, N., and Elledge, S. J. (2002) The SUMO-1 isopeptidase Smt4 is linked to centromeric cohesion through SUMO-1 modification of DNA topoisomerase II. *Mol. Cell*. **9**, 1169–82

140. Montpetit, B., Hazbun, T. R., Fields, S., and Hieter, P. (2006) Sumoylation of the budding yeast kinetochore protein Ndc10 is required for Ndc10 spindle localization and regulation of anaphase spindle elongation. *J. Cell Biol.* **174**, 653–663

141. Westman, B. J., Verheggen, C., Hutten, S., Lam, Y. W., Bertrand, E., and Lamond, A. I. (2010) A proteomic screen for nucleolar SUMO targets shows SUMOylation modulates the function of Nop5/Nop58. *Mol. Cell*. **39**, 618–31

142. Zhang, X. D., Goeres, J., Zhang, H., Yen, T. J., Porter, A. C. G., and Matunis, M. J. (2008) SUMO-2/3 Modification and Binding Regulate the Association of CENP-E with Kinetochores and Progression through Mitosis. *Mol. Cell*. **29**, 729–741

143. Liu, Y. Y., Zhang, Y.-D., Guo, L., Huang, H.-Y., Zhu, H., Huang, J.-X., Zhou, S.-R., Dang, Y.-J., Li, X., and Tang, Q.-Q. (2013) Protein Inhibitor of Activated STAT 1 (PIAS1) Is Identified as the SUMO E3 Ligase of CCAAT/Enhancer-Binding Protein β (C/EBPβ) during Adipogenesis. *Mol. Cell. Biol.* **33**, 4606–17

144. Li, L., Zhou, Y., Sun, L., Xing, G., Tian, C., Sun, J., Zhang, L., and He, F. (2007) NuSAP is degraded by APC/C-Cdh1 and its overexpression results in mitotic arrest dependent of its microtubules' affinity. *Cell. Signal.* **19**, 2046–55

145. Hu, C.-K. K., Ozlu, N., Coughlin, M., Steen, J. J., and Mitchison, T. J. (2012) Plk1 negatively regulates PRC1 to prevent premature midzone formation before cytokinesis. *Mol. Biol. Cell*. **23**, 2702–2711

146. Kurasawa, Y., Earnshaw, W. C., Mochizuki, Y., Dohmae, N., and Todokoro, K. (2004) Essential roles of KIF4 and its binding partner PRC1 in organized

central spindle midzone formation. *EMBO J.* **23**, 3237–3248

147. Kellogg, E. H., Howes, S., Ti, S.-C., Ramírez-Aportela, E., Kapoor, T. M., Chacón, P., and Nogales, E. (2016) Near-atomic cryo-EM structure of PRC1 bound to the microtubule. *Proc. Natl. Acad. Sci. U. S. A.* **113**, 9430–9

148. Mellacheruvu, D., Wright, Z., Couzens, A. L., Lambert, J.-P., St-Denis, N. a, Li, T., Miteva, Y. V, Hauri, S., Sardiu, M. E., Low, T. Y., Halim, V. a, Bagshaw, R. D., Hubner, N. C., Al-Hakim, A., Bouchard, A., Faubert, D., Fermin, D., Dunham, W. H., Goudreault, M., Lin, Z.-Y., Badillo, B. G., Pawson, T., Durocher, D., Coulombe, B., Aebersold, R., Superti-Furga, G., Colinge, J., Heck, A. J. R., Choi, H., Gstaiger, M., Mohammed, S., Cristea, I. M., Bennett, K. L., Washburn, M. P., Raught, B., Ewing, R. M., Gingras, A.-C., and Nesvizhskii, A. I. (2013) The CRAPome: a contaminant repository for affinity purification–mass spectrometry data. *Nat. Methods*. **10**, 730–736

149. Hutchins, J. R. A., Toyoda, Y., Hegemann, B., Poser, I., Hériché, J.-K., Sykora, M. M., Augsburg, M., Hudecz, O., Buschhorn, B. A., Bulkescher, J., Conrad, C., Comartin, D., Schleiffer, A., Sarov, M., Pozniakovsky, A., Slabicki, M. M., Schloissnig, S., Steinmacher, I., Leuschner, M., Ssykor, A., Lawo, S., Pelletier, L., Stark, H., Nasmyth, K., Ellenberg, J., Durbin, R., Buchholz, F., Mechtler, K., Hyman, A. A., and Peters, J.-M. (2010) Systematic analysis of human protein complexes identifies chromosome segregation proteins. *Science*. **328**, 593–9

150. Joseph, J., Liu, S., Jablonski, S. A., Yen, T. J., and Dasso, M. (2004) The RanGAP1-RanBP2 Complex Is Essential for Microtubule-Kinetochore Interactions In Vivo. *Curr. Biol.* **14**, 611–617

151. Joseph, J., Tan, S.-H., Karpova, T. S., McNally, J. G., and Dasso, M. (2002) SUMO-1 targets RanGAP1 to kinetochores and mitotic spindles. *J. Cell Biol.* **156**, 595–602

152. Söderberg, O., Gullberg, M., Jarvius, M., Ridderstråle, K., Leuchowius, K.-J., Jarvius, J., Wester, K., Hydbring, P., Bahram, F., Larsson, L.-G., and Landegren, U. (2006) Direct observation of individual endogenous protein complexes in situ by proximity ligation. *Nat. Methods*. **3**, 995–1000

153. Huttlin, E. L., Ting, L., Bruckner, R. J., Gebreab, F., Gygi, M. P., Szpyt, J., Tam, S., Zarraga, G., Colby, G., Baltier, K., Dong, R., Guarani, V., Vaites, L. P., Ordureau, A., Rad, R., Erickson, B. K., Wühr, M., Chick, J., Zhai, B., Kolippakkam, D., Mintseris, J., Obar, R. a., Harris, T., Artavanis-Tsakonas, S., Sowa, M. E., De Camilli, P., Paulo, J. a., Harper, J. W., and Gygi, S. P. (2015) The BioPlex Network: A Systematic Exploration of the Human Interactome. *Cell*. **162**, 425–440

154. Verbakel, W., Carmeliet, G., and Engelborghs, Y. (2011) SAP-like domain in nucleolar spindle associated protein mediates mitotic chromosome loading as well as interphase chromatin interaction. *Biochem. Biophys. Res. Commun.* **411**, 732–7

155. Bernier-Villamor, V., Sampson, D. a, Matunis, M. J., and Lima, C. D. (2002)

Structural basis for E2-mediated SUMO conjugation revealed by a complex between ubiquitin-conjugating enzyme Ubc9 and RanGAP1. *Cell*. **108**, 345–56

156. Schimmel, J., Eifler, K., Otti Sigurðsson, J., Cuijpers, S. A., Hendriks, I. A., Verlaan-de Vries, M., Kelstrup, C. D., Francavilla, C., Medema, R. H., Olsen, J. V, and Vertegaal, A. C. (2014) Uncovering SUMOylation Dynamics during Cell-Cycle Progression Reveals FoxM1 as a Key Mitotic SUMO Target Protein. *Mol. Cell*. **53**, 1053–1066

157. Schou, J., Kelstrup, C. D., Hayward, D. G., Olsen, J. V, and Nilsson, J. (2014) Comprehensive identification of SUMO2/3 targets and their dynamics during mitosis. *PLoS One*. **9**, e100692

158. Lamoliatte, F., Caron, D., Durette, C., Mahrouche, L., Maroui, M. A., Caron-Lizotte, O., Bonneil, E., Chelbi-Alix, M. K., and Thibault, P. (2014) Large-scale analysis of lysine SUMOylation by SUMO remnant immunoaffinity profiling. *Nat. Commun.* **5**, 5409

159. Harlow, E., and Lane, D. (1999) *Using antibodies: a laboratory manual*

160. Suzuki, A., Badger, B. L., and Salmon, E. D. (2015) A quantitative description of Ndc80 complex linkage to human kinetochores. *Nat. Commun.* 10.1038/ncomms9161

161. Suzuki, A., Badger, B. L., Wan, X., Deluca, J. G., and Salmon, E. D. (2014) The Architecture of CCAN Proteins Creates a Structural Integrity to Resist Spindle Forces and Achieve Proper Intrakinetochore Stretch. *Dev. Cell*. **30**, 717–730

162. Wątroba, M., Dudek, I., Skoda, M., Stangret, A., Rzodkiewicz, P., and Szukiewicz, D. (2017) Sirtuins, epigenetics and longevity. *Ageing Res. Rev.* **40**, 11–19

163. Osborne, B., Bentley, N. L., Montgomery, M. K., and Turner, N. (2016) The role of mitochondrial sirtuins in health and disease. *Free Radic. Biol. Med.* **100**, 164–174

164. Frye, R. A. (1999) Characterization of five human cDNAs with homology to the yeast SIR2 gene: Sir2-like proteins (Sirtuins) metabolize NAD and may have protein ADP-ribosyltransferase activity. *Biochem. Biophys. Res. Commun.* **260**, 273–279

165. Du, J., Zhou, Y., Su, X., Yu, J. J., Khan, S., Jiang, H., Kim, J., Woo, J., Kim, J. H., Choi, B. H., He, B., Chen, W., Zhang, S., Cerione, R. A., Auwerx, J., Hao, Q., and Lin, H. (2011) Sirt5 Is a NAD-Dependent Protein Lysine Demalonylase and Desuccinylase. *Science.* **334**, 806–809

166. Peng, C., Lu, Z., Xie, Z., Cheng, Z., Chen, Y., Tan, M., Luo, H., Zhang, Y., He, W., Yangţ, K., Zwaans, B. M. M., Tishkoff, D., Ho, L., Lombard, D., Heţ, T.-C., Dai, J., Verdin, E., Ye, Y., and Zhao, Y. (2011) The First Identification of Lysine Malonylation Substrates and Its Regulatory Enzyme. *Mollecular Cell. Proteomics*. **10**, 1–12

167. Tan, M., Peng, C., Anderson, K. A., Chhoy, P., Xie, Z., Dai, L., Park, J., Chen, Y., Huang, H., Zhang, Y., Ro, J., Wagner, G. R., Green, M. F., Madsen, A. S., Schmiesing, J., Peterson, B. S., Xu, G., Ilkayeva, O. R., Muehlbauer, M. J., Braulke, T., Mühlhausen, C., Backos, D. S., Olsen, C. A., McGuire, P. J., Pletcher, S. D., Lombard, D. B., Hirschey, M. D., and Zhao, Y. (2014) Lysine glutarylation is a protein posttranslational modification regulated by SIRT5. *Cell Metab.* **19**, 605–617

168. Nakagawa, T., Lomb, D. J., Haigis, M. C., and Guarente, L. (2009) SIRT5 Deacetylates Carbamoyl Phosphate Synthetase 1 and Regulates the Urea Cycle. *Cell*. **137**, 560–570

169. Ogura, M., Nakamura, Y., Tanaka, D., Zhuang, X., Fujita, Y., Obara, A., Hamasaki, A., Hosokawa, M., and Inagaki, N. (2010) Overexpression of SIRT5 confirms its involvement in deacetylation and activation of carbamoyl phosphate synthetase 1. *Biochem. Biophys. Res. Commun.* **393**, 73–78

170. Rubio, V. (1993) Structure-function studies in carbamoyl phosphate synthetases. *Biochem. Soc. Trans.* **21**, 198–202

171. Lin, Z. F., Xu, H. B., Wang, J. Y., Lin, Q., Ruan, Z., Liu, F. B., Jin, W., Huang, H. H., and Chen, X. (2013) SIRT5 desuccinylates and activates SOD1 to eliminate ROS. *Biochem. Biophys. Res. Commun.* **441**, 191–195

172. McCord, J. M., and Fridovich, I. (1969) Superoxide Dismutase an enzymatic function for erythrocuprein. *J. Biol. Chem.* **244**, 6049–6065

173. Park, J., Chen, Y., Tishkoff, D. X. X., Peng, C., Tan, M., Dai, L., Xie, Z., Zhang, Y., Zwaans, B. M. M. M. M., Skinner, M. E. E., Lombard, D. B. B., and Zhao, Y. (2013) SIRT5-Mediated Lysine Desuccinylation Impacts Diverse Metabolic Pathways. *Mol. Cell*. **50**, 919–930

174. Skowyra, D., and Craig, K. L. (1997) F-Box Proteins Are Receptors that Recruit Phosphorylated Substrates to the SCF Ubiquitin-Ligase Complex. *Cell*. **91**, 209–219

175. Koh, J. L. Y., Ding, H., Costanzo, M., Baryshnikova, A., Toufighi, K., Bader, G. D., Myers, C. L., Andrews, B. J., and Boone, C. (2010) DRYGIN: a database of quantitative genetic interaction networks in yeast. *Nucleic Acids Res.* **38**, D502–D507

176. Matsushita, N., Yonashiro, R., Ogata, Y., Sugiura, A., Nagashima, S., Fukuda, T., Inatome, R., and Yanagi, S. (2011) Distinct regulation of mitochondrial localization and stability of two human Sirt5 isoforms. *Genes to Cells*. **16**, 190–202

177. Jiang, L., Xiong, J., Zhan, J., Yuan, F., Tang, M., Zhang, C., Cao, Z., Chen, Y., Lu, X., Li, Y., Wang, H., Wang, L., Wang, J., Zhu, W.-G., and Wang, H. (2017) Ubiquitin-specific peptidase 7 (USP7)-mediated deubiquitination of the histone deacetylase SIRT7 regulates gluconeogenesis. *J. Biol. Chem.* **292**, 13296–13311

178. Gao, D., Inuzuka, H., Korenjak, M., Tseng, A., Wu, T., Wan, L., Kirschner, M., Dyson, N., and Wei, W. (2009) Cdh1 Regulates Cell Cycle through Modulating the Claspin/Chk1 and the Rb/E2F1 Pathways. *Mol. Biol. Cell*. **20**, 3305–3316

179. Ohtsubo, M., Theodoras, A. M., Schumacher, J., Roberts, J. M., and Pagano, M. (1995) Human Cyclin E, a Nuclear Protein Essential for the G 1 -to-S Phase Transition. *Mol. Cell. Biol.* **15**, 2612–2624

180. Lee, H.-J., Jedrychowski, M. P., Vinayagam, A., Wu, N., Shyh-Chang, N., Hu, Y., Min-Wen, C., Moore, J. K., Asara, J. M., Lyssiotis, C. A., Perrimon, N., and Kirschner, M. W. (2017) Proteomic and Metabolomic Characterization of a Mammalian Cellular Transition from Quiescence to Proliferation Cell Reports Resource Proteomic and Metabolomic Characterization of a Mammalian Cellular Transition from Quiescence to Proliferation. *Cell Rep.* **20**, 721–736

181. Igci, M., Kalender, M. E., Borazan, E., Bozgeyik, I., Bayraktar, R., Bozgeyik, E., Camci, C., and Arslan, A. (2016) High-throughput screening of Sirtuin family of genes in breast cancer. *Gene*. **586**, 123–128

182. Lu, W., Zuo, Y., Feng, Y., and Zhang, M. (2014) SIRT5 facilitates cancer cell growth and drug resistance in non-small cell lung cancer. *Tumour Biol.* **35**, 10699–10705